GAC-MAC
WINNIPEG
2013

AT THE
CENTRE OF
THE CONTINENT

AU
CENTRE DU
CONTINENT

FIELD TRIP GUIDEBOOK

Pirate Island - Paint Lake by Nancy-lynne Hughes

Field Trip Guidebook FT-A1 / Open File OF2013-4

The Rice Lake mine trend, Manitoba: regional setting, host rock stratigraphy and structural evolution of a classical Archean orogenic gold system

S.D. Anderson

Held in conjunction with

GAC®-MAC • AGC®-AMC

Joint Annual Meeting • Congrès annuel conjoint

May 22–24, 2013

This field trip was sponsored by the Mineral Deposits Division of the Geological Association of Canada

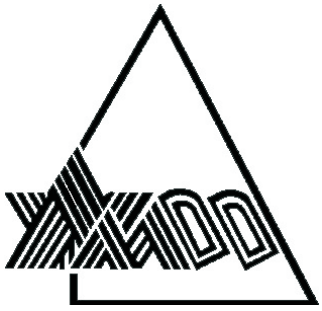

In-kind support provided by San Gold Corporation

Open File OF2013-4

Field Trip Guidebook FT-A1

The Rice Lake mine trend, Manitoba: regional setting, host rock stratigraphy and structural evolution of a classical Archean orogenic gold system

by S.D. Anderson

Geological Association of Canada–Mineralogical Association of Canada Joint Annual Meeting, Winnipeg

May, 2013

Innovation, Energy and Mines

Hon. Dave Chomiak
Minister

Grant Doak
Deputy Minister

Mineral Resources Division

John Fox
Assistant Deputy Minister

Manitoba Geological Survey

C.H. Böhm
A/Director

Manitoba

Anderson, S.D. 2013: The Rice Lake mine trend, Manitoba: regional setting, host rock stratigraphy and structural evolution of a classical Archean orogenic gold system; Geological Association of Canada–Mineralogical Association of Canada Joint Annual Meeting, Field Trip Guidebook FT-A1; Manitoba Innovation, Energy and Mines, Manitoba Geological Survey, Open File OF2013-4, 47 p.

NTS grid: 52M

Keywords: Manitoba; Rice Lake; Archean; Superior province; North Caribou terrane; Uchi subprovince; Rice Lake greenstone belt; Bidou, Gem or San Antonio assemblage; Rice Lake mine trend; San Antonio, Rice Lake, 007 or Hinge deposit; quartz-carbonate veins; orogenic or shear-hosted gold deposits

Published by:

Manitoba Innovation, Energy and Mines
Manitoba Geological Survey
360–1395 Ellice Avenue
Winnipeg, Manitoba
R3G 3P2 Canada
Telephone: (800) 223-5215 (General Enquiry)
(204) 945-4154 (Publication Sales)
Fax: (204) 945-8427
E-mail: minesinfo@gov.mb.ca
Website: manitoba.ca/minerals

This publication is available to download free of charge at manitoba.ca/minerals

SAFETY INFORMATION

General Information

The Geological Association of Canada (GAC) recognizes that its field trips may involve hazards to the leaders and participants. It is the policy of the GAC to provide for the safety of participants during field trips, and to take every precaution, reasonable in the circumstances, to ensure that field trips are run with due regard for the safety of leaders and participants. Field trip safety is a shared responsibility. The GAC has a responsibility to take all reasonable care to provide for the safety of the participants on its field trips. Participants have a responsibility to give careful attention to safety-related matters and to conduct themselves with due regard to the safety of themselves and others while on the field trips.

Field trip participants should be aware that any geological fieldwork, including field trips, can present significant safety hazards. Foreseeable hazards of a general nature include inclement weather, slips and falls on uneven terrain, falling or rolling rock, insect bites or stings, animal encounters and flying rock from hammering. **The provision and use of appropriate personal protective equipment (e.g., rain gear, sunscreen, insect repellent, safety glasses, work gloves and sturdy boots) is the responsibility of each participant.** Each field trip vehicle will be equipped with a moderate sized first-aid kit, and the lead vehicle will carry a larger, more comprehensive kit of the type used by the Manitoba Geological Survey for remote field parties.

Participants should be prepared for the possibility of inclement weather. In Manitoba, the weather in May is highly unpredictable. The average daily temperature in Winnipeg is 12°C, with record extremes of 37°C and -11°C. North-central Manitoba (Thompson) has an average daily temperature of 7°C, with record extremes of 33°C and -18°C (*Source:* Environment Canada). Consequently, participants should be prepared for a wide range of temperature and weather conditions, and should plan to dress in layers. A full rain suit and warm sweater are essential. Gloves and a warm hat could prove invaluable if it is cold and wet, and a sunhat and sunscreen might be just as essential in the heat and sun.

Above all, field trip participants are responsible for acting in a manner that is safe for themselves and their co-participants. This responsibility includes using personal protective equipment (PPE) when necessary or when recommended by the field trip leader, or upon personal identification of a hazard requiring PPE use. It also includes informing the field trip leaders of any matters of which they have knowledge that may affect their health and safety or that of co-participants. Field Trip participants should pay close attention to instructions from the trip leaders and GAC representatives at all field trip stops. Specific dangers and precautions will be reiterated at individual localities.

Specific Hazards

Some of the stops on this field trip may require short hikes, in some cases over rough, rocky, uneven or wet terrain. Participants should be in good physical condition and accustomed to exercise. Sturdy footwear that provides ankle support is strongly recommended. Some participants may find a hiking stick a useful aid in walking safely. Steep outcrop surfaces require special care, especially after rain. Access to bush outcrops may require traverses across muddy or boggy areas; in some cases it may be necessary to cross small streams or ditches. Field trip leaders are responsible for identifying such stops and making participants aware well in advance if waterproof footwear is required. Field trip leaders will also ensure that participants do not go into areas for which their footwear is inadequate for safety. In all cases, field trip participants must stay with the group.

Other field trip stops are located adjacent to roads, some of which may be prone to fast-moving traffic. At these stops, participants should pay careful attention to oncoming traffic, which may be distracted by the field trip group. Participants should exit vehicles on the shoulder-side of the road, stay off roads when examining or photographing outcrops, and exercise extreme caution in crossing roads.

Road cuts or rock quarries also present specific hazards, and participants MUST behave appropriately for the safety of all. Participants must be aware of the danger from falling debris and should stay well back from overhanging cliffs or steep faces. Participants must stay clear of abrupt drop-offs at all times, stay with the field trip group, and follow instructions from leaders.

Participants are asked to refrain from hammering rock. It represents a significant hazard to the individual and other participants, and is in most cases unnecessary. Many stops on this field trip include outcrop with unusual features that should be preserved for future visitors. If a genuine reason exists for collecting a sample, please inform the field trip leader, and then make sure it is done safely and with concern for others, ideally after the main group has departed the outcrop.

Subsequent sections of this guidebook contain the stop descriptions and outcrop information for the field trip. In addition to the general precautions and hazards noted above, the introductions for specific localities make note of any specific safety concerns. Field trip participants must read these cautions carefully and take appropriate precautions for their own safety and the safety of others.

TABLE OF CONTENTS

TABLES

FIGURES

Introduction

The Rice Lake mine trend is located 155 km northeast of Winnipeg, Manitoba, in the central portion of the Archean Rice Lake greenstone belt of the western Superior Province. The trend is hosted by 2.73–2.72 Ga volcanic, volcaniclastic, epiclastic and subvolcanic intrusive rocks, and includes several significant gold deposits, the largest of which is the Rice Lake (a.k.a. San Antonio) deposit at Bissett. Within the trend, auriferous quartz-carbonate veins are hosted by brittle-ductile shear zones and cogenetic arrays of shear and tensile fractures, and preferentially formed within chemically favourable or competent rocks, or along strength-anisotropies, during regional compressional deformation. With total production of 1.7 million ounces of gold, and current reserves and resources of 3.5 million ounces in nine deposits (Ginn and Michaud, 2013; Table 1), the Rice Lake mine trend is the most significant lode gold camp in Manitoba and is currently the focus of intensive exploration and mining by San Gold Corporation.

In 2002, the Manitoba Geological Survey initiated a program of 1:20 000 scale bedrock mapping, structural analysis, lithogeochemistry, U-Pb geochronology and Sm-Nd isotopic analysis in the Rice Lake greenstone belt, with the intent of providing an improved geological context and predictive framework for mineral exploration. Bedrock mapping at Rice Lake took place in 2004 and 2005 and the results of this work were released in 2008 (Anderson, 2008). Detailed stratigraphic and structural mapping of the mine trend at 1:5000 scale took place in 2011 (Anderson, 2011a, b, c), utilizing high-resolution light detection and ranging (LiDAR) data provided by San Gold Corporation.

This guidebook includes an overview of the regional setting of the Rice Lake belt, and the stratigraphy, geochemistry and structural geology of Neoarchean supracrustal rocks at Rice Lake, in light of new results from government and industry geoscience. Also included is a road log and descriptions of field trip stops that will facilitate understanding of the stratigraphic setting, structural controls and tectonic evolution of the mine trend. Readers interested in other, or more detailed, aspects of the local geology are referred to reports by Anderson (2008, 2011a, b, 2013), parts of which are excerpted here.

Previous work

Early geological investigations of the Rice Lake area by the Geological Survey of Canada and Manitoba Geological Survey documented the setting and general characteristics of lode-gold deposits (e.g., Moore, 1914; Dresser, 1917; Cooke, 1922; De Lury, 1927; Wright, 1923, 1932; Stockwell, 1938, 1940, 1945; Davies, 1953, 1963). Of these, Stockwell (1938) provided the most comprehensive and detailed description of the Rice Lake mine trend. In 1985, the mine trend was remapped at 1:10 000 scale by the Geological Survey of Canada in support of detailed studies of the Rice Lake deposit and its hostrocks (Tirschmann, 1986; Ames, 1988; Lau, 1988; Ames et al., 1991; Lau and Brisbin, 1996), which took place under the auspices of the 1984–1989 Canada-Manitoba Mineral Development Agreement (MDA). Aspects of this work were summarized by Poulsen et al. (1986, 1996) and Poulsen (1987, 1989). Mineral occurrences in the area were documented by Theyer (1994a). Additional studies focused specifically on the Rice Lake deposit include those of Reid (1931), Bragg (1943), Gibson and Stockwell (1948), Whiting (1989) and Rhys (2001)

Regional setting

The Rice Lake greenstone belt (RLB) is one of several strands of Neoarchean and Mesoarchean supracrustal rocks that define the western segment of the volcano-plutonic Uchi subprovince (Card and Ciesielski, 1986; Stott and Corfu, 1991) of the western Superior province (Figure 1). The western Uchi subprovince includes the Red Lake and Birch-Uchi greenstone belts in Ontario and is flanked to the north by the mainly metaplutonic Berens River subprovince and to the south by metasedimentary rocks and derived gneiss, migmatite and granitoid plutonic rocks of the English River subprovince (Card and Ciesielski, 1986). Thurston et al. (1991) included the Berens River subprovince and the Mesoarchean portions of the Uchi subprovince in the continental 'North Caribou terrane' (NCT), now widely regarded as the Mesoarchean protocraton around which Mesoarchean and Neoarchean terranes were accreted during the protracted assembly of the western Superior province (e.g., Stott and Corfu, 1991; Williams et al., 1992; Corfu et al., 1998; Whalen et al., 2003; Percival et al., 2006b). Mesoarchean portions of the Uchi subprovince in Manitoba are bounded to the

Table 1: Rice Lake mine trend production, reserves and resources (after Ginn and Michaud, 2013).

as at December 31, 2012	Tons	Au grade (oz/ton)	Au grade (g/tonne)	Ounces Au
Production[1]	8,096,900	0.21	7.2	1,715,500
Reserve (proven and probable)	1,699,200	0.15	5.1	252,600
Resource (measured and indicated)[2]	3,429,900	0.19	6.5	655,100
Resource (inferred)	16,517,100	0.17	5.8	2,852,500
Total[3]	28,043,900	0.18	6.2	5,223,100

[1] Cumulative production (1927, 1933-68, 1980-83, 1997-2001, 2007-12)
[2] Includes proven and probable reserve
[3] Production + total resource

south by the Wanipigow fault and described herein as part of the NCT. Using the terminology of Stott et al. (2010), the English River subprovince is herein referred to as the English River basin (ERB). South of Rice Lake, the Manigotagan fault sharply defines the north boundary of this basin and is continuous with the Sydney Lake–Lake St. Joseph fault in Ontario (Figure 1).

Stratigraphic nomenclature

Stockwell (1945) assigned the supracrustal rocks of the RLB to the Rice Lake group and the overlying San Antonio formation. A revised stratigraphic scheme developed by the MGS in the early 1970s had the Rice Lake group divided into the mainly metavolcanic Wallace Lake, Bidou Lake and Gem Lake subgroups and the metasedimentary Edmunds Lake formation (*see* Campbell, 1971; Weber, 1971a). Poulsen et al. (1996) proposed one additional unit, the mainly metavolcanic Garner Lake subgroup, based on subsequent work at Garner Lake (e.g., Brommecker et al., 1993; Poulsen et al., 1993, 1994; Davis, 1994). Poulsen et al. (1996) also proposed an alternative tectonostratigraphic nomenclature, wherein the supracrustal components of the RLB are subdivided into six distinct assemblages: the Mesoarchean Wallace assemblage, the Mesoarchean–Neoarchean Garner assemblage, and the Neoarchean Bidou, Gem, Edmunds and San Antonio assemblages (Figure 2, Table 2). Broadly comparable assemblages are recognized in other locations along the south margin of the NCT (Percival et al., 2006a, b), thereby providing a basis for regional correlations.

North Caribou terrane

In Manitoba, the south margin of the NCT includes five principal components: 1) ca. 3.01–2.99 Ga tonalitic basement; 2) nonconformably overlying ca. 2.99–2.92 Ga platform-rift sequences (Wallace assemblage); 3) ca. 2.94–2.90 Ga tonalite–granodiorite plutons; 4) ca. 2.90–2.85 Ga volcano-sedimentary rocks (Garner assemblage); and 5) ca. 2.75–2.70 Ga tonalite–granodiorite–granite plutons of the Wanipigow River plutonic complex (Corfu and Stone, 1998; Bailes et al., 2003; Whalen et al., 2003; Bailes and Percival, 2005; Percival et al., 2006a, b; Sasseville et al., 2006; Anderson, 2013). Vestiges of Mesoarchean basement are uniquely well preserved along the south margin of the NCT in Manitoba and consist of juvenile tonalite-diorite-gabbro-anorthosite suites of the East Shore and English Lake complexes, which are interpreted to have formed in a primitive oceanic arc (Whalen et al., 2003). Mafic gneiss in the English Lake complex preserves evidence of high-grade (~12 kbar; ~850°C) metamorphism at ca. 3.0 Ga, suggesting that the NCT had attained continental thickness by that time (Percival et al., 2006a).

Wallace assemblage

The Wallace assemblage is best preserved along the east shore of Lake Winnipeg and at Wallace Lake, at the south margin of the NCT (Figure 2). Basal quartz arenite and pebble conglomerate contain single age-populations of ca. 2.99 Ga detrital zircons and are conformably overlain by ca. 2.98–2.92 Ga komatiite, tholeiitic basalt and iron formation (Davis, 1994; Percival

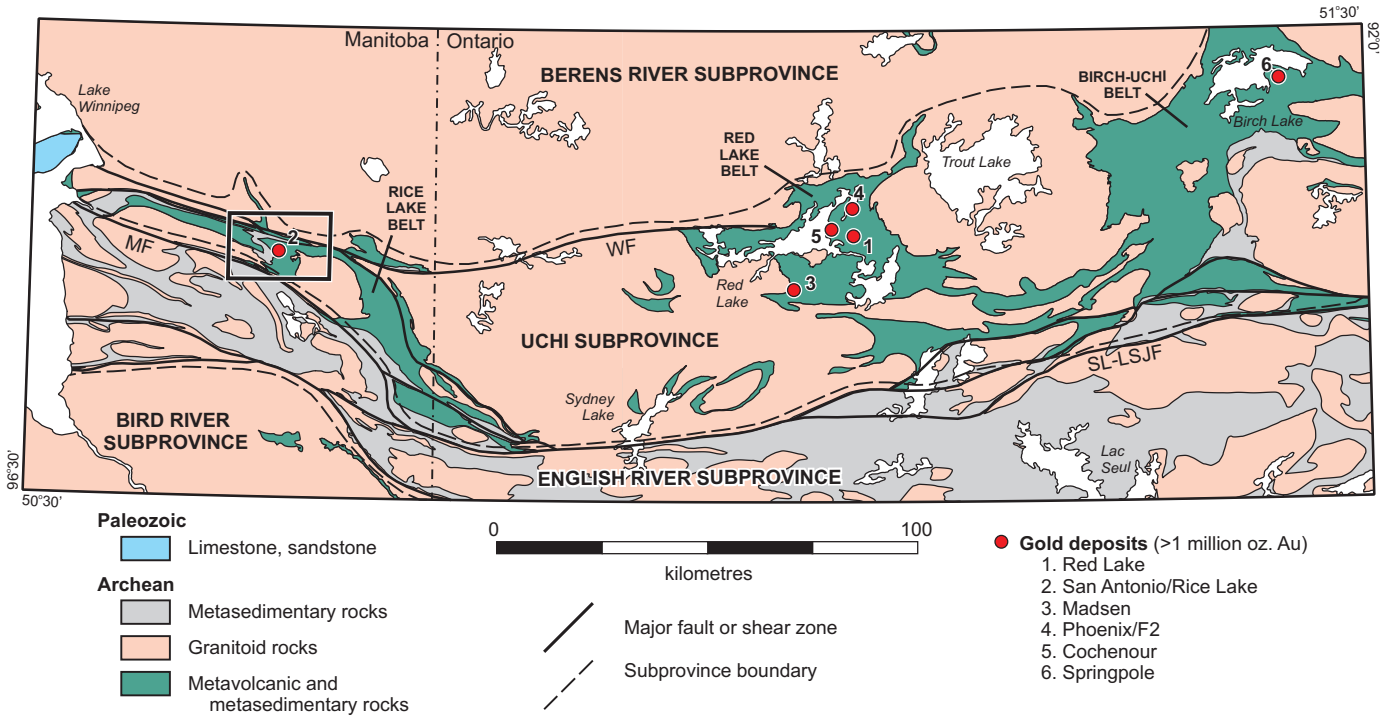

Figure 1: *Regional geological setting of the Rice Lake belt in the western Uchi Subprovince (modified after Lemkow et al., 2006). Rectangle indicates the Rice Lake area. Abbreviations: MF, Manigotagan fault; SL–LSJF, Sydney Lake–Lake St. Joseph fault; WF, Wanipigow fault.*

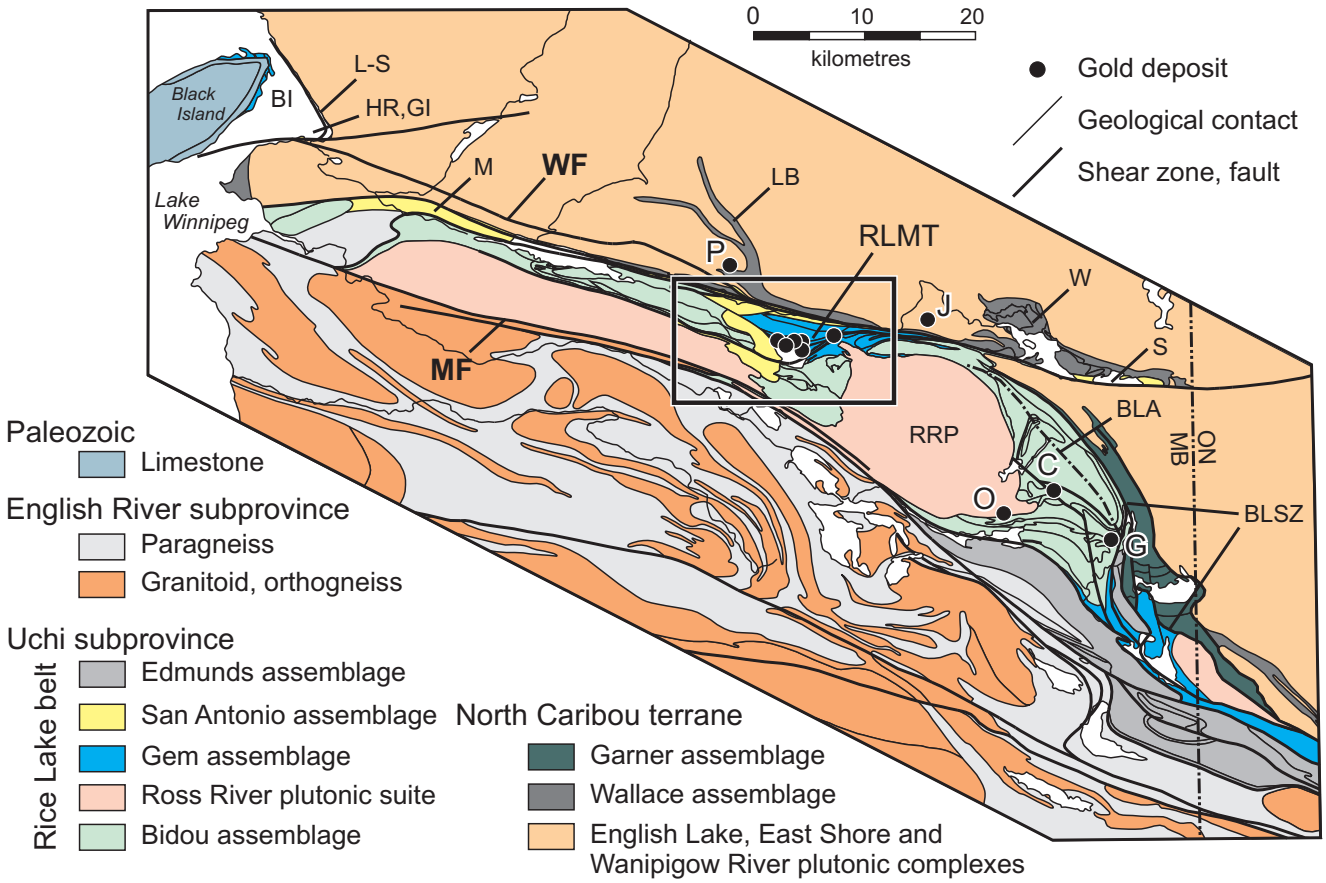

Figure 2: *Simplified geology of the Rice Lake belt, showing the principal lithotectonic assemblages, major gold deposits and location of the field trip area (rectangle). Abbreviations: BLA, Beresford Lake anticline; BLSZ, Beresford Lake shear zone; BI, Black Island assemblage; C, Central Manitoba deposit; GI, Guano Island assemblage; G, Gunnar deposit; HR, Hole River assemblage; J, Jeep deposit; LB, Little Beaver assemblage; L-S, Lewis-Storey assemblage; M, Manigotagan assemblage; MF, Manigotagan fault; O, Ogama-Rockland deposit; P, Poundmaker deposit; RLMT, Rice Lake mine trend; RRP, Ross River pluton; S, Siderock assemblage; W, Wallace assemblage; WF, Wanipigow fault.*

et al., 2006a; Sasseville et al., 2006). This sequence is thought to record uplift, erosion and stabilization of the proto-continental mass by ca. 2.98 Ga, followed by plume-influenced extension and rifting of the protocraton to form a long-lived oceanic basin (Percival et al., 2006b). As suggested by Percival et al. (2006a, b), the Wallace assemblage is likely correlative with komatiite-bearing assemblages in the Red Lake belt in Ontario, including the ca. 2.99–2.96 Ga Balmer and ca. 2.94–2.92 Ga Ball assemblages (Stott and Corfu, 1991; Sanborn-Barrie et al., 2001). The Balmer assemblage is interpreted to record plume-influenced extension and rifting of the protocraton, whereas the Ball assemblage is thought to represent a primitive arc to intra-arc rift built on extended continental crust of the NCT (Stott and Corfu, 1991; Tomlinson et al., 1998; Sanborn-Barrie et al., 2001; Percival et al., 2006b). Minor dikes and plutons of ca. 2.94–2.92 Ga tonalite–granodiorite along the NCT margin in Manitoba (Turek et al., 1989; Davis, 1994; Percival et al., 2006a; Sasseville et al., 2006) likely represent local manifestations of this magmatism.

Garner assemblage

The Garner assemblage has a stratigraphic thickness of at least 8 km and occurs as a fault-bounded panel at the south margin of the NCT in the southeast portion of the Rice Lake belt (Anderson, 2013; Figure 2). Intermediate–felsic volcaniclastic and derived epiclastic rocks in the lower portion of the assemblage show geochemical affinity to modern continental arcs and are intruded by the ca. 2.87 Ga (Davis, 1994) mafic–ultramafic Garner Lake intrusive complex. Arkosic sandstone and pebble conglomerate at the base of the upper portion overlie an erosional unconformity and contain locally-sourced 2.87 Ga detrital zircons (Davis, 1994). They are successively overlain by ca. 2.85 Ga intermediate–felsic volcanic rocks, magnetite-chert iron formation and subaqueous komatiitic and tholeiitic basalt flows derived from a strongly depleted source, which Hollings et al. (1999) attributed to a mantle plume that impinged on the NCT margin. The Garner assemblage thus appears to be analogous to Archean 'plume-influenced' rift sequences documented elsewhere (e.g., Thurston and Chivers, 1990; Bleeker et al., 1999; Percival et al., 2006a). Stratigraphic, geochemical and age constraints suggest possible correlations to the Bruce Channel (ca. 2.89 Ga) and Trout Bay (ca. 2.85 Ga) assemblages in the Red Lake belt, which are interpreted as continental-arc and oceanic-plateau successions, respectively (Sanborn-Barrie et al., 2001).

Table 2: Tectonostratigraphic assemblages and correlations in the western Uchi subprovince.

Assemblage	Age constraints	Equivalent units (MB)	Equivalent units (ON)	Key rock-types and chemical affinity	Depositional setting	Tectonic significance
San Antonio	<2.705 Ga	Guano Island; Hole River; Manigotagan; Siderock	None known	Quartz greywacke, conglomerate, turbiditic greywacke	Subaerial fault-bounded fluvial basin; basal angular unconformity	Post-accretion, pre-orogenic; denudation of NCT margin
Edmunds	<2.71 Ga (lower); <2.70 Ga (upper); >2.69 Ga	English River	Bee Lake (Kangaroo Formation)	Turbiditic greywacke, mudstone, conglomerate, iron formation; minor TH to CA basalt	Submarine fan; mature arc-rift basin; basal conformity	Regionally extensive intra-arc basin; uplift and denudation of NCT margin
Gem	<2.73 Ga; ca. 2.72 Ga	Black Island; Rainy Lake Road, Townsite and Round Lake units	Bee Lake (Odd and Anderson formations); St. Joseph	TH to CA basalt, basaltic-andesite; CA ADR; hypabyssal intrusions; epiclastic rocks	Subaerial to shallow subaqueous arc-rift basin	Restricted extensional basin in Bidou arc; slab rollback?
Bidou	<2.75 Ga (lower); 2.73 Ga (upper)	Black Island (part of); Independence Lake unit	Confederation	TH basalt and gabbro; CA dacite, rhyolite; turbiditic greywacke and conglomerate	Mature back-arc basin (lower); subaqueous volcanic arc (upper)	Oceanic or marginal arc–back-arc complex; northward subduction
Garner	>2.87 Ga (lower); ca. 2.85 Ga (upper)	None known	Bruce Channel and Trout Bay	CA ADR; peridotite, pyroxenite; arkose; iron formation; komatiite-KB; TH basalt and gabbro	Subaqueous volcanic arc (lower); intra-arc rift (upper)	Continental arc
Wallace	<2.99 Ga; >2.92 Ga	Lewis-Story; Little Beaver	Balmer (±Ball)	Arkosic 'grit'; quartzite; iron formation; carbonate; komatiite-KB; TH basalt and gabbro	Shallow marine continental platform and restricted rift basins	Stabilization of NCT; initial rifting

ADR, andesite-dacite-rhyolite; CA, calcalkalic; KB, komatiitic basalt; NCT, North Caribou terrane; TH, tholeiitic

Wanipigow River plutonic complex

The Wanipigow River plutonic complex represents the southwest portion of a vast domain of composite granitoid batholiths that extends north and east of the Rice Lake belt for several hundred kilometres. It includes suites of calcalkalic tonalite, granodiorite and granite that were emplaced during an essentially continuous pulse of magmatism between 2.75 and 2.69 Ga (Corfu and Stone, 1998). Early suites, consisting mostly of hornblende tonalite and granodiorite emplaced between 2.75 and 2.72 Ga, are chemically analogous to modern magmatic arcs (Corfu and Stone, 1998). Contemporaneous mafic–felsic volcanic rocks of calcalkalic and tholeiitic affinity in the ca. 2.75–2.73 Ga Confederation assemblage of the Red Lake and Birch-Uchi belts in Ontario are interpreted to record construction and localized rifting of this continental arc (Stott and Corfu, 1991; Hollings and Kerrich, 2000; Sanborn-Barrie et al., 2001; Percival et al., 2006b).

Wanipigow fault

In the western and central portions of the Rice Lake belt, the south boundary of the NCT is defined by the Wanipigow fault, which is one of the principal structures of the region (Figure 2) and is interpreted to represent a long-lived crustal-scale fault of the type associated with major terrane boundaries and orogenic gold districts elsewhere. It trends east-southeast and, though poorly exposed, is delineated by fault-bounded basins of fluvial-alluvial siliciclastic rocks and a topographic lineament. It is characterized by a steeply dipping zone of interleaved tectonite, mylonite and phyllonite that ranges up to 1.5 km wide and contains kinematic evidence of a multi-phase movement history (Anderson, 2008). Supracrustal rocks on either side of this fault contain comparable metamorphic mineral assemblages, suggesting that the strike-slip component of movement was dominant. The fault bifurcates toward the east at Wallace Lake, where a northern splay is traced eastward along strike as a topographic lineament towards Red Lake, Ontario (Figure 1); offset of the greenstone-granitoid contact suggests approximately 20 km of net dextral displacement (Figure 2). The southern splay, known as the Beresford Lake shear zone, trends southeast through the Beresford Lake area and separates Mesoarchean and Neoarchean assemblages of the NCT and Uchi subprovince, respectively (Figure 2). Further along strike in Ontario, it appears to merge with the Sydney Lake–Lake St. Joseph fault.

Uchi subprovince

The Uchi subprovince in Manitoba consists of subaqueously deposited volcanic and derived epiclastic rocks, synvolcanic gabbro sills and tonalite–granodiorite plutons, and unconformably overlying terrestrial and marine siliciclastic rocks, which collectively define the RLB south of the Wanipigow fault. The exposed portion of the belt trends southeast for a distance of 145 km from the eastern extent of Paleozoic cover at Lake Winnipeg to just east of the Manitoba-Ontario border, and ranges up to 15 km wide (Figure 2). Regional aeromagnetic

data indicate that the belt extends at least 150 km to the west beneath Paleozoic cover, where it widens considerably. The eastern extent of the RLB in Ontario is referred to as the Bee Lake belt.

Major volcanism in the Manitoba segment of the Uchi subprovince spanned roughly 30 m.y., between 2.75 and 2.72 Ga, whereas overlying sedimentary successions were deposited shortly after cessation of major volcanism, within a roughly 20 m.y. time interval between 2.72 and 2.70 Ga (Krogh et al., 1974; Ermanovics and Wanless, 1983; Turek et al., 1989; Turek and Weber, 1991; Davis, 1994, 1996; Percival et al., 2006a; Sasseville et al., 2006; Anderson, 2008, 2013). Following the terminology of Poulsen et al. (1996), volcanic rocks south of the Wanipigow fault are subdivided into the Bidou and Gem assemblages, whereas the younger sedimentary successions are subdivided into the Edmunds and San Antonio assemblages (Figure 2). The volcanic assemblages are distinguished by geochemical signatures and U-Pb ages, and are intruded by voluminous tonalite–granodiorite plutons of the Ross River plutonic suite. As outlined below, these assemblages are interpreted to record back-arc, arc and arc-rift magmatism and synorogenic sedimentation within a north-verging subduction-accretion complex that developed over a span of roughly 50 m.y. along the NCT margin (e.g., Stott and Corfu, 1991; Poulsen et al., 1996; Sanborn-Barrie et al., 2001; Bailes et al., 2003; Bailes and Percival, 2005; Percival et al., 2006a, b; Anderson, 2008, 2013).

Bidou assemblage

The Bidou assemblage (ca. 2.75–2.73 Ga) defines the map-scale Beresford Lake anticline in the core of the RLB and is intruded by ca. 2.73–2.72 Ga tonalite–granodiorite plutons, of which the Ross River pluton is the most prominent example (Figure 2; Turek et al., 1989; Bailes et al., 2003; Percival et al., 2006a; Anderson, 2008). At the type locality east of the pluton, the Bidou assemblage is approximately 6–7 km thick and consists of intercalated basalt flows, gabbro sills and marine sedimentary rocks, overlain by a thick accumulation of calcalkalic felsic volcaniclastic rocks. Subaqueous basalt flows and subvolcanic gabbro sills in the lower portion of the assemblage are chemically similar to MORB erupted at steady-state spreading centres in relatively mature (>100 km wide) back-arc basins (Bailes and Percival, 2005) and alternate with intervals of marine turbidite with a maximum depositional age of ca. 2.75 Ga (Anderson, 2013). Juvenile isotopic signatures and the absence of older (>2.75 Ga) inherited or detrital zircons suggest an intra-oceanic setting; the basal contact of this assemblage is nowhere exposed. The absence of Mesoarchean detrital zircons further suggests a depositional setting isolated from the NCT margin. The upper portion ranges up to 2.4 km in thickness and consists of coarse volcaniclastic rocks derived from ca. 2.73 Ga (Turek et al., 1989) calcalkalic porphyritic dacite, which represents the minimum age for the Bidou assemblage as a whole. Probable correlatives occur south of Rice Lake (i.e., the Independence Lake unit of Anderson, 2008) and at Black Island on Lake Winnipeg (i.e., the Black Island rhyolite of Bailes and Percival, 2005). The available age constraints also indicate a correlation to the 2.75–2.73 Ga Confederation assemblage in the Red Lake and Birch-Uchi belts, which is interpreted as an extended, and locally rifted, continental arc (Sanborn-Barrie et al., 2001; Percival et al., 2006a).

Gem assemblage

At the type locality in the southeast portion of the Rice Lake belt, the Gem assemblage conformably overlies the Bidou assemblage and ranges up to 2 km thick. It consists of volcanic flows, primary and variably reworked volcaniclastic rocks, hypabyssal intrusions, and derived epiclastic rocks, deposited between 2.73 and 2.72 Ga in subaqueous to subaerial settings (Anderson, 2013). Unlike the markedly bimodal Bidou assemblage, the volcanic rocks vary in composition from primitive basalt to high-SiO_2 rhyolite and include distinctive FII-FIII–type (Lesher et al., 1986) rhyolite flows, suggesting an analogy to modern and ancient rifts. A wide diversity in eruptive settings and styles, coupled with abrupt lateral and vertical facies changes, and the presence of rhyolite flows, indicate proximal deposition in a volcanic complex comprising multiple eruptive centres. Age-equivalent rocks at Rice Lake (i.e., the Rainy Lake Road, Townsite and Round Lake units of Anderson, 2008) and at Black Island on Lake Winnipeg (the Gray Point and Drumming Point sequences of Bailes and Percival, 2005) include geochemical analogues of rocks at the type locality. Associated epiclastic rocks either lack detrital zircons or are exclusively of Neoarchean provenance, suggesting deposition in sites remote from the NCT. Age-equivalent rocks in Ontario include the ca. 2.72 Ga Anderson formation of the Bee Lake belt (Rogers and McNicoll, unpublished; cited by Lemkow et al., 2006) and the ca. 2.72–2.71 Ga St. Joseph assemblage (Stott and Corfu, 1991; Corfu and Stott, 1993) of the Lake St. Joseph belt, the latter of which is interpreted to represent a continental- or marginal-arc setting (Stott and Corfu, 1991).

Ross River plutonic suite

The Bidou and Gem assemblages are intruded by tonalite–granodiorite plutons of the Ross River plutonic suite and hypabyssal porphyry intrusions emplaced between 2.73 and 2.72 Ga (Turek et al., 1989; Turek and Weber, 1991; Anderson, 2008). The namesake pluton dominates the central portion of the Rice Lake belt and appears to consist of two nested stocks, each of which is zoned outward from a granodioritic core to a tonalitic margin. Igneous zircons from the granodioritic core of the western stock yielded a U-Pb age of 2724 ±2 Ma (Anderson, 2008), which is taken as the best estimate of the emplacement age. Prominent apophyses extend outwards toward the northwest and southeast, imparting a sigmoidal shape to the pluton. West of Rice Lake, a homogeneous sheet-like intrusion of ca. 2.72 Ga (Anderson, unpublished data, 2008) tonalite intrudes the Bidou assemblage and is nonconformably overlain by fluvial-alluvial siliciclastic rocks of the San Antonio assemblage (Stockwell, 1945; Davies, 1963).

Edmunds assemblage

Along the south margin of the Rice Lake belt, sedimentary rocks and basaltic flows of the Edmunds assemblage conformably overlie the Bidou and Gem assemblages, and define the

north flank of the English River basin. Distinctive lower and upper facies associations record deposition below wave-base in a coarsening-upward submarine fan at least 2.5 km thick (Anderson, 2013). The upper facies association (UFA) consists of distal greywacke-mudstone turbidite, conglomerate, massive quartz-lithic greywacke and iron formation that were deposited in a channellized lower- to mid-fan setting, with a maximum depositional age of ca. 2.71 Ga (Davis, 1996; Anderson, 2013). Proximal greywacke-mudstone turbidites, coarse polymictic conglomerate, iron formation and basalt flows in the upper facies association (UFA) were deposited after 2.71 Ga (Davis, 1996) in a channellized, upper-fan to feeder-channel setting. Detrital zircons from five greywacke samples at different stratigraphic levels include three distinct age populations (ca. 3.0, 2.93 and 2.73 Ga; Davis, 1996; Anderson, 2013), and indicate that the proportion of Mesoarchean detritus increases upsection, consistent with progressive uplift and erosion of the NCT during sedimentation. Abundant tonalite and quartzite clasts in the UFA were likely sourced from NCT basement (3.01–2.99 Ga; Whalen et al., 2003) or were recycled from its cover sequence (2.98–2.92 Ga; Davis, 1994; Percival et al., 2006a; Sasseville et al., 2006). Basaltic flows in the UFA have diverse geochemical signatures (N-MORB–, E-MORB– and arc-like) and are intercalated with coarse-clastic rocks, consistent with an extensional setting (Anderson, 2013). In Ontario, correlative rocks contain tonalite boulders dated at 2703 ±2 Ma and are intruded by 2696 +3/–2 Ma granodiorite plutons (Rogers and McNicoll, unpublished; cited by Lemkow et al., 2006), which constrains the latest stages of marine sedimentation to ca. 2.7 Ga.

San Antonio assemblage

Crossbedded arenite and polymictic conglomerate of the San Antonio assemblage define a series of fluvial-alluvial, fault-bounded, basins along the NCT-Uchi interface (Figure 2). Weber (1971b) interpreted these rocks as continental-delta deposits and noted their similarity to synorogenic molasse sequences. At Rice Lake, these rocks define a 1.2 km thick succession that trends across regional strike and overlies the Bidou and Gem assemblages on an angular unconformity (Stockwell, 1938; Poulsen et al., 1996; Anderson, 2008). Along the south margin of the basin, these rocks overlie tonalite of the Ross River plutonic suite and include clast-supported tonalite-boulder conglomerate that is thought to record deposition by either debris-flow or rock-fall mechanisms (Stockwell, 1938; Weber, 1971b). U-Pb ages from detrital zircons just above the unconformity indicate a maximum depositional age of 2705 ±5 Ma (Percival et al., 2006a). In contrast to the volcanic assemblages, no intrusions are known to cut the San Antonio assemblage and detrital zircon populations include abundant Mesoarchean grains (Percival et al., 2006a; Anderson, 2008), which were likely sourced from the NCT. Local equivalents are found in the Hole River (<2.71 Ga) and Guano Island (<2.73 Ga) assemblages at Lake Winnipeg (Percival et al., 2006a), and the Siderock Lake assemblage (<2.71 Ga) at Siderock Lake (Sasseville et al., 2006), all of which postdate major arc magmatism.

English River basin

The English River basin is an east-trending belt of medium- to high-grade metasedimentary rocks and associated granitoid plutonic rocks that ranges up to 50 km wide and flanks the Uchi subprovince to the south over a strike length of more than 700 km. In Manitoba, this belt ranges from 15 to 40 km wide and is bounded to the north by the Manigotagan fault, a subvertical mylonite that is traced for more than 100 km along strike in Manitoba and is continuous with the Sydney Lake–Lake St. Joseph fault in Ontario (Figure 1). The metasedimentary rocks consist mainly of submarine fan turbidites deposited after cessation of major volcanism in adjacent terranes (Davis, 1996). Detrital zircon ages span a range from 3.1 to 2.7 Ga, indicating that the sediment was derived from the NCT and Uchi subprovince, and was at least locally deposited after 2704 Ma (Corfu et al., 1995; Davis, 1996); regional constraints require sedimentation mainly between 2.72 and 2.7 Ga. These rocks are thought to represent higher grade equivalents to the Edmunds assemblage. Various tectonic scenarios have been postulated for the English River basin, including fore-arc (Breaks, 1991; Hrabi and Cruden, 2006), back-arc (Pan et al., 1998) or syncollisional foreland (Davis, 1998) basins. Hoffman (1989) and Card (1990) interpreted the English River basin as an accretionary prism that incorporated a precursor fore-arc basin adjacent to a volcanic arc represented by the Uchi subprovince.

The sedimentary succession was intruded by voluminous diorite-tonalite-granodiorite plutons at ca. 2.7 Ga, prior to regional deformation and high-T–low-P metamorphism at ca. 2.69 Ga (Corfu et al., 1995), related to terminal collision of the North Caribou and Winnipeg River terranes (Percival et al., 2006a, b). Metamorphic mineral assemblages indicate that peak metamorphism varied from middle greenschist facies in the north to localized granulite facies in the south (e.g., McRitchie and Weber, 1971; Breaks, 1991). Late-tectonic granite plutonism at ca. 2.66 Ga (Turek et al., 1989) and ca. 2.66 Ga titanite ages (Corfu et al., 1995) record the waning stages of thermotectonism at the present level of exposure.

Economic geology

The Rice Lake greenstone belt hosts hundreds of lode gold occurrences and several significant deposits and past-producing mines, mostly clustered around the margins of the Ross River pluton (Figure 2). The largest known deposits are located northwest of the pluton along the Rice Lake mine trend and include the Rice Lake, Hinge and 007 deposits. Other significant deposits (e.g., Central Manitoba, Gunnar and Ogama-Rockland), constitute a lesser trend southeast of the pluton. Several occurrences and deposits are also hosted by Mesoarchean supracrustal and intrusive rocks of the NCT along the north margin of the Wanipigow fault (e.g., Jeep and Poundmaker; Figure 2).

Gold deposits in the belt have been described by numerous previous workers, beginning with the work of Moore (1914) on the original discovery at Rice Lake and culminating with the overview by Poulsen et al. (1996). Individual deposits or occurrences, including their exploration history, were described by Theyer and Yamada (1989), Theyer and Ferreira (1990) and Theyer (1994a, b). Particularly useful descriptions of historical mines were provided by Stockwell (1938), Stockwell and Lord

(1939) and Davies (1953). The Rice Lake deposit is described by Reid (1931), Stockwell (1938, 1940), Bragg (1943), Gibson and Stockwell (1948), Stephenson (1972), Poulsen et al. (1986), Ames (1988), Lau (1988), Poulsen (1989), Ames et al. (1991), Lau and Brisbin (1996) and Rhys (2001).

In the Rice Lake belt, gold mineralization is almost invariably hosted by quartz-carbonate vein systems in discrete brittle-ductile shear zones or complex networks of shear and tensile fractures. Although the hostrocks are variable, the larger deposits occur in gabbro sills (Rice Lake, Central Manitoba), basalt flows (007, Gunnar) and dacitic volcaniclastic rocks (Hinge), within stratified sections of volcaniclastic and epiclastic rocks. In these deposits, significant ore also occurs at the contacts between rock types, in settings that highlight the importance of hostrock chemistry and competency contrasts in localizing ore. Auriferous shear-hosted veins are found in granitoid plutons of the Ross River plutonic suite (e.g., Ogama-Rockland). Shear-hosted quartz-carbonate veins are also found in the San Antonio assemblage, although none are known to contain significant gold values (Stockwell, 1938; Davies, 1953).

In all deposits, the principal controlling structures are ductile and brittle-ductile shear zones that vary from parallel to transverse to the local hostrock anisotropy and, in general, dip steeply northwest or northeast. As noted by Stockwell (1938), veins exhibit a high degree of structural control and are better developed in more competent rocks. Shear-hosted (i.e., fault-fill) veins vary from laminated to massive to brecciated, often within the same vein, and typically pinch and swell along strike and down-dip. Thicker veins, or portions of veins, are often associated with inflection points in the host shear zones, indicating that they were emplaced by hydrothermal infilling of dilational jogs. Most shear zones are associated with arrays of kinematically linked extension and oblique-extension veins that locally intensify into stockwork-breccia systems. Coupled with the structural geometry of the arrays, vein textures indicate synkinematic emplacement under brittle-ductile rheological conditions.

In the well-studied Rice Lake deposit, two major vein sets are preferentially developed in the leucocratic portion of a thick gabbro sill and comprise northeast-trending fault-fill veins and northwest-trending stockwork-breccia veins. The planar fault-fill veins exhibit multiple generations of laminated quartz, planar slip-surfaces, quartz-matrix breccias, stylolitic pressure-solution seams and oblique extension veins, resulting from cyclical stress accumulation, dissolution, fluid-pressure build-up, shear failure, dilation, fluid ingress, hydraulic fracturing and hydrothermal sealing (i.e., fault-valve behaviour; Sibson et al., 1988; Cox, 1995). As described by several authors (e.g., Stockwell, 1938; Lau, 1988; Lau and Brisbin, 1996), the geometry and kinematics of the controlling structures indicate that they accommodated subhorizontal northeast–southwest shortening (present co-ordinates). Similar models were proposed by Davies (1953) and Brommecker (1991, 1996), based on the geometry and kinematics of auriferous shear zones to the west and east of the Ross River pluton, respectively. In some deposits, most notably SG1 east of Rice Lake, the mineralized veins are intensely transposed, indicating they were emplaced prior to the latest increments of ductile deformation.

The auriferous veins are typically composed of quartz, with subordinate carbonate (ankerite>calcite); minor albite, chlorite and sericite; and rare tourmaline and fuchsite. Sulphide minerals comprise mostly pyrite, with minor chalcopyrite and rare sphalerite, galena and telluride minerals (Stephenson, 1972). The pyrite generally accounts for less than 5 vol. % of veins and occurs as scattered crystals and irregular blebs within or along the margins, or is concentrated along slip surfaces or stylolitic pressure-solution seams. Arsenopyrite is associated with gold mineralization only along the margins of the belt, where it typically occurs as finely disseminated needles in the wallrocks. Gold occurs as free grains associated with or as minute inclusions in pyrite (Stephenson, 1972), with a typical grade of 6–10 grams/tonne. The gold ores are characterized by high Au:Ag ratios (>5:1), and very low concentrations of base metals (Cu, Pb, Zn) and pathfinder elements (e.g., As, Bi, B, Sb, W). Fluid-inclusion studies of vein quartz from the Rice Lake deposit (Diamond et al., 1990) indicate low-salinity aqueous-carbonic fluids.

Wallrock alteration varies from negligible to intense and is typically zoned outward, from proximal ankerite-sericite/chlorite-pyrite±albite to distal chlorite-calcite, consistent with significant additions of CO_2 and K, and lesser S and Na (Ames et al., 1991). Alteration overprints the regional greenschist-facies metamorphic mineral assemblages (e.g., Ames et al., 1991). Most veins exhibit evidence of wallrock sulphidization in the form of distinct 'haloes' containing up to 10% coarse pyrite. Thick zones of altered and sulphidized wallrock with negligible vein quartz locally constitute ore in the Rice Lake deposit (Bragg, 1943). Larger deposits are associated with zones of relatively 'clean' ankerite-sericite phyllonite that serve as important guides to ore. The Rice Lake deposit exhibits a significant vertical extent (>2 km) yet displays negligible variation in vein mineralogy, texture and structure.

The above characteristics identify the gold deposits as classical 'greenstone-hosted vein' deposits, also known as 'mesothermal' or 'mother lode'–type deposits (Poulsen et al., 2000). Groves et al. (1998) referred to these types of deposits as 'orogenic' to emphasize their spatial association with accretionary orogens and the synkinematic and synmetamorphic timing of lode emplacement (e.g., Kerrich and Wyman, 1990; Hodgson, 1993; Kerrich and Cassidy, 1994). The preferred genetic model for this deposit type involves fluids generated by thermal equilibration of accreted sedimentary rocks during the clockwise P-T-t evolution of accretionary orogens (e.g., Kerrich and Cassidy, 1994; McCuaig and Kerrich, 1998). The resulting fluids are thought to migrate upward along transcrustal faults into subsidiary brittle-ductile shear and fracture arrays in the middle to upper crust, where gold is deposited in synkinematic and synmetamorphic quartz-carbonate veins due to physical and/or chemical changes in the ore fluid brought about by pressure fluctuations, wallrock sulphidization reactions, phase separation and/or fluid mixing.

Structural geology and deformation history

As described by Anderson (2008, 2011b), structural overprinting and field relationships in the central Rice Lake belt indicate six generations (G_1–G_6) of ductile and brittle-ductile

deformation structures (Table 3). Only the G_3 and G_4 fabrics are pervasive; they record regional deformation under mid-crustal (greenschist-facies) metamorphic conditions. The upper age limit for this deformation is provided by the 2705 Ma maximum depositional age of the San Antonio assemblage (Percival et al., 2006a). Each generation is described briefly below (*after* Anderson, 2008, 2011b). Planar fabrics, linear fabrics and folds are herein denoted by S_x, L_x and F_x, respectively, where 'x' indicates the assigned generation. Shortening directions (e.g., northwest–southeast) are given with respect to present geographical co-ordinates.

The deformation history of the Rice Lake belt involved at least five episodes (D_1–D_5; Table 3; Figure 3), two of which (D_1 and D_2) predated the San Antonio assemblage. As outlined below, the distinction between deformation episode (D_X) and generation of deformation structure (G_Y) is made to emphasize that one episode (D_2) involved regional tilting of strata without fabric development, whereas another episode (D_5) involved multiple increments of progressive deformation during which three generations (G_4–G_6) of fabric were developed (see below).

G_1 structures, D_1 deformation

The earliest fabric in the Rice Lake area is observed in clasts of phyllite in a heterolithic clastic dike near the base of the Gem assemblage. Very fine grained phyllosilicate minerals in these clasts define a penetrative foliation (S_1) that predates entrainment in the dike. In some clasts, quartz (±feldspar) exhibits undulose extinction, lattice-preferred orientation, serrated grain margins and a weak shape-preferred orientation, which are indicative of dynamic recrystallization under greenschist-facies metamorphic conditions. The unimodal (ca. 2.72 Ga; Anderson, 2008) zircon population in the clastic dike and the delicate shapes of the phyllite clasts indicate they were proximally sourced. As described by Anderson (2008), map patterns and facies associations east of Rice Lake indicate a highly discordant fault at the contact between the Bidou and Gem assemblages (Figure 4). The fault is marked by hypabyssal intrusions, hydrothermal alteration and exhalative sulphide mineralization, and bounds a relatively restricted marine basin in its hangingwall. It is thus interpreted to represent a synvolcanic subsidence structure related to extension and incipient rifting of the Bidou volcanic arc. Exhumed rocks in the footwall of this fault are considered to be the most likely source of the phyllite clasts in the clastic dikes. The associated fabric is assigned to the first (G_1) generation of structures and the synvolcanic faulting to the D_1 episode of deformation (Figure 3).

D_2 deformation

Map patterns of the San Antonio and Gem assemblages in the Horseshoe Lake area (Figure 4) indicate two temporally distinct deformation episodes (D_2 and D_3). The D_2 episode is not associated with any meso- or microscale deformation structures, but is indicated by the angular unconformity at the base of the San Antonio assemblage. In particular, the near-orthogonal orientation of the unconformity with respect to primary stratification in the Bidou and Gem assemblages indicates that these rocks were tilted into a near-vertical orientation and partially exhumed prior to deposition of the San Antonio assemblage (Figure 3). This tilting is ascribed to the D_2 deformation episode, which may mark the onset of accretion along the NCT margin.

Table 3: Summary of ductile and ductile-brittle deformation in the Rice Lake area.

Generation	Shortening direction[1]	Mesoscopic structure	Macroscopic structure	Deformation episode and inferred tectonic significance
G_1	?	Penetrative to finely-spaced S_1 foliation in phyllite fragments in clastic dikes	Synvolcanic subsidence structures (normal faults)	D_1 : arc-extension; initiation of back-arc spreading?
	?	None observed	Early tilting of the Bidou and Gem assemblages	D_2 : arc-accretion and back-arc basin inversion?
G_2	?	Local, weak, layer-parallel S_2 foliation in San Antonio assemblage	Thrust fault at top of San Antonio assemblage	D_3 : basin inversion; continued accretion and/or initial crustal thickening
G_3	NE-SW	Regional WNW-trending S_3; steep L_3 stretching lineation; upright F_3 folds; conjugate brittle-ductile shear zones	Macroscopic folds (BLA, HLA, GCS); sinistral-reverse shear in WF	D_4 : collisional tectonics; crustal thickening and sinistral transpression; Au mineralization
G_4	NW-SE	Regional, WSW-trending, S_4 crenulation cleavage; F_4 Z-folds		Early-D_5 : onset of terminal collision; dextral transcurrent shear
G_5	NW-SE	Regional S_5 shear-band cleavage; mylonitic S_5 in NW-trending high-strain zones; shallow L_5 lineation; F_5 Z-folds	Main-stage dextral shear in WF and subsidiary structures; coaxial flattening in NCSZ	Main-D_5 : terminal collision; dextral transcurrent shear
G_6	E-W	Open, north-trending F_6 crenulations	Open fold in the Bidou and Gem assemblages at Rice Lake	Late-D_5 : butress effect on Ross River pluton; continued dextral transcurrent shear

Abbreviations: BLA, Beresford Lake anticline; GCS, Gold Creek syncline; HLA, Horseshoe Lake anticline; NCSZ, Normandy Creek shear zone; WF, Wanipigow fault

[1] inferred trend of maximum principal far-field stress axis; based on present orientation of associated fabric elements

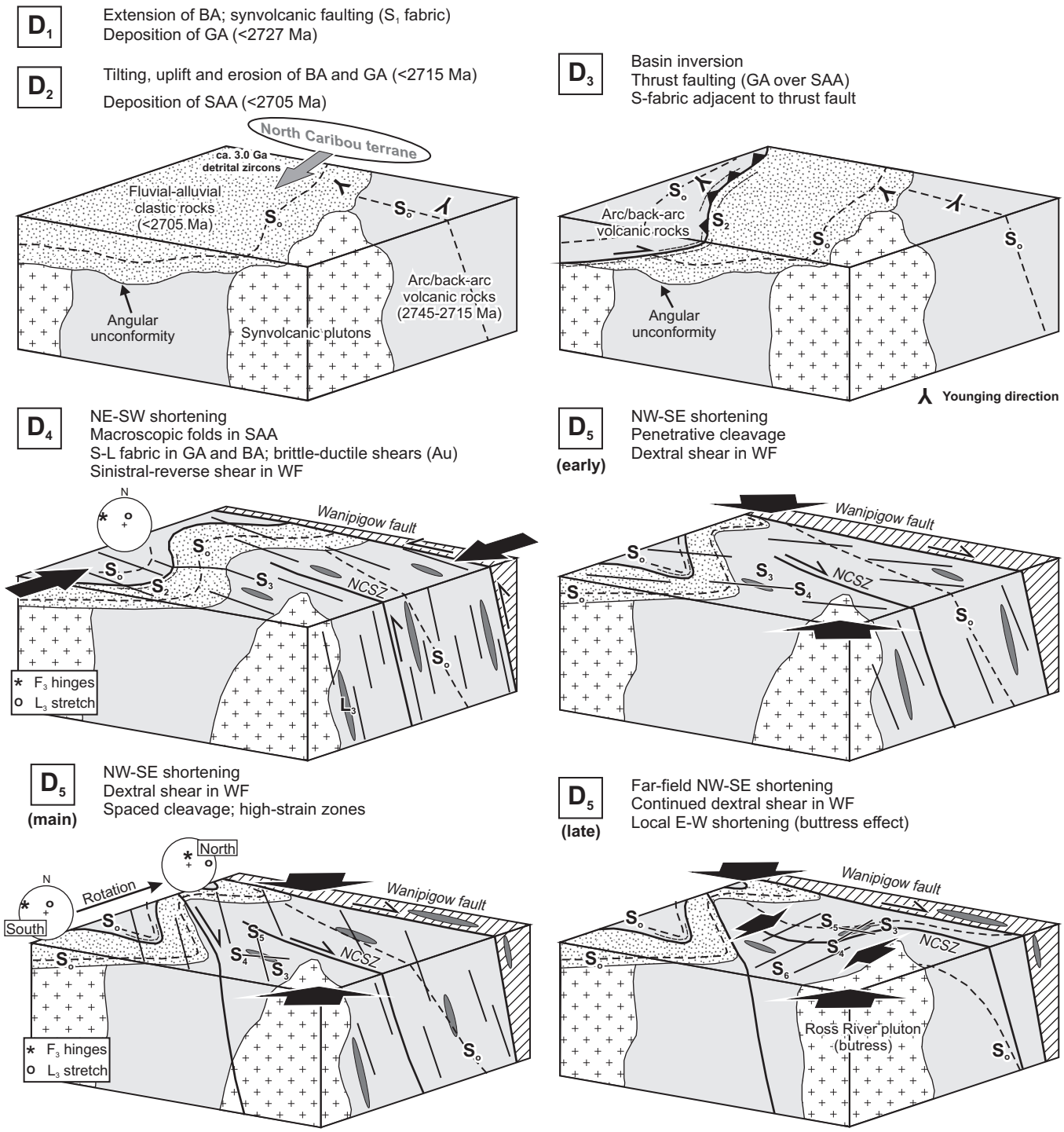

Figure 3: *Schematic block diagrams illustrating the structural evolution of the Rice Lake area. Not depicted is the D_1 deformation, which is interpreted to be associated with extensional faulting in the Bidou assemblage prior to D_2 tilting. Abbreviations: BA, Bidou assemblage; GA, Gem assemblage; NCSZ, Normandy Creek Shear Zone; SAA, San Antonio assemblage; WF, Wanipigow fault.*

G_2 structures, D_3 deformation

Structures of the second generation (G_2) are best-developed along and within the western contact of the San Antonio assemblage. They consist of a penetrative and continuous shape fabric (S_2), defined by fine-grained sericite and elongate quartz grains, which roughly parallels bedding and is folded around the hinges of F_3 folds. At the contact, the west-younging San Antonio assemblage is structurally overlain to the west by intermediate volcaniclastic and epiclastic rocks that are intruded by gabbro sills and quartz-feldspar porphyry dikes, and are correlated with the Gem assemblage on the basis of comparable rock types and geochemistry. Both assemblages young to the west and are folded by the F_3 Horseshoe Lake anticline (Figure 4). The resulting older-over-younger map pattern (Figure 3) is interpreted to result from thrust-faulting and tectonic inversion of the San Antonio basin during the D_3 episode of regional deformation, which may record the onset of collisional orogenesis along the NCT margin.

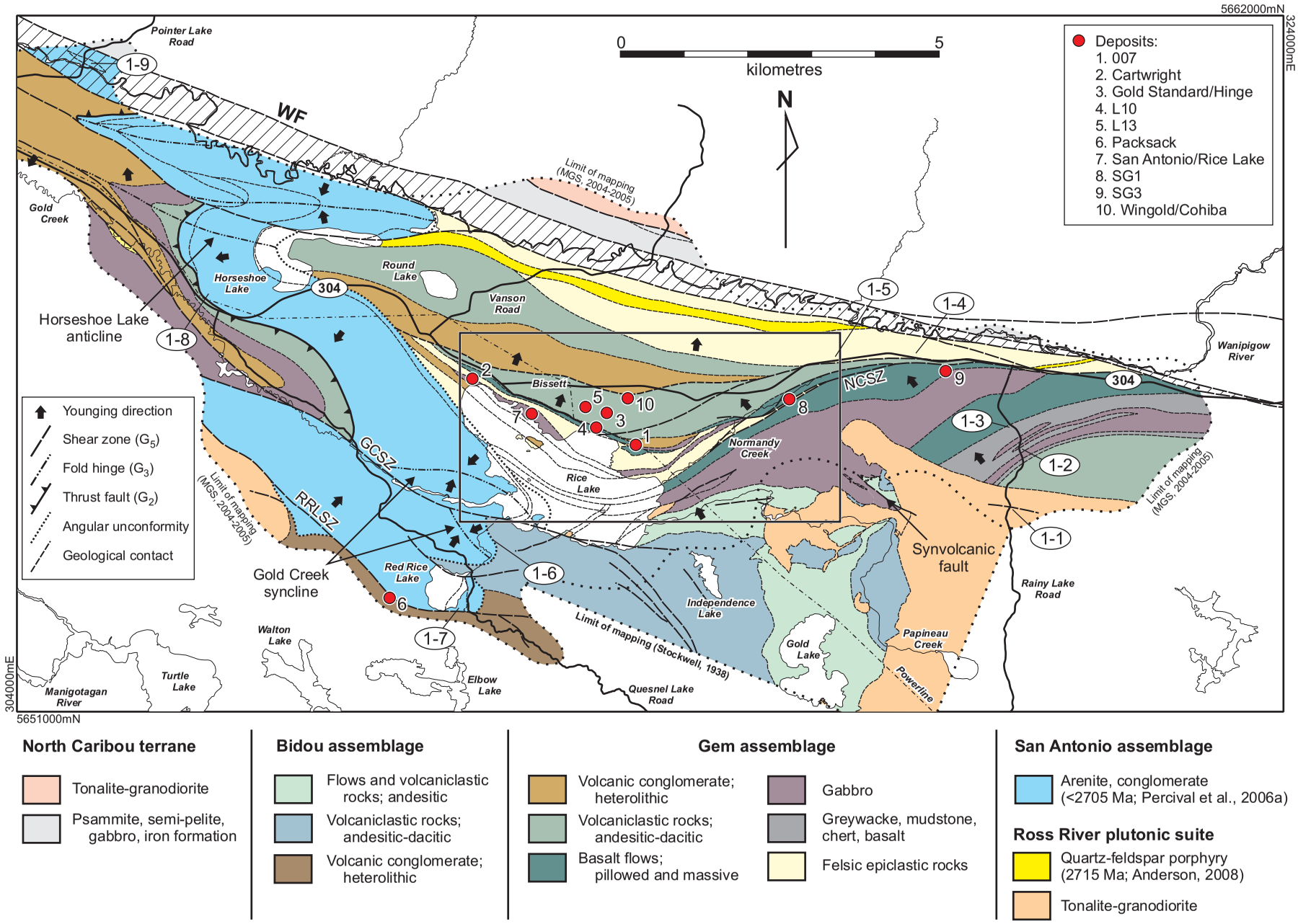

Figure 4: *Geology of the Rice Lake area, after Map GR2008-1-1 (Anderson, 2008), showing the locations of major gold deposits and the stops for Day 1of the field trip (1-1 to 1-9). Abbreviations: GCSZ, Gold Creek Shear Zone; NCSZ, Normandy Creek Shear Zone; RRLSZ, Red Rice Lake Shear Zone; WF, Wanipigow fault (indicated by hachured pattern).*

G_3 structures, D_4 deformation

Structures of the third generation (G_3) are pervasive in the Rice Lake area and formed at mid-crustal depths in response to regional compression. Flattened and stretched primary features define a pervasive planar-linear (S-L) shape fabric in the Bidou and Gem assemblages. The shape fabric is also defined by a continuous foliation (chlorite-actinolite±sericite) that generally trends west-northwest and dips steeply to moderately north. The L_3 stretching lineation plunges moderately to the northeast in the plane of the S_3 fabric. The axial ratios of deformed primary features are typically in the range 2–5:1 (Y:Z, X:Z and X:Y); finite strain determinations performed by Lau and Brisbin (1996) indicate strain ellipsoids that vary from constrictional to flattening type. The G_3 shape fabric is generally symmetric. At Rice Lake, the S_3 fabric is oriented at a shallow counterclockwise angle to bedding (which thus faces east on S_3) and mesoscopic examples of F_3 folds are very rare. From north to south across the Rice Lake area, the L_3 lineation exhibits a systematic change in trend and plunge, from steeply or moderately northeast plunging in the south to shallowly east plunging in the north, which is interpreted to result from reorientation during transcurrent shear along the Wanipigow fault (Figure 5; Poulsen et al., 1986).

West of Rice Lake, the S_3 fabric passes continuously into the San Antonio assemblage, where it is prominently defined by flattened pebbles; the L_3 fabric is generally not well developed. The S_3 fabric is axial planar to the Horseshoe Lake anticline (HLA) and Gold Creek syncline (GCS), which are the most prominent closures in a macroscopic train of F_3 folds that trends across the belt (Figure 4). These folds are tight, steeply inclined, and overturned to the southwest. The GCS plunges shallowly to the northwest, whereas the HLA plunges steeply to the north. On the shared limb of the HLA and GCS south of Horseshoe Lake, the S_3 fabric is refracted toward the west-southwest (Figure 5). The F_3 fold train terminates at the base of the San Antonio assemblage and does not extend into the underlying Bidou and Gem assemblages (Figure 4), indicating that the axis of maximum shortening during folding was oriented subparallel to the unconformity but suborthogonal to strata in the underlying volcanic units. Hence, the clastic rocks deformed by buckling and folding, with some flattening, whereas the volcanic rocks experienced flattening and subvertical stretching without buckling.

In general, minor fold hinges and bedding-cleavage (S_0-S_3) intersection lineations associated with the GCS plunge shallowly northwest or southeast, whereas those in the HLA plunge

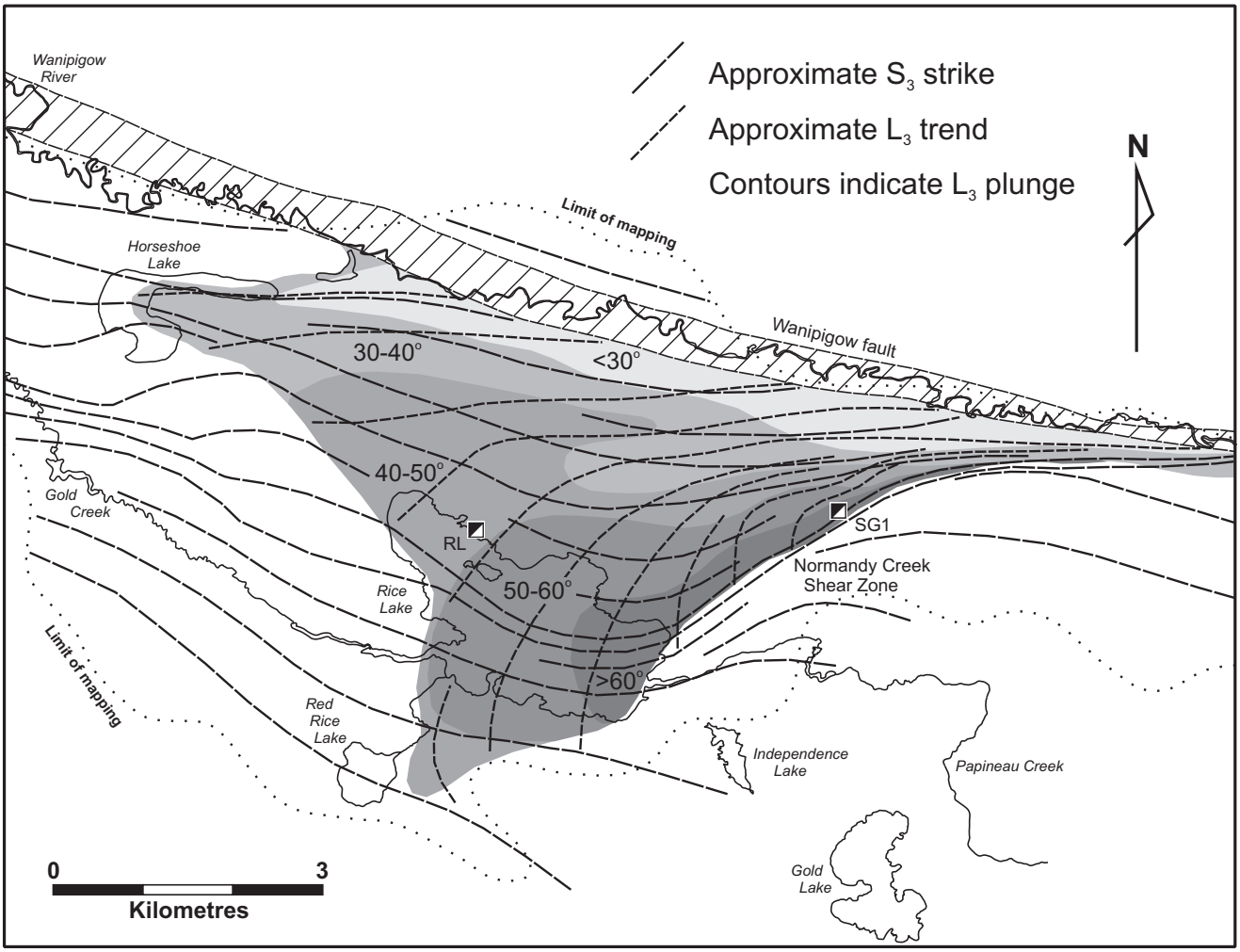

Figure 5: *Schematic map showing the trends of the S_3 and L_3 fabrics (dashed lines) and the plunge of the L_3 lineation (contours) in the Rice Lake area. The systematic change in trend and plunge of the L_3 lineation along the margin of the Wanipigow fault was originally described by Poulsen et al. (1986). Abbreviations: RL, Rice Lake mine (A-shaft); SG1, SG1 mine (portal).*

more steeply. In the footwall of the San Antonio assemblage, this change in F_3 plunge is mimicked by the systematic change, from south to north, in the trend and plunge of the L_3 lineation, which maintains a near-orthogonal angular relationship with the macroscopic hinge in the adjacent segment of the F_3 fold train. Towards the north, these structures appear to have been reoriented, in a sympathetic manner, in response to transcurrent shear along the south margin of the Wanipigow fault, as suggested by Poulsen et al. (1986).

As illustrated in Figure 3, the G_3 deformation was strongly partitioned at Rice Lake into three distinct structural domains: 1) sinistral-oblique noncoaxial shearing within the Wanipigow fault, 2) upright subhorizontal folding in rocks structurally above the angular unconformity at the base of the San Antonio assemblage, and 3) bulk flattening and subvertical stretching in rocks below the unconformity. The bulk geometry and kinematics of the G_3 structures are compatible with major northeast–southwest shortening of the belt in a regional regime of sinistral transpression. As described in detail in a later section of this guidebook dealing specifically with the structural geology of the Rice Lake mine trend, this transpressive deformation was coeval with the auriferous quartz-carbonate vein systems at Rice Lake (Anderson, 2011a, b), and a similar kinematic framework was proposed for vein systems east of the Ross River pluton (Brommecker, 1991, 1996). This shortening is assigned to the D_4 episode of regional deformation and likely coincided with main-stage collisional orogenesis along the NCT margin.

G_4 structures, D_5 deformation (early)

Throughout the Rice Lake area, the S_3 fabric is overprinted by a finely spaced crenulation cleavage assigned to the G_4 generation. The S_4 cleavage trends west or southwest, dips steeply northwest and typically strikes 20–30° counter-clockwise to the S_3 fabric. It is often best preserved as a finely spaced crenulation cleavage within flattened clasts defining the regional G_3 fabric. The S_4 cleavage transects meso- and macroscopic F_3 folds, and intersects S_3 to form a crenulation lineation that plunges at moderate angles to the northeast, subparallel to the L_3 stretching lineation. The S_4 fabric is axial planar to rare, open to tight, Z-asymmetric folds that plunge moderately north. The G_4 structures overprint alteration and auriferous vein systems in the Rice Lake mine trend and appear to have accommodated weak northwest–southeast shortening, during the transition to a different kinematic frame. This deformation is assigned to an early increment of the D_5 episode of regional deformation, which marked the onset of late-orogenic dextral transcurrent shear (Figure 3; early D_5).

G_5 structures, D_5 deformation (main)

Fifth-generation (G_5) ductile deformation structures are pervasive in the Rice Lake area but are only penetrative in discrete high-strain zones, including the Gold Creek, Normandy Creek and Red Rice Lake shear zones (Figure 4). These fabrics are also penetrative and pervasive within the Wanipigow and Manigotagan faults, and their subsidiary structures, along both margins of the Rice Lake belt (Percival et al., 2006a; Sasseville et al., 2006; Anderson, 2008). The G_5 high-strain zones are characterized by penetrative mylonitic foliations (S_5) defined by foliated sericite, chlorite and domains of dynamically recrystallized quartz and feldspar. These zones are subvertical and trend west-northwest to north-northwest, except where overprinted by later structures (see below). Quartz-filled pressure fringes, stretched clasts, quartz ribbons or ridge-in-groove striations define a shallow plunging L_5 lineation. Packets of open to tight, upright, asymmetrical (Z) F_5 folds are a characteristic feature of G_5 high-strain zones and plunge variably, from shallowly east to steeply north. On the margins of the G_5 high-strain zones, the S_5 fabric is locally manifested as a spaced shear-band cleavage that trends northwest or north-northwest and dips subvertically. Dextral kinematic indicators are well developed on horizontal outcrop surfaces and typically include S-C fabrics, σ-porphyroclast systems, shear bands and asymmetric boudins. The geometry and kinematics of the G_5 structures indicate that they accommodated strongly partitioned north-northwest–south-southeast shortening during the progressive D_5 deformation episode (Figure 3).

G_6 structures, D_5 deformation (late)

The latest generation of ductile deformation (G_6) is associated with an open upright syncline that trends north through Rice Lake (Figure 4). A weak crenulation cleavage (S_6) in the hinge of this fold is locally associated with upright symmetric folds that plunge at moderate angles to the northeast. The S_6 cleavage generally dips steeply to the east-southeast and is best developed along the south shoreline of Rice Lake. The G_6 structures accommodated east-west shortening, perhaps in response to a buttressing effect along the northwestern margin of the Ross River pluton, and resulting strain perturbation in the hangingwall of the Normandy Creek shear zone, during the late-stage of the D_5 deformation episode (Figure 3; late D_5).

Tectonic interpretation

As outlined above, the Rice Lake greenstone belt and adjacent portions of neighbouring domains record approximately 360 million years of Archean crustal evolution in two major phases of crustal growth, separated by nearly 100 million years of apparent quiescence (Table 4, 5). An accretionary tectonic process is strongly implicated by the progressive younging of supracrustal assemblages from north to south across the region (Figure 6). A comparable history is apparent in greenstone belts over at least 500 km of strike length (e.g., Stott and Corfu, 1991; Percival et al., 2006b), indicating that this process operated at a regional scale.

The older phase of crustal growth (ca. 3.01–2.85 Ga) is recorded by volcano-plutonic rocks of the North Caribou terrane (NCT) and by detrital zircons of the same age in much younger (ca. 2.7 Ga) sedimentary rocks in adjacent domains (Table 4, 5). Crustal growth during this phase was likely characterized by complex interactions between arc and mantle-plume magmatism (e.g., Hollings et al., 1999; Whalen et al., 2003), with coeval deposition of supracrustal assemblages in mostly continental settings. This time interval is thought to include the initial development and stabilization of NCT continental crust, represented by the ca. 3.01–2.99 Ga English Lake and East Shore intrusive complexes, and subsequent plume-influenced uplift, extension and rifting of this crust to form a south-facing

Table 4: Summary of U-Pb geochronological data from the south margin of the North Caribou terrane.

Sample number	Rock type (subunit)	Location	Ziron Age		Type	Reference
NORTH CARIBOU TERRANE						
Wanipigow River plutonic complex (continental successor arc)						
C66	Granite	Job L.	2703	±2	I	Corfu and Stone, 1998
C65	Biotite tonalite	Bloodvein R.	2705	±4	I	Corfu and Stone, 1998
GSC 72-39	Augen granodiorite	L. Winnipeg	2715	±10	I	Krogh et al., 1974
	Granodiorite	Eagle L.	2720	±5	I	McNicoll and Rogers, unpub.
C67	Granodiorite	Olive L.	2722	±2	I	Corfu and Stone, 1998
96-03-1116	Biotite granite	Garner L.	2726	±1	I	Anderson, 2013
M705	Tonalite	Wallace L.	2731	±10	I	Turek et al., 1989
C63	Biotite tonalite	Douglas L.	2734	±2	I	Corfu and Stone, 1998
C64	Hornblende tonalite	Donald L.	2736	±3	I	Corfu and Stone, 1998
GSC 72-46	Tonalite	Obukowin L.	2737	±10	I	Krogh et al., 1974
96-03-1261	QFP dike	Garner L.	2747	±2	I	Anderson, 2013
PBA00-2859	Granite dike	English L.	2749	±2	I	Percival et al., 2006a
Garner assemblage (rifted continental arc)						
96-02-1050	Dacite	Garner L.	2851	±1	I	Anderson, 2013
DD93-6	Pegmatitic gabbro	Garner L.	2870	±1	I	Davis, 1994
96-02-1067	Pegmatitic tonalite	Garner L.	2870	±1	I	Anderson, 2013
DD93-9	Arkose	Garner L.	2871	±2	D	Davis, 1994
Wanipigow River plutonic complex (continental arc; intrusive into basement and Wallace assemblage)						
M708	Granodiorite	Jeep mine	2880	±9	I	Turek et al., 1989
GSC 72-4	Orthogneiss	L. Winnipeg	2900	±10	I	Krogh et al., 1974
CS98-238	Tonalite dike	Wallace L.	2921	±1	I	Sasseville et al., 2006
DD93-15	Tonalite dike	Wallace L.	2921	±3	I	Davis, 1994
CS98-209-2	Dacite dike	Wallace L.	2922	±2	I	Sasseville et al., 2006
M708	Granodiorite	Jeep mine	2923	±16	I	Turek et al., 1989
PBA00-2844	Biotite granodiorite	Rice R.	2941	± 2	I	Percival et al., 2006a
PBA00-2621B	Rhyolite porpyrhy sill	L. Winnipeg	2978	±3	I	Percival et al., 2006a
Wallace assemblage (platform-rift sequence)						
PBA99-2026	Paragneiss (Little Beaver)	Wanipigow R.	<2975		D	McNicoll and Percival, unpub.
PBA00-2581B	Quarzite (Lewis-Storey)	L. Winnipeg	<2991		D	Percival et al., 2006a
DD93-14	Quartz arenite (Conley)	Wallace L.	<2999		D	Davis, 1994
02-89-09	Tonalite boulder (Conley)	Wallace L.	3010	±13	I	Turek and Weber, 1991
East Shore and English Lake plutonic complexes (basement)						
PBA99-2067	Gabbro	English L.	2992	±2	I	Whalen et al., 2003
PBA99-2153	Mafic gneiss	English L.	2997	±4	M	Percival et al., 2006a
PBA00-2068	Anorthosite	English L.	2998	±3	I	Whalen et al., 2003
PBA00-2621A	Tonalite	L. Winnipeg	2999	±2	I	Whalen et al., 2003
GSC 74-40	Tonalite	L. Winnipeg	2999	±10	I	Krogh et al., 1974
WXP99-168	Tonalite gneiss	English L.	2999	±1	I	Whalen et al., 2003
MA-27	Tonalite dike	English L.	3003	±3	I	Turek and Weber, 1994
PBA99-2048	Tonalite dike	English L.	3006	±2	I	Whalen et al., 2003
WXP99-130	Tonalite	Poundmaker mine	3007	±1	I	Whalen et al., 2003

D, detrital (youngest population mode or single-grain analysis); I, igneous (crystallization age); M, metamorphic

Table 5: Summary of U-Pb geochronological data from the Rice Lake belt and English River basin.

Sample number	Rock type (subunit)	Location	Ziron Age		Type	Reference
Syn- to post-orogenic intrusions (mostly in English River basin)						
SL-94-6	Leucogranite	Separation Rapids	2646	±2	I	Larbi et al., 1999
M710	Granite	Black L.	2663	±7	I	Turek et al., 1989
96-02-1056	Diorite	Garner L.	2665	±16	I	Anderson, unpub.
C-88-34	Granodiorite	Fletcher L.	2684	±3	M	Corfu et al., 1995
GSC 72-38	Orthogneiss	Manigotagan R.	2690	±10	M	Krogh et al., 1974
	Granodiorite	Wingiskus L.	2696	±3	I	McNicoll and Rogers, unpub.
C-88-34	Granodiorite	Fletcher L.	2698	±2	I	Corfu et al., 1995
UCHI SUBPROVINCE						
Edmunds assemblage (submarine fan; north margin of regional intra-arc English River basin)						
	Granodiorite boulder (UFA)	Eagle L.	<2703		D	McNicoll and Rogers, unpub.
DD93-1	Greywacke (UFA)	Moose R.	2705	±2	D	Davis, 1994
DD93-12	Greywacke (LFA)	Gem L.	2712	±2	D	Davis, 1994
DD93-3	Greywacke (LFA)	Beresford L.	2725	±2	D	Davis, 1994
96-06-2059	Greywacke (UFA)	Lily L.	<2732		D	Anderson, 2013
96-02-1004	Greywacke (LFA)	Gem L.	<2738		D	Anderson, 2013
San Antonio assemblage (fault-bounded fluvial-alluvial basins)						
DD93-13	Arenite (San Antonio)	Red Rice L.	<2705		D	Percival et al., 2006a
PBA99-2143	Arkose (Hole River)	L. Winnipeg	<2708		D	Percival et al., 2006a
CS98-107-2	Greywacke (Siderock)	Siderock L.	<2709		D	Sasseville et al., 2006
PBA99-2128	Arkose (Guano Island)	L. Winnipeg	<2728		D	Percival et al., 2006a
96-05-1622-1	Greywacke (San Antonio)	Wanipigow R.	<2732		D	Anderson, 2008
Ross River plutonic suite (oceanic arc and intra-arc rift)						
96-04-1384	QFP sill/dike	Round L.	2715	±2	I	Anderson, 2008
GSC 72-1	Quartz diorite	Deer I.	2715	±10	I	Krogh et al., 1974
96-07-2287	Granodiorite	Manigotagan R.	2717	±2	I	Anderson, unpub.
96-03-RRP	Biotite granodiorite	Rainy L.	2724	±1	I	Anderson, 2008
96-07-2150	Quartz porphyry dike	Lily L.	2727	±1	I	Anderson, 2013
M702	Tonalite	Ogama mine	2728	±8	I	Turek et al., 1989
M711	Feldspar porphyry	Gunnar mine	2731	±13	I	Turek et al., 1989
02-89-21	QFP dike	Beresford L.	2733	±6	I	Turek and Weber, 1991
Gem assemblage (intra-arc rift)						
	Felsic tuff (Anderson)	Bee L.	2718	±3	I	McNicoll and Rogers, unpub.
DD93-11	Rhyolite breccia	Gem L.	2722	±2	I	Davis, 1994
07-00-272-2-1	Basalt (Grey Point)	Black I.	2723	±6	I	Percival et al., 2006a
96-04-1450-2	Volcanic sandstone (Townsite)	Rice L.	<2723		D	Anderson, 2008
96-05-MRF	Volcanic sandstone	Gem L.	<2724		D	Anderson, 2013
96-03-1285	Conglomerate (Rainy Lake Rd.)	Rainy Lake Rd.	<2727		D	Anderson, 2008
96-06-1845	Dacitic lapilli-tuff	Gem L.	2727	±2	I	Anderson, 2013
M716	Volcanic sandstone (Townsite)	Rice L.	2729	±3	I	Turek et al., 1989
Bidou assemblage (oceanic back-arc - arc complex)						
M703	Dacite (The Narrows)	Stormy L.	2731	±3	I	Turek et al., 1989
EE-74-BLI-4A	Rhyolite (Black Island)	Black I.	2732	±10	I	Ermanovics and Wanless, 1983
96-05-SL	Greywacke (Stormy Lake)	Beresford L.	2734	±2	D	Anderson, 2013
96-05-SLF	Greywacke (Stovel Lake)	Tinney L.	<2736		D	Anderson, 2013
96-05-SLF	Greywacke (Stovel Lake)	Tinney L.	2745	±5	D	Anderson, 2013

D, detrital (youngest population mode or single-grain analysis); I, igneous (crystallization age);
LFA, lower facies association; M, metamorphic; UFA, upper facies association

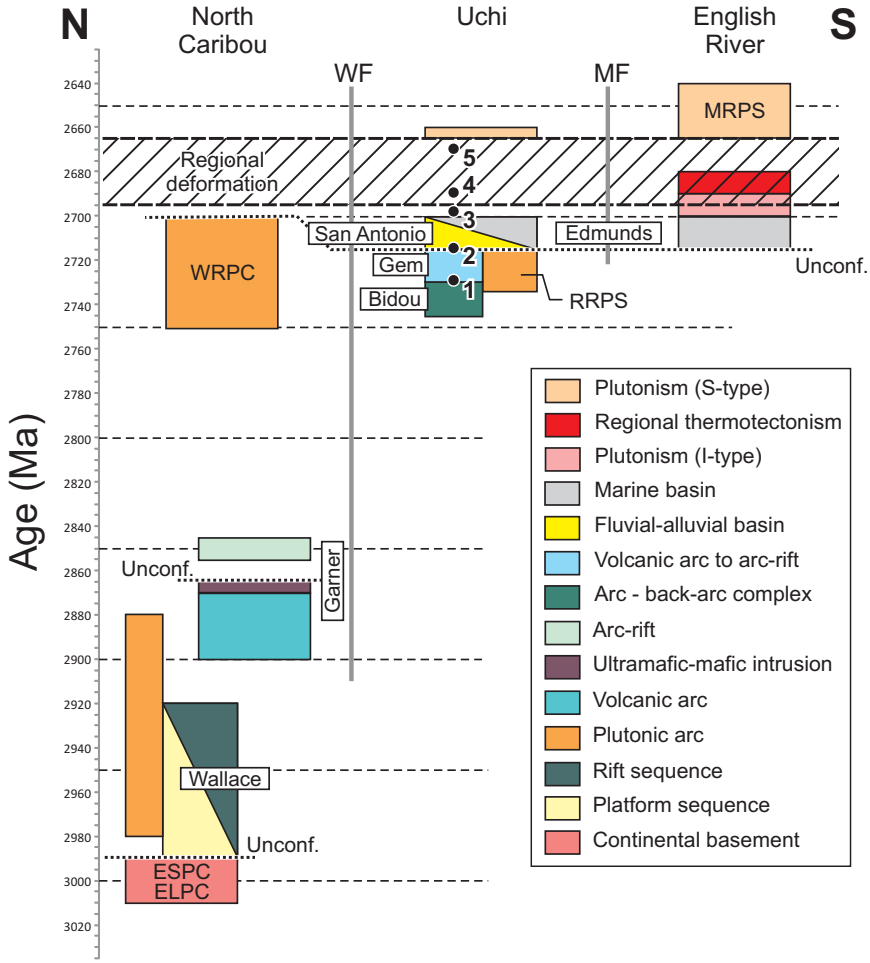

Figure 6: *Time-space correlation diagram illustrating the ca. 360 m.y. tectonic evolution at the south margin of the North Caribou terrane in Manitoba (see Tables 4 and 5). Numbered dots indicate the approximate time of deformation episodes in the Rice Lake area (see Figure 3, Table 3). ELPC, English Lake plutonic complex; ESPC, East Shore plutonic complex; Manigotagan River plutonic suite; RRPS, Ross River plutonic suite; WRPC, Wanipigow River plutonic complex.*

(present configuration) continental margin and long-lived oceanic basin, represented by platform-rift sequences of the ca. 2.98–2.92 Ga Wallace assemblage (Davis, 1994; Percival et al., 2006a; Sasseville et al., 2006). The ca. 2.89–2.85 Ga Garner assemblage is thought to record the subsequent construction and plume-influenced uplift, extension and rifting of a volcanic arc situated on, or marginal to, the NCT (Figure 7; Anderson, 2013). Although the age of this arc remains poorly constrained, it was intruded by the mafic–ultramafic Garner Lake intrusive complex at ca. 2.87 Ga (Davis, 1994), indicating that it had achieved significant thickness by that time.

The younger phase of crustal growth (ca. 2.75–2.65 Ga) is well-represented by granitoid rocks across all domains (Table 4, 5) and is interpreted to reflect a dynamic convergent margin setting associated with renewed northward subduction beneath the NCT (Stott and Corfu, 1991) following an apparent magmatic hiatus of close to 100 million years. Accretion, driven by northward subduction of oceanic crust, is thought to have terminated at ca. 2.71 Ga and was closely followed by collisional orogenesis related to convergence and final amalgamation of the North Caribou and Winnipeg River continental terranes (e.g., Stott and Corfu, 1991; Corfu et al., 1995; Sanborn-Barrie et al., 2001; Percival et al., 2006a, b). This phase of crustal growth appears to have involved a systematic progression from early continental-arc and oceanic arc–back-arc magmatism, to synorogenic sedimentation, regional thermotectonism, and late-orogenic emplacement of peraluminous granite plutons (Figure 7b–e; Stott and Corfu, 1991; Corfu et al., 1995; Poulsen et al., 1996; Corfu and Stone, 1998; Bailes et al., 2003; Percival et al., 2006a; Anderson, 2008).

Continental-arc magmatism is recorded by granitoid plutons of the Wanipigow River plutonic complex (ca. 2.73–2.72 Ga; Corfu and Stone, 1998) and contemporaneous volcanic rocks of the Confederation assemblage (ca. 2.75–2.73 Ga) in Ontario, which are attributed to construction and localized rifting of a continental arc on the south margin of the NCT (Stott and Corfu, 1991; Hollings and Kerrich, 2000; Sanborn-Barrie et al., 2001; Percival et al., 2006b). Bimodal volcanic rocks of the Bidou assemblage (ca. 2.75–2.73 Ga), interpreted to represent an arc–back-arc complex, underwent extension prior to deposition of the chemically-diverse Gem assemblage (ca. 2.73–2.72 Ga) in shallow subaqueous rift basins (Figure 7b, c; Bailes and Percival, 2005; Anderson, 2013). Juvenile isotopic signatures and the absence of older (>2.75 Ga) inherited or detrital zircons are compatible with an intra-oceanic setting isolated from the NCT margin. Initiation of this arc complex was attributed to

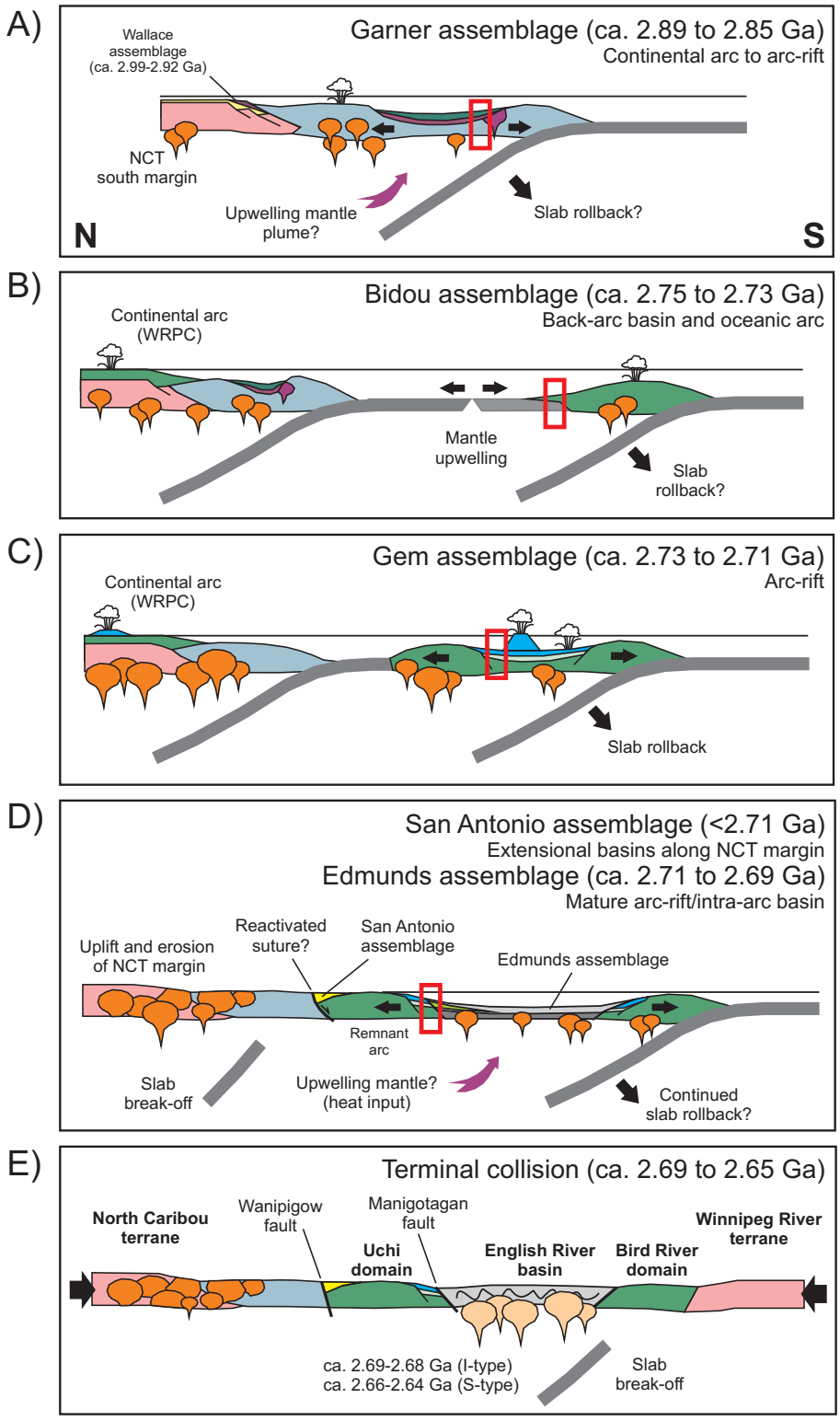

Figure 7: *Schematic sections illustrating a postulated tectonic evolution for the south margin of the North Caribou terrane (NCT) through 250 m.y. of geological time. Red rectangles indicate the inferred geodynamic settings of the type localities of supracrustal assemblages:* ***a)*** *ca. 2.89–2.85 Ga deposition of the Garner assemblage in a continental-arc to arc-rift setting;* ***b)*** *ca. 2.75–2.73 Ga deposition of the Bidou assemblage in an oceanic arc–back-arc complex outboard of the NCT margin, with coeval continental-arc magmatism inboard of the margin;* ***c)*** *ca. 2.73–2.71 Ga deposition of the Gem assemblage in an intra-arc rift setting, with continued continental-arc magmatism inboard of the NCT margin;* ***d)*** *deposition of the ca. 2.71–2.69 Ga Edmunds assemblage in a mature arc-rift basin after cessation of major arc magmatism and coeval with synorogenic fluvial-alluvial sedimentation (San Antonio assemblage) in fault-bounded, probably extensional basins along the NCT margin;* ***e)*** *ca. 2.69–2.65 Ga terminal collision of the North Caribou and Winnipeg River terranes, resulting in tectonic burial, regional thermotectonism, crustal-scale faulting (with an evolution from early sinistral to late dextral kinematics) and voluminous granitoid magmatism. Abbreviation: WRPC, Wanipigow River plutonic complex. See text for discussion.*

subduction zone step-back by Percival et al. (2006a), possibly in response to early accretion events suggested by evidence of ca. 2.74–2.73 Ga deformation in the Red Lake belt (Sanborn-Barrie et al., 2001). At Red Lake, penetrative regional deformation and main-stage gold mineralization are constrained between ca. 2.72 and 2.71 Ga (Dubé et al., 2004), indicating that orogenic activity was locally ongoing in the late stages of arc volcanism.

Cessation of major arc volcanism in the Uchi domain was followed in rapid succession by renewed extension, erosional denudation of the NCT, coarse-clastic sedimentation, and regional thermotectonism related to terminal collision with the Winnipeg River terrane. Coarse-clastic sedimentary rocks of the San Antonio assemblage were deposited in areally-restricted basins at the NCT-Uchi interface (Figure 7d), suggesting an important tectonic control on basin subsidence, probably by reactivation of early accretionary faults or sutures. Considered in the context of coeval uplift of the NCT margin and subsidence of the orogen-scale English River basin, extensional (as opposed to strike-slip; e.g., Corcoran and Mueller, 2007) fault reactivation is considered the most likely scenario, and thus implicates a synorogenic phase of crustal extension, as has been suggested for 'Timiskaming-type' sedimentary basins in the Abitibi greenstone belt of Ontario (Bleeker, 2012).

Submarine turbiditic sedimentary rocks and basaltic flows of the Edmunds assemblage at the north margin of the English River basin contain three distinct age populations of detrital zircons (ca. 3.0, 2.93 and 2.73 Ga). The proportion of Mesoarchean detritus increases up-section, consistent with progressive uplift and erosion of the NCT. Coeval eruption of NMORB-, EMORB- and arc-like basaltic lavas suggests an analogy to complex rift settings in modern arcs or back-arc basins, and a geodynamic evolution from incipient arc-rift (Gem assemblage) to a more mature intra-arc basin (Figure 7d). The short time interval between sedimentation (<2.71 Ga) and the orogenic peak (ca. 2.69 Ga) in the adjacent and partly equivalent English River basin requires some combination of rapid crustal thickening, perhaps by internal imbrication (Corfu et al., 1995) or thick-skinned overthrusting by the NCT margin (Percival et al., 2006a), coupled with accelerated heat input from upwelling mantle, possibly in response to slab break-off (Corfu et al., 1995) or crustal extension (Pan et al., 1998).

Regional orogenesis, attributed to terminal collision of the North Caribou and Winnipeg River terranes (Figure 7e), is manifest in the Rice Lake belt as multiple generations of ductile and brittle ductile deformation structures that formed under greenschist to (local) amphibolite-facies metamorphic conditions. Regional G_3 structures record northeast–southwest shortening, bulk sinistral transpression and coeval development of orogenic gold deposits. Regional constraints indicate that transpressive deformation was probably also coeval with major orogenesis in the English River basin, which also involved penetrative ductile deformation, high-T–low-P metamorphism and the development of crustal-scale sinistral-oblique shear zones (ca. 2.69–2.68 Ga; Breaks, 1991; Corfu et al., 1995; Bethune et al., 2006). Regional G_4-G_5 structures record a distinctly different kinematic frame associated with northwest–southeast shortening of the Rice Lake belt under conditions of waning temperature and pressure. These fabrics are penetrative and pervasive within the Wanipigow and Manigotagan faults, and their subsidiary structures, along both margins of the Rice Lake belt (Percival et al., 2006a; Sasseville et al., 2006; Anderson, 2008), and are interpreted in the context of a progressive, partitioned, dextral transcurrent shear during the later stages of collisional orogenesis.

Rice Lake mine trend: geology and stratigraphy

Supracrustal rocks south of the Wanipigow fault (WF) in the Rice Lake area include the Neoarchean Bidou, Gem and San Antonio assemblages (Figure 4); however, only the Gem assemblage is described in detail here, as it is the principal host to gold mineralization in the Rice Lake mine trend. The Gem assemblage includes three lithostratigraphic units, each of which is characterized by distinctive lithological associations. Contact relationships and younging criteria indicate that these units conformably overlie the Bidou assemblage and define a north-younging stratigraphic succession, the base of which is intruded from the southeast by the synvolcanic Ross River plutonic suite (Figure 4). To the west and north, the Gem assemblage is truncated by the basal unconformably of the San Antonio assemblage and the Wanipigow fault, respectively.

South of Rice Lake, the Independence Lake unit of the Bidou assemblage consists of intermediate volcanic and volcaniclastic rocks, and heterolithic volcanic conglomerate (Figure 4, 8; Anderson, 2008). The section here is at least 2.5 km thick and is interpreted to represent a lateral equivalent to ca. 2.73 Ga volcaniclastic rocks that define the top of the assemblage at the type locality east of the Ross River pluton (i.e., The Narrows formation; Campbell, 1971; Turek et al., 1989). Bed forms are rare, but typically dip at shallow to moderate angles to the north; sparse younging criteria indicate that these rocks are upright. Northeast-trending dikes of Fe-tholeiitic gabbro are interpreted to represent feeders to chemically similar flows and intrusions in the overlying Gem assemblage. The contact between these units is conformable at Rice Lake. Along strike to the east, the contact is a highly discordant synvolcanic fault (Anderson, 2008).

The geology of the Rice Lake area is dominated by intermediate–felsic volcaniclastic rocks and synvolcanic tonalite–granodiorite intrusions (Figure 4, 8; Anderson, 2008). Bulk compositions are mostly dacitic and trace element signatures are very uniform; in the interest of brevity, their geochemical attributes are described collectively here.

Most of these rocks are subalkaline and calcalkalic, although some have elevated Nb in relation to Y suggestive of mildly alkaline affinities. Chondrite-normalized trace element profiles are smoothly-sloped (Figure 9a), with enriched and fractionated light REE (La/Yb_N = 9.4–57.8; La/Sm_N = 3.3–6.3) and fractionated heavy REE (Gd/Yb_N = 1.7–6.9); negative Eu anomalies are lacking (Eu/Eu* = 0.9–1.5). All samples exhibit strong negative Nb anomalies (Figure 9b), with generally weak positive Zr and weak negative Ti. A subset of the these samples is characterized by high Mg numbers, high contents of Cr, Ni and Sr, anomalously low contents of Y and Yb, strongly fractionated REE patterns and correspondingly high Sr/Y and $(La/Yb)_N$ ratios, and are thus analogous to adakites (e.g., Martin et

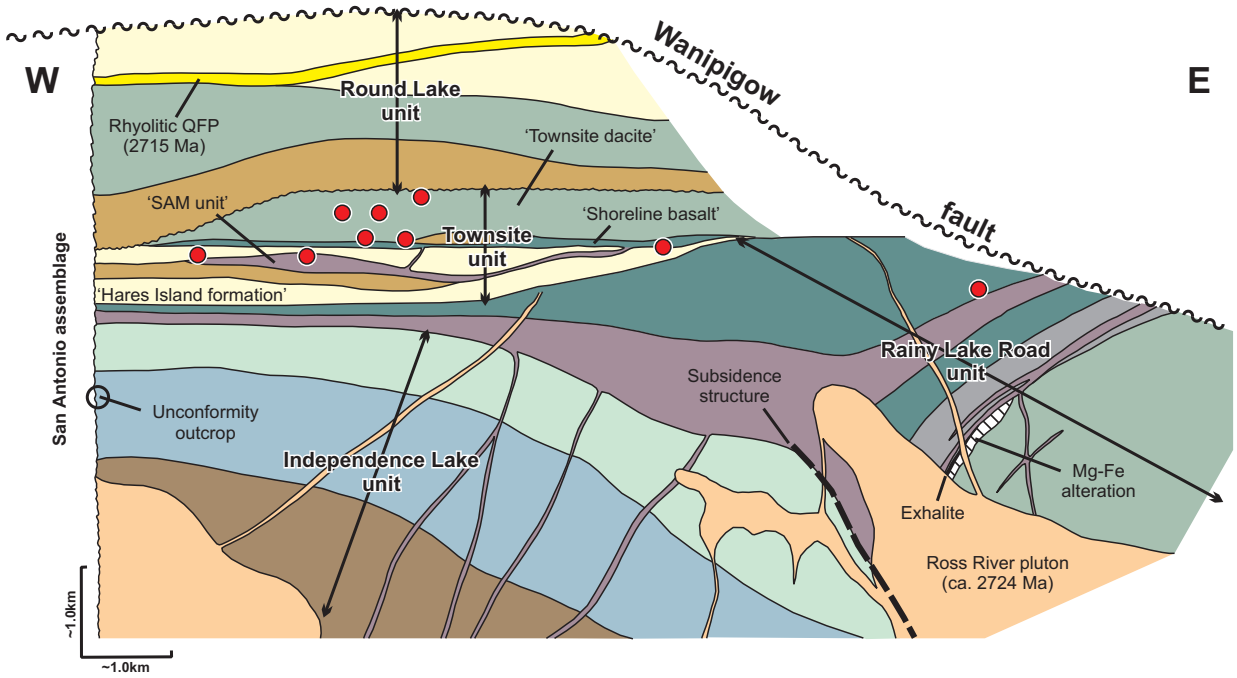

Figure 8: *Schematic lithostratigraphy of the Rice Lake section of the Bidou and Gem assemblages (vertical section, looking toward present-day north). For simplicity, the geology north of the Wanipigow fault and west of the San Antonio assemblage is excluded. The red circles indicate the approximate stratigraphic locations of the major gold deposits. The heavy grey dashed line indicates the approximate location of the postulated synvolcanic fault east of Rice Lake. The thickness of the exhalite (chert) and solid sulphide horizon in the Rainy Lake Road unit is exaggerated.*

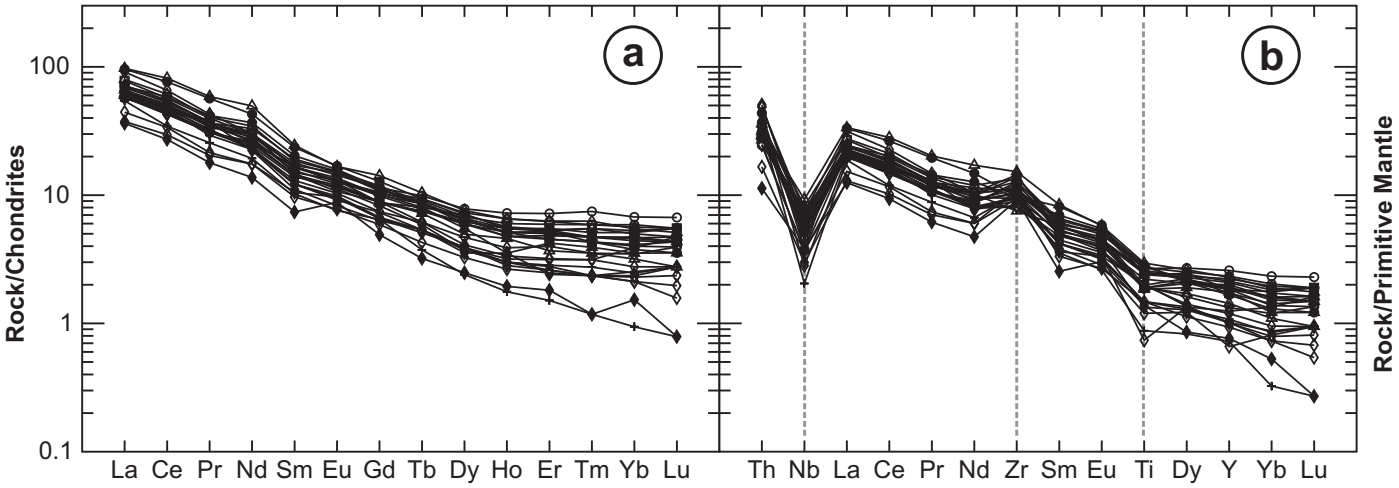

Figure 9: *Chondrite-* ***(a)*** *and primitive mantle-normalized* ***(b)*** *extended-element plots for intermediate–felsic volcanic and plutonic rocks from the Rice Lake area (Independence Lake unit, n = 5; Rainy Lake Road unit, n = 2; Ross River plutonic suite, n = 7; Round Lake unit, n = 5, Townsite unit, n = 7). Normalizing values are from Sun and McDonough (1989).*

al., 2005; Richards and Kerrich, 2007). Dacite at the base of the Gem assemblage has an initial ε_{Nd} of 0.3 and a model age of 3.03 Ga, whereas quartz-feldspar porphyry rhyolite near the top has an initial ε_{Nd} of 1.1 and a model age of 2.94 Ga.

Metamorphic mineral assemblages throughout the area south of the WF indicate low to middle greenschist facies regional metamorphism, with the exception of narrow zones along the margins of the larger plutons of the Ross River suite, which locally contain upper greenschist facies assemblages. However, the prefix 'meta' is not utilized and the rocks are described in terms of known or inferred protolith.

Gem assemblage

The Gem assemblage at Rice Lake is informally subdivided into the Rainy Lake Road, Townsite and Round Lake units. Although each has traditionally been considered part of the Bidou assemblage (e.g., Anderson, 2008), these correlations can no longer be sustained in light of new geochemical and

age constraints (Anderson, 2013). As shown schematically in Figure 8, abrupt lateral and vertical facies transitions, evidence of deep erosional scouring and the predominance of coarse epiclastic deposits, some of which were significantly reworked in subaerial settings, also point toward a more dynamic shallow-marine depositional setting, in contrast to the basinal-marine setting inferred for the Bidou assemblage.

Rainy Lake Road unit

The Rainy Lake Road (RLR) unit ranges up to at least 2.5 km thick and includes three distinct lithostratigraphic sections (lower, middle and upper), which are intruded by voluminous gabbro sills and the ca. 2.72 Ga Ross River pluton. Despite its proximity to the Wanipigow fault, the main body of this unit is characterized by an anomalously low state of strain, and thus contains well-preserved primary features. At Rice Lake, only the uppermost section is exposed, and is less than 200 m thick.

The RLR unit is best exposed along the Rainy Lake road, which branches to the south off Provincial Road 304 approximately 7.5 km east of Bissett (Figure 4). Aphyric to coarsely plagioclase-phyric felsic volcaniclastic rocks constitute the lower section and may, in part, be equivalent to similar rocks along strike to the west in the Independence Lake unit. Moderate to strong, fracture-controlled (i.e., stringer-style) chlorite-garnet alteration near the top of this unit is capped by laminated sulphidic sedimentary rocks and minor lenses of solid pyrite, indicating that basin subsidence and initial infilling were at least locally accompanied by hydrothermal circulation and discharge (exhalation). The stringer alteration is suggestive of close proximity to a fault-controlled discharge site, and thus supports the inference of a synvolcanic subsidence structure in this location (Figure 4, 8).

The middle section of the RLR unit is dominated by thin-bedded greywacke-mudstone turbidites but also includes minor heterolithic volcanic conglomerate, felsic volcaniclastic rocks, pillowed basalt flows and laminated chert, all of which are intruded by abundant hypabyssal sills and dikes of basalt. Bedding generally dips at moderate angles to the northwest. Normally-graded beds, load casts and slump-structures indicate subaqueous deposition from downslope turbidity flows, most likely in a relatively quiescent and short-lived marine basin, which formed in the hangingwall of the subsidence structure to the west. Detrital zircons from volcanic conglomerate near the top of this section indicate a maximum age of 2727 ±2 Ma for the late increments of basin infilling (Anderson, 2008).

The upper section of the RLR unit overlaps the subsidence structure and consists of pillowed and massive basalt flows, voluminous dikes and sills of gabbro, and a large gabbro laccolith that is rooted to the south in the subsidence structure (Figure 10). The basalt and gabbro are mostly Fe-tholeiitic and exhibit relatively flat profiles on extended-element plots normalized to normal mid-ocean-ridge basalt (NMORB), with weakly fractionated light REE and heavy REE, and weak negative Nb anomalies (Figure 11a). In relation to NMORB, the light REE are generally weakly enriched, whereas the heavy REE are mostly depleted, and most samples exhibit evidence of weak Zr depletion. Basalt from the RLR unit has an initial ε_{Nd} of 1.4, consistent with minor crustal contamination. The HFSE

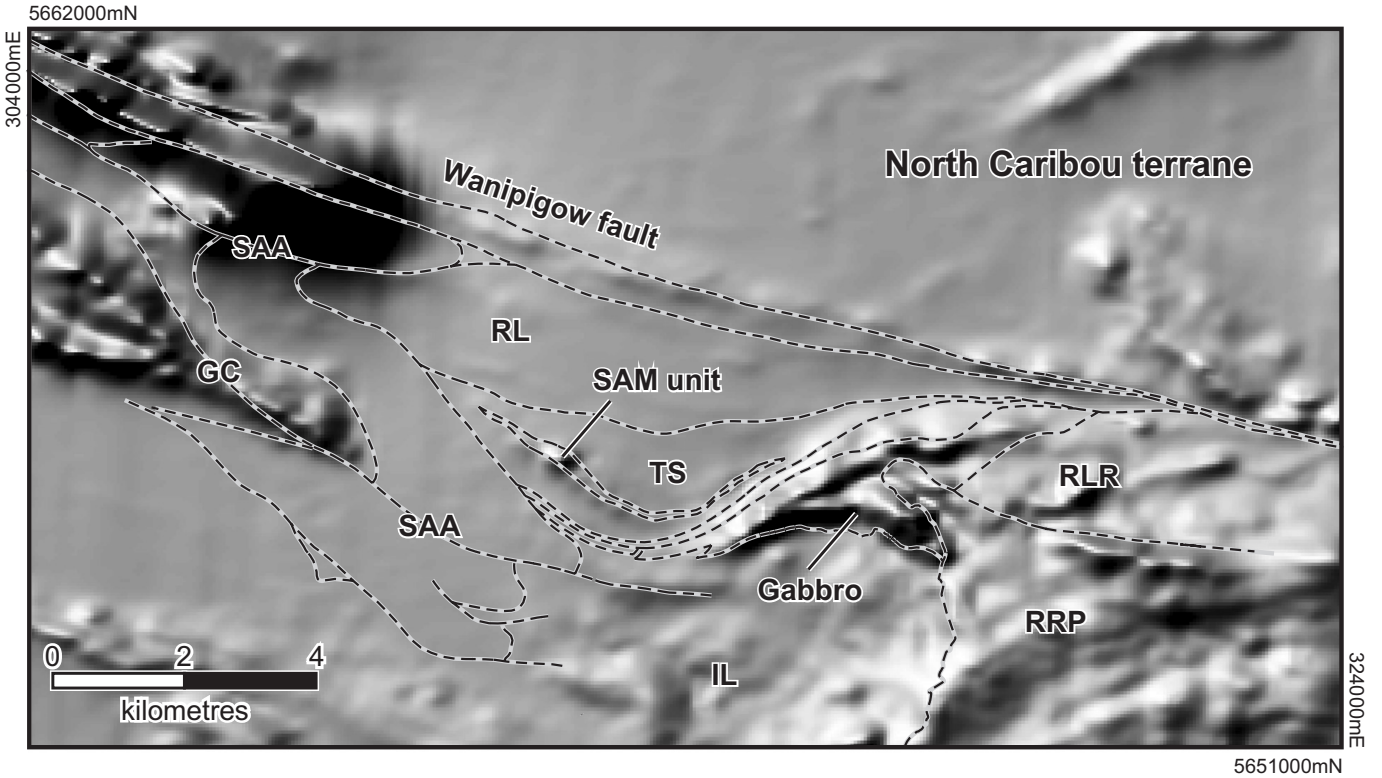

Figure 10: *Aeromagnetic total-field relief map of the Rice Lake area, showing the laccolithic cross-sectional shape of the gabbro intrusion east of Rice Lake. Data from the Geological Survey of Canada (1986). Simplified contacts and faults shown as thin dashed lines. Abbreviations: GC, Gold Creek unit; IL, Independence Lake unit; RL, Round Lake unit; RLR, Rainy Lake road unit; RRP, Ross River pluton; SAA, San Antonio assemblage; SAM sill, San Antonio mine sill; TS, Townsite unit.*

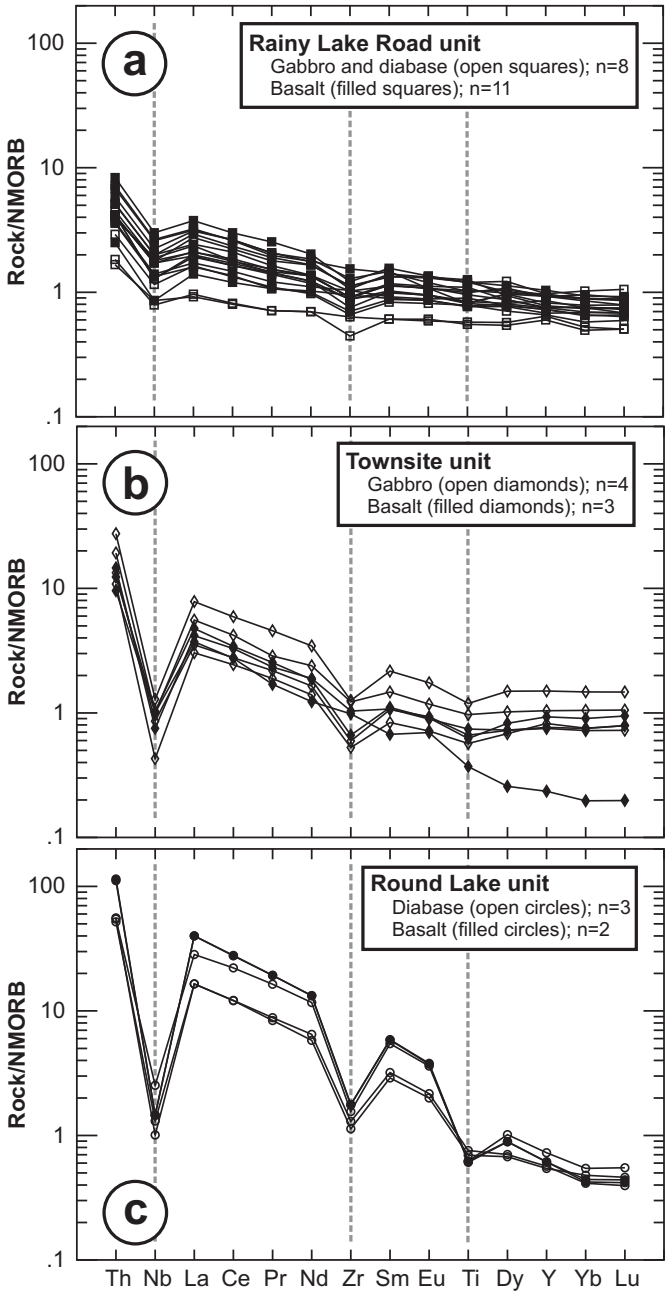

Figure 11: *Normal mid-ocean-ridge basalt (NMORB)-normalized extended-element plots for mafic volcanic and plutonic rocks from the Rice Lake area: a) Rainy Lake Road unit (basalt and gabbro); includes diabase dikes cutting the underlying Independence Lake unit of the Bidou assemblage; b) Townsite unit (basalt and gabbro); c) Round Lake unit (basalt); includes diabase dikes cutting the underlying Townsite and Rainy Lake Road units. Normalizing values are from Sun and McDonough (1989).*

and REE abundances of these rocks are comparable in most respects to basalt erupted in modern back-arc–basin settings (e.g., Gribble et al., 1998; Fretzdorff et al., 2002; Sinton et al., 2003). Northeast-trending diabase dikes in the underlying Independence Lake unit have similar geochemical signatures, and are interpreted to represent feeders to the RLR unit.

To the north, the contact with the Townsite unit coincides with the trace of the Normandy Creek shear zone (NCSZ); although unexposed, it is presumed to be depositional. The RLR and Townsite units both contain dikes of sanukitoid-affinity basalt that are interpreted to represent feeders to sanukitoid-affinity mafic volcanic rocks in the overlying Round Lake unit. An angular discordance between the Townsite and RLR units is indicated by facing criteria on either side of the NCSZ, where bedding faces in opposite directions on the S_3 fabric. Syn- to early-post–depositional tilting of the RLR unit in the hanging-wall of the subsidence structure would readily account for this discordance, and is in keeping with the observed lithofacies and basin geometry. Although it is not possible to entirely rule out a fault contact, any such fault would have to be an early low-angle structure that is stitched to the west by the San Antonio assemblage.

Townsite unit

The Townsite (TS) unit is the major host to gold mineralization in the Rice Lake area and largely defines the Rice Lake mine trend (Figure 12). The western portion of this unit strikes to the west-northwest and dips moderately to the northeast, whereas the eastern portion strikes to the west-southwest and dips steeply to the northwest. Felsic volcanic sandstone and heterolithic volcanic conglomerate at the base are interstratified with mafic to intermediate flows and associated volcaniclastic rocks, and are overlain to the north by a thick interval of plagioclase-phyric intermediate to felsic volcaniclastic rocks. Using the local mine terminology, these units correspond, respectively, to the 'Hares Island formation', 'Shoreline basalt' and 'Townsite dacite' (e.g., Poulsen et al., 1996). Epiclastic rocks at the base of the unit are intruded by gabbro sills and slightly discordant dikes, the thickest of which hosts the Rice Lake deposit and is referred to as the 'SAM unit'; it is interpreted as a subvolcanic equivalent to the 'Shoreline basalt' (e.g., Ames, 1988; Anderson, 2008). The TS unit ranges up to 1.3 km in thickness. A stratigraphic column is provided in Figure 13.

As described previously, the basal contact of the TS unit is unexposed, but field relationships are interpreted to indicate a depositional contact with the underlying RLR unit. The western boundary is defined by the angular unconformity at the base of the San Antonio assemblage, which dips steeply northeast and is overturned in this location, such that the TS unit and San Antonio assemblage are arranged 'back-to-back'. The TS unit is overlain to the north by the Round Lake unit along a deeply incised erosional contact (Figure 8).

Felsic volcanic sandstone

Felsic volcanic sandstone, with minor pebble to cobble volcanic conglomerate and mudstone, defines three major map units in the lower portion of the TS unit. These rocks were described as tuff and arkose by Stockwell (1938) and as lithic arenite by Tirschmann (1986). The lower unit is at least 150 m thick and is best exposed on the small islands south of Hares Island on Rice Lake; it is also exposed in several locations along the NCSZ, where it defines the immediate footwall to gold mineralization in the SG1 deposit. The medial unit is well exposed along the eastern shoreline of the lake, where it is approximately 300 m thick, and tapers out along strike to both

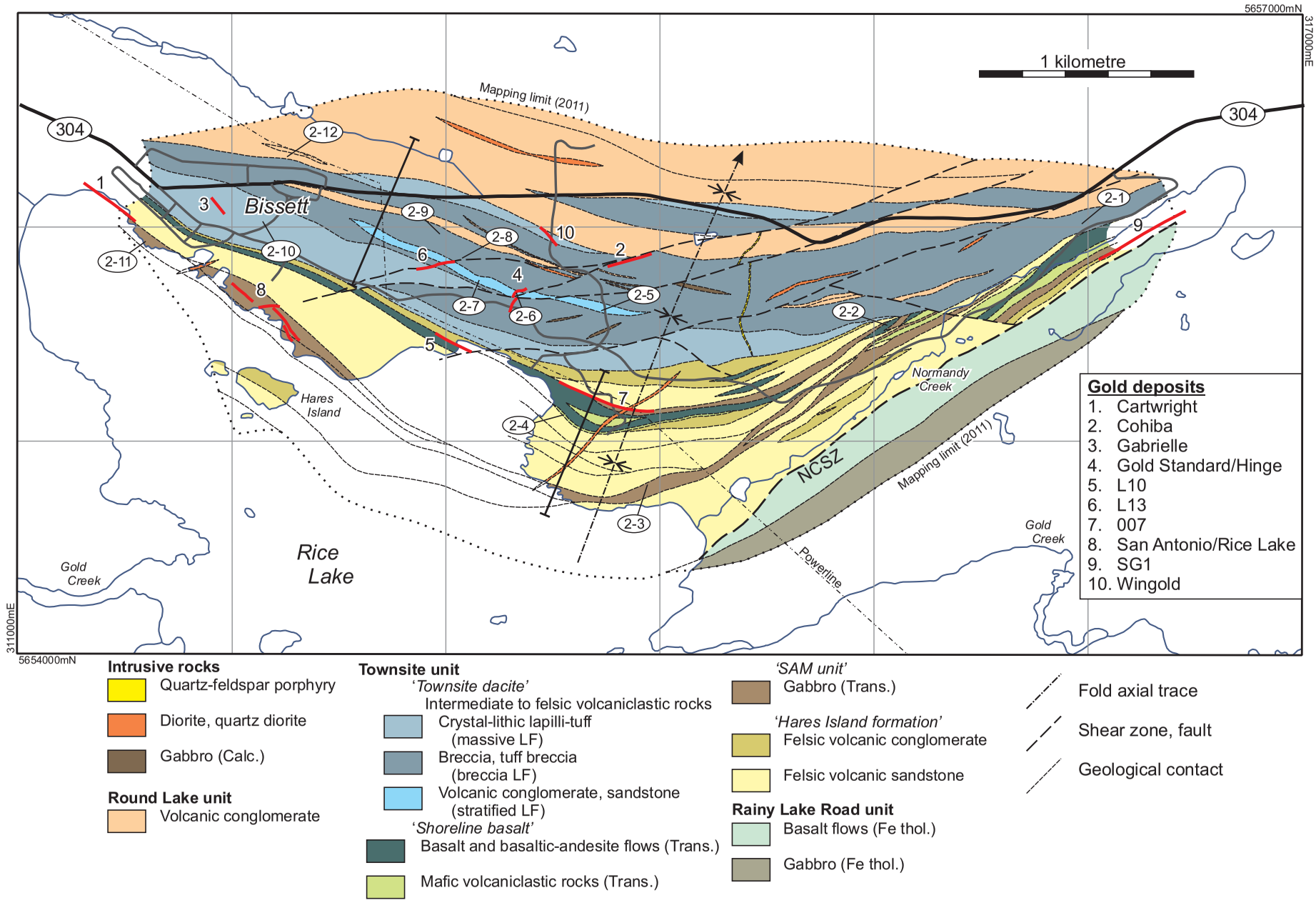

Figure 12: *Geology of the Rice Lake mine trend, simplified from (Anderson, 2011c). Map location is indicated on Figure 4. Major gold deposits are shown in the approximate locations of their up-dip projections (heavy red lines). Abbreviations: Calc., calcalkalic; Fe thol., Fe tholeiitic; LF, lithofacies; NCSZ, Normandy Creek shear zone; Trans., transitional tholeiitic-calcalkalic. Heavy black lines indicate the line of section for Figure 13. Numbered ellipses (2-1 to 2-12) indicate the stop locations for Day 2 of the field trip.*

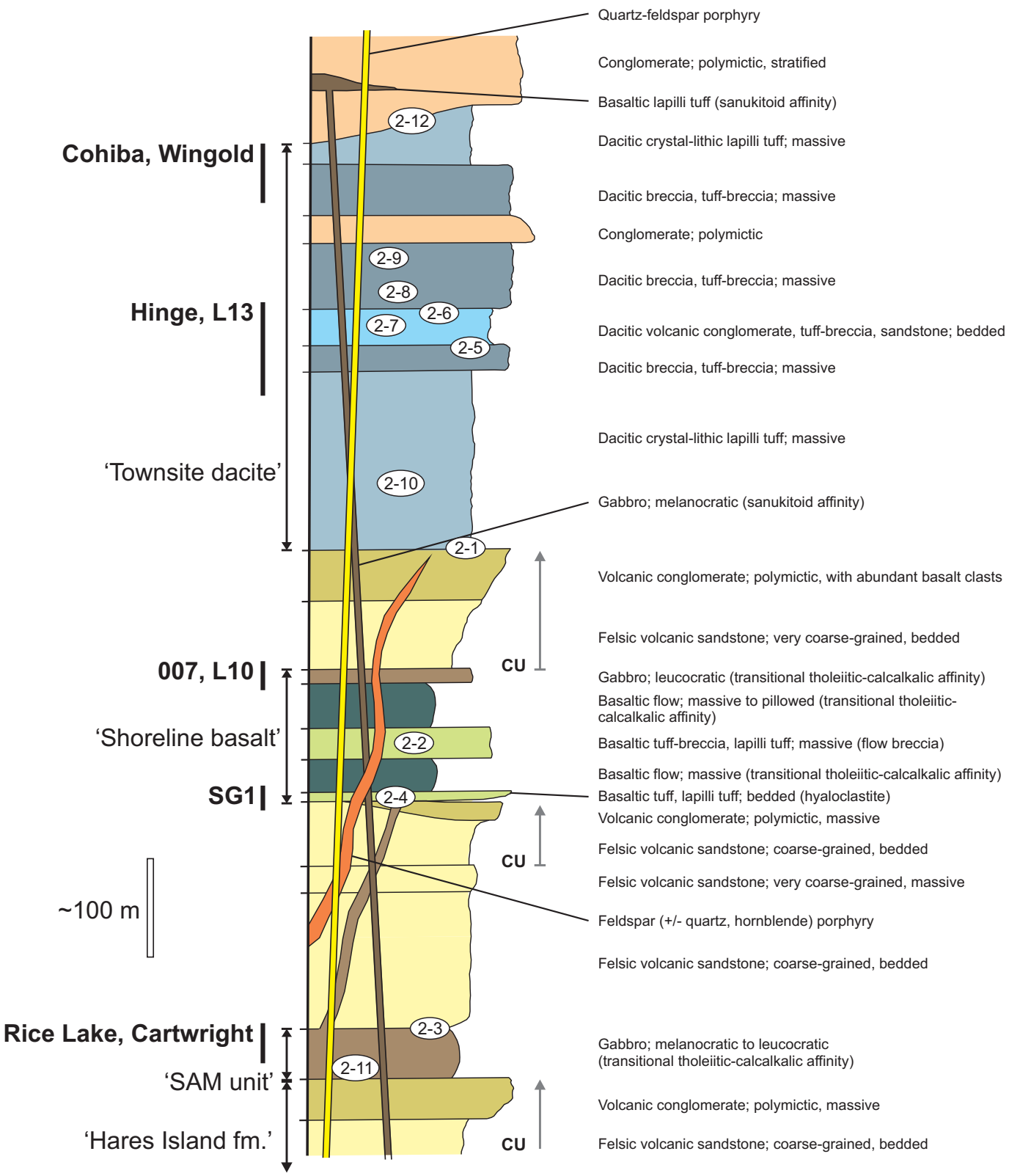

Figure 13: *Schematic, composite stratigraphic column for the Townsite unit, showing the major stratigraphic units, the approximate position of the major gold deposits, and the cross-cutting relationships of mafic–felsic dikes. CU, coarsening-upward. Line of section indicated on Figure 12. Numbered ellipses indicate the approximate stratigraphic positions of stops for Day 2 of the field trip.*

the east and west. This lenticular sandstone unit is bounded to the south by the SAM unit and to the north by the Shoreline basalt. The upper unit overlies the Shoreline basalt east of Rice Lake and also defines a lens-like body that ranges up to approximately 100 m thick. This unit defines the immediate hangingwall to gold mineralization in the 007 deposit and is exposed along strike to the east in several small outcrops north and south of the SG1 road, where it includes minor basalt flows. Each of the sandstone units is capped by heterolithic volcanic conglomerate, thus defining three distinct coarsening-upward cycles (Figure 13) suggestive of proximal suprafan-lobe and channel-fill deposits in a progradational submarine fan.

The felsic volcanic sandstone weathers white to light brown or grey and is medium to very coarse grained. It contains coarse grains of feldspar and quartz, the latter distinguishing it from superficially similar sandstone beds higher in the stratigraphy. It varies from well-bedded, with minor interbeds of pebble to cobble volcanic conglomerate and volcanic mudstone, to massive. Beds in these intervals are planar and massive to normally-graded; crossbedding is absent. Consistent normal size-grading and local scours indicate tops to the north. A sample of felsic volcanic sandstone collected from a sedimentary dike just below the base of the TS unit contains a unimodal population of ca. 2.72 Ga detrital zircons (Anderson, 2008).

Felsic volcanic conglomerate

Discontinuous units of heterolithic volcanic conglomerate cap each of the felsic volcanic sandstone units (Figure 12, 13). The lower conglomerate unit is best exposed on the north side of Hares Island in Rice Lake, where it is homogeneous and massive, and ranges up to 190 m thick. The medial unit is approximately 40 m thick in the immediate footwall of the Shoreline basalt where it is crossed by the powerline, and appears to taper out along strike in both directions. Outcrops along the SG1 road provide the best exposures of the upper unit, which also has a pronounced lenticular shape, and ranges up to 60 m thick within a strike length of 1.6 km.

The conglomerate is typically clast supported and poorly sorted, and varies from crudely stratified to massive. It consists of subangular to well-rounded clasts of intermediate and felsic volcanic rock that range up to 50 cm across. The matrix consists of medium- to coarse-grained, pebbly volcanic sandstone that contains up to 20% feldspar and quartz crystals. The northern unit contains angular clasts of variably epidotized amygdaloidal basalt, and is intruded by dikes and sills of texturally similar basalt. In the context of a submarine-fan model, these conglomerate units most likely represent high-density debris flows deposited in upper-fan channels.

Gabbro

The epiclastic rocks at the base of the TS unit host two laterally extensive gabbro intrusions, the southern of which hosts most of the gold mineralization in the Rice Lake and Cartwright deposits and is informally referred to as the 'SAM unit'. This unit is traced over a strike length of 5 km on surface, and has been traced by drilling for an additional 700–800 m to the northwest of Rice Lake. In the mine, this unit has been traced more than 2 km down dip and remains open at depth. The western segment ranges up to 120 m thick, dips moderately to the northeast and appears to cut slightly downsection toward the east, whereas the eastern segment ranges up to 80 m thick, dips steeply to the northwest, and cuts significantly upsection toward the east into immediate footwall of the Shoreline basalt. The contacts are well exposed in several locations and are typically sharp, planar and discordant to bedding in the country rock. Large rafts and roof pendants of felsic volcanic sandstone within the SAM unit indicate its intrusive nature. The northern gabbro intrusion ranges up to 50 m thick and is discontinuously exposed over a strike length of 2.0 km in the hangingwall of the Shoreline basalt. Each of these units is intruded by sills and dikes of sparsely amygdaloidal basalt, which typically have thick chilled margins and are interpreted as feeders to overlying basaltic flows.

The gabbro is fine to medium grained and equigranular, with a subophitic texture, and varies from melanocratic to leucocratic. Leucogabbro is most extensive near the top of the thick western segment of the SAM unit, where it ranges up to 90 m thick and is interpreted to result from in situ magmatic differentiation. An outcrop of layered gabbro on a small island in Rice Lake consists of irregular wisps, clots and discontinuous contorted layers (2–10 cm thick) of leucogabbro in melagabbro, and perhaps represents the interface between these subunits.

Gabbro in the TS unit exhibits weakly to moderately sloped profiles on NMORB-normalized extended-element plots (La/Yb_N = 1.7–11.1), with moderately enriched and fractionated light REE, generally unfractionated heavy REE, prominent negative Nb anomalies and weak negative Zr and Ti anomalies (Figure 11b), suggesting an affinity to modern volcanic-arc magmas (e.g., Perfit et al., 1980; Kelemen et al., 1990). Similar geochemical characteristics in overlying basalt flows are interpreted to indicate a comagmatic relationship and a resurgence of arc-magmatism subsequent to extension and incipient rifting.

Mafic volcaniclastic rocks

Mafic volcaniclastic rocks appear to be confined to a relatively restricted stratigraphic interval at the base of the uppermost of the three suprafan-lobe successions described above (Figure 12). These rocks are spatially associated with basalt and basaltic andesite flows (see below), to which they appear to be genetically related, and thus collectively define the 'Shoreline basalt'. The mafic volcaniclastic rocks range up to 50 m thick and, in places, contain minor interlayers of felsic volcanic sandstone and conglomerate. At the type locality, which is located approximately 100 m east of Rice Lake in the immediate footwall of the 007 deposit, this unit is situated at the contact between felsic-volcanic sandstone (south) and massive basalt (north).

The mafic volcaniclastic rocks weather light brown or green and are dark green on fresh surfaces. They consist of monolithic tuff, lapilli tuff, lapillistone, tuff breccia and breccia, which were derived from aphyric to very sparsely plagioclase-phyric basalt and basaltic andesite. The clasts typically contain sparse (<10%) quartz or carbonate amygdules up to 1.5 cm across. In most localities, a high proportion of the clasts

exhibit wispy, shard-like or cuspate shapes and show evidence of formerly glassy margins, indicative of primary hyaloclastite deposits.

Laminated to thin-bedded tuff and lapilli tuff define the base of the unit in most locations, and include minor interbeds of felsic volcanic sandstone. In the western portion, this tuffaceous unit is exposed in three locations over a strike length of approximately 700 m and varies from 2.5 to 10 m thick. Normally graded beds and scours in these locations indicate tops to the north. Massive to crudely stratified intervals (<15 m thick) of monolithic lapilli tuff and lapillistone locally overlie these rocks and consist of closely packed, angular to subangular lapilli with delicate shard-like or cuspate shapes. This material is interlayered with, or overlain by, massive layers of clast-supported monolithic breccia and tuff breccia, which contain very angular to subangular basaltic clasts up to 30 cm across. At the type locality, these rocks define a coarsening upward sequence in the footwall of a massive basalt flow and are interpreted to record a distal to proximal facies transition within an apron of resedimented and in-situ hyaloclastite.

Basalt and basaltic andesite flows

Basalt and basaltic andesite flows are confined to a relatively restricted stratigraphic interval at or just above the base of the uppermost of the three suprafan-lobe successions. The flows range up to 100 m thick and are interstratified on a variety of scales with mafic volcaniclastic rocks and minor felsic epiclastic rocks. They are best exposed in shoreline outcrops in the northeastern portion of Rice Lake, but are also well exposed in scattered outcrops along strike to the northeast. The northern contact of this unit hosts significant Au mineralization in the L10 and 007 deposits, whereas the southern contact hosts the SG1 deposit. As described by Stockwell (1938), this unit was traced northwest by drilling beneath the covered area north of the Rice Lake mine, and is exposed at two locations in Bissett.

The basalt (and basaltic andesite) weather light green to reddish-brown and are dark green on fresh surfaces. They are typically aphyric with a very fine grained intergranular texture. Sparsely porphyritic basalt contains 2–10% euhedral to subhedral plagioclase laths that are 1–3 mm in length. Most specimens are moderately to strongly altered, such that the primary mineral assemblage is completely replaced by secondary chlorite, epidote and carbonate. Flow types include massive, pillowed and brecciated. All three flow types are locally observed in single outcrops; however, the exposure is generally insufficient to determine the flow organization. In some locations, massive flows transition upward into pillowed or brecciated basalt. Pillowed flows consist of bun-shaped pillows 20–50 cm across, with subordinate amoeboid pillows up to 1.5 m in length. Pillow cores are sparsely amygdaloidal, moderately to strongly epidotized and locally plagioclase phyric. Amygdules are round and less than 5 mm in diameter, and variably contain epidote, quartz, calcite and/or hematite. Pillow selvages are 0.5–1.5 cm thick and strongly chloritized. Brecciated flows consist of blocky to very irregular to wispy fragments of fine-grained amygdaloidal basalt, some of which show evidence of chilled margins. These flows range up to 10 m thick and tend to be strongly epidotized.

The basalt has weakly to moderately sloped profiles on NMORB-normalized extended-element plots (Figure 11b), with moderately enriched and fractionated light REE, generally unfractionated heavy REE, prominent negative Nb anomalies and weak negative Zr and Ti anomalies, suggesting an affinity to modern volcanic-arc basalt.

Intermediate to felsic volcaniclastic rocks

Intermediate to felsic volcaniclastic rocks at the top of the TS unit are informally referred to as the 'Townsite dacite' and include three distinct lithofacies. This unit ranges up to 500 m thick north of Rice Lake and is well exposed in a large outcrop ridge that extends east from Bissett for just over 5.0 km along strike. To the east, the unit thins considerably toward the confluence of the WF and the NCSZ, and is less than 100 m thick in the hangingwall of the SG1 deposit. To the west, the unit appears to be truncated by a deep erosional scour at the base of the Round Lake unit. Significant gold deposits are restricted to the upper portion of this unit (Cohiba, L13, Hinge and Wingold), in intervals that contain a strong primary anisotropy (i.e., bedding; Figure 12).

The 'massive' lithofacies consists of massive to very crudely stratified crystal-lithic lapilli tuff, which has a bulk composition varying between dacite and high-silica andesite. This lithofacies defines the base of the map unit in its western and central portions, where it ranges up to 190 m thick, and is also locally present in the upper and eastern portions of the unit, where it appears to define diffuse layers up to several tens of metres thick. The crystal-lithic lapilli tuff weathers pale green-grey and is dark green on fresh surfaces. It tends to be homogeneous, with a seriate-porphyritic texture defined by euhedral to subhedral plagioclase crystals (<1 cm; 20–45%) in an aphanitic to fine-grained matrix of feldspar, quartz and phyllosilicate minerals. The crystals vary from euhedral (tabular) to angular (broken) to subrounded, and commonly display oscillatory zoning. The crystal component also includes trace to 2% blue quartz (<5 mm) and black amphibole (<3 mm). Subtle variations in the size and proportion of crystals or lithic clasts define a crude stratification in some outcrops. The lithic component consists of subrounded to angular clasts (<10 cm) of crystal tuff, aphyric andesite, amygdaloidal basalt or sulphidic mudstone, and includes possible examples of felsic pumice (Tirschmann, 1986; Anderson, 2008). The latter three clast types commonly have wispy shapes, which preclude significant transport or reworking. The proportion of clasts is typically <5%, but ranges up to 20% in some locations. As described by Anderson (2008), the preferred depositional model for the crystal-lithic lapilli tuff involves 1) initial fragmentation by explosive eruption of crystal-rich magma; 2) syneruptive elutriation of the fine fraction to produce high concentrations of coarse plagioclase crystals; 3) final deposition in a shallow subaqueous, or locally subaerial, setting as primary pyroclastic or resedimented grain-flow deposits.

Breccia and tuff breccia of the 'breccia' lithofacies dominate the upper and eastern portions of the unit, and host significant mineralization in the Cohiba deposit (Figure 12). These rocks are generally monolithic, matrix-supported and poorly-sorted, and vary from massive to crudely stratified. They consist

of very angular to subrounded blocks of crystal-lithic lapilli tuff that range in size up to 1.0 m (generally 5–40 cm). These blocks are typically more coarsely and densely plagioclase phyric than the matrix, although the clasts and matrix in some localities are texturally similar and indistinct. Some outcrops consist of very angular interlocking clasts with less than 5% matrix material. Clast margins vary from sharp to diffuse, perhaps as a consequence of in situ disaggregation of weakly indurated material. Rare examples of angular, joint-bounded clasts of crystal-lithic lapilli tuff indicate at least local derivation from well-indurated material. Some outcrops contain aphyric basalt and andesite clasts that have wispy shapes, ragged terminations and vesicular textures suggestive of juvenile vitriclasts. Near the base, this lithofacies includes widely spaced, discontinuous layers (<1 m thick) of thin-bedded volcanic sandstone and pebble conglomerate that are normally-graded and contain low-angle crossbeds and scours. The breccia lithofacies is interpreted to represent secondary mass-flow deposits generated by gravitational instability of partially indurated primary pyroclastic or syneruptive sedimentary deposits.

The 'stratified' lithofacies consists of interlayered volcanic conglomerate and volcanic sandstone, defining a well-stratified, lenticular unit near the interface between the massive and breccia lithofacies. This lithofacies ranges up to 50 m thick and is traced along strike for approximately 1.5 km. The surface trace coincides with the up-dip projections of the Hinge and L13 deposits. The conglomerate layers range up to 15 m thick and are poorly sorted, matrix supported and unstratified. Most layers are massive with thin (<50 cm) reversely graded bases and normally graded tops consistent with high-density debris flows; basal contacts are sharp and scoured. Interlayers of volcanic sandstone vary up to 1.5 m thick and are normally graded, with sharp scoured bases, consistent with sedimentation from high-density turbidity currents. Collectively, the volcanic conglomerate and sandstone are interpreted to record influxes of reworked detritus during a transition from grain-flow–dominated to mass-flow–dominated sedimentation.

Round Lake unit

The Round Lake (RL) unit defines the top of the Gem assemblage at Rice Lake and consists of a basal heterolithic volcanic conglomerate, overlain by a thick succession of volcaniclastic and epiclastic rocks that exhibits increasingly felsic bulk compositions, from andesitic through dacitic to rhyolitic (Figure 4). Unlike underlying units, mafic intrusions are apparently absent in all but the lowermost portions of the RL unit (e.g., Stockwell, 1938), and the constituent volcanic rocks are commonly hornblende phyric. This unit ranges up to 1.7 km thick and is truncated to the north by the WF. Apparent finite strain generally increases toward the east, and the aspect ratios of deformed clasts in horizontal outcrop surfaces near the confluence of the NCSZ and WF locally exceed 100:1. Near the top of this unit, a slightly discordant body of quartz-feldspar porphyry (Figure 4), interpreted to represent a hypabyssal intrusion, returned a U-Pb zircon age of 2715 ±2 Ma and thus provides a minimum age for the Gem assemblage (Anderson, 2008). This unit is unconformably overlain to the west by the San Antonio assemblage.

Conglomerate near the base of the RL unit includes basaltic lapilli tuff, interpreted as a scoria deposit, with geochemical attributes of the late Archean sanukitoid suite. Dikes and sills of sanukitoid basalt and gabbro intrude the TS unit, and have also been identified in the RLR unit. They are characterized by 45–51 wt. % SiO_2, 0.8–1.0 wt. % TiO_2 and 9–11 wt. % Fe_2O_3, with high Mg numbers (61–70). NMORB-normalized extended-element plots exhibit steeply-sloped profiles, with extreme La/Yb_N ratios of 20.2–55.8 (Figure 11c), strongly enriched and fractionated light REE, depleted and fractionated heavy REE, and pronounced negative Nb, Zr and Ti anomalies. Chromium and nickel values are highly elevated, ranging from 231 to 408 ppm (average 322 ppm) and from 101 to 402 ppm (average 233 ppm), respectively. A sample of the basaltic lapilli tuff has an initial ε_{Nd} value of 1.2, suggesting minor interaction with isotopically evolved crust. As described by Shirey and Hanson (1984), the unique chemistry of the sanukitoid suite (high Mg#, Cr and Ni, with strongly enriched light REE and LILE) is attributed to partial melting of sub-arc mantle peridotite that was extensively metasomatized by slab-derived fluids (e.g., Stern, 1989; Stern et al., 1989).

Rice Lake mine trend: structural geology of vein systems

Deformation structures within the mine trend are correlated on the basis of orientation, style and overprinting relationships with the generations (G_1–G_6) of regional structure described above (Anderson, 2008, 2011b). Only the G_3 structures are further described here, as they represent the principal structural control on gold mineralization in the mine trend. They include early ductile and later brittle-ductile structures, attributed to progressive deformation. G_1 and G_2 structures are only observed outside the mine trend and clearly pre-date gold mineralization, whereas the G_4 crenulation cleavage is pervasive and post-dates mineralization, thereby constraining its structural timing. G_5 structures also post-date mineralization but are only pervasive in the NCSZ, which coincides with a northeast trending topographic low and is poorly exposed.

Patterns of orientation define two structural domains, corresponding to the western and eastern limbs of the open F_6 syncline that trends north through Rice Lake (Figure 12). In the western domain, beds generally strike to the west-northwest and dip moderately to the northeast (Figure 14a, whereas in the eastern domain they generally strike to the west-southwest and dip steeply to the northwest (Figure 14g). Minor mafic to intermediate dikes are typically oriented at shallow (~10–20°) counter-clockwise angles to bedding; the exception being a quartz-feldspar porphyry dike in the eastern domain (Figure 14b, h).

Ductile G_3 structures

The earliest ductile deformation structures in the mine trend are the pervasive S_3-L_3 shape fabrics, which are defined by flattened and stretched clasts and pillows, and a continuous foliation of fine-grained chlorite, actinolite and sericite. The S_3 fabric in the western domain generally strikes to the west-northwest and dips steeply or moderately to the northeast, whereas this fabric in the eastern domain generally strikes to the west-

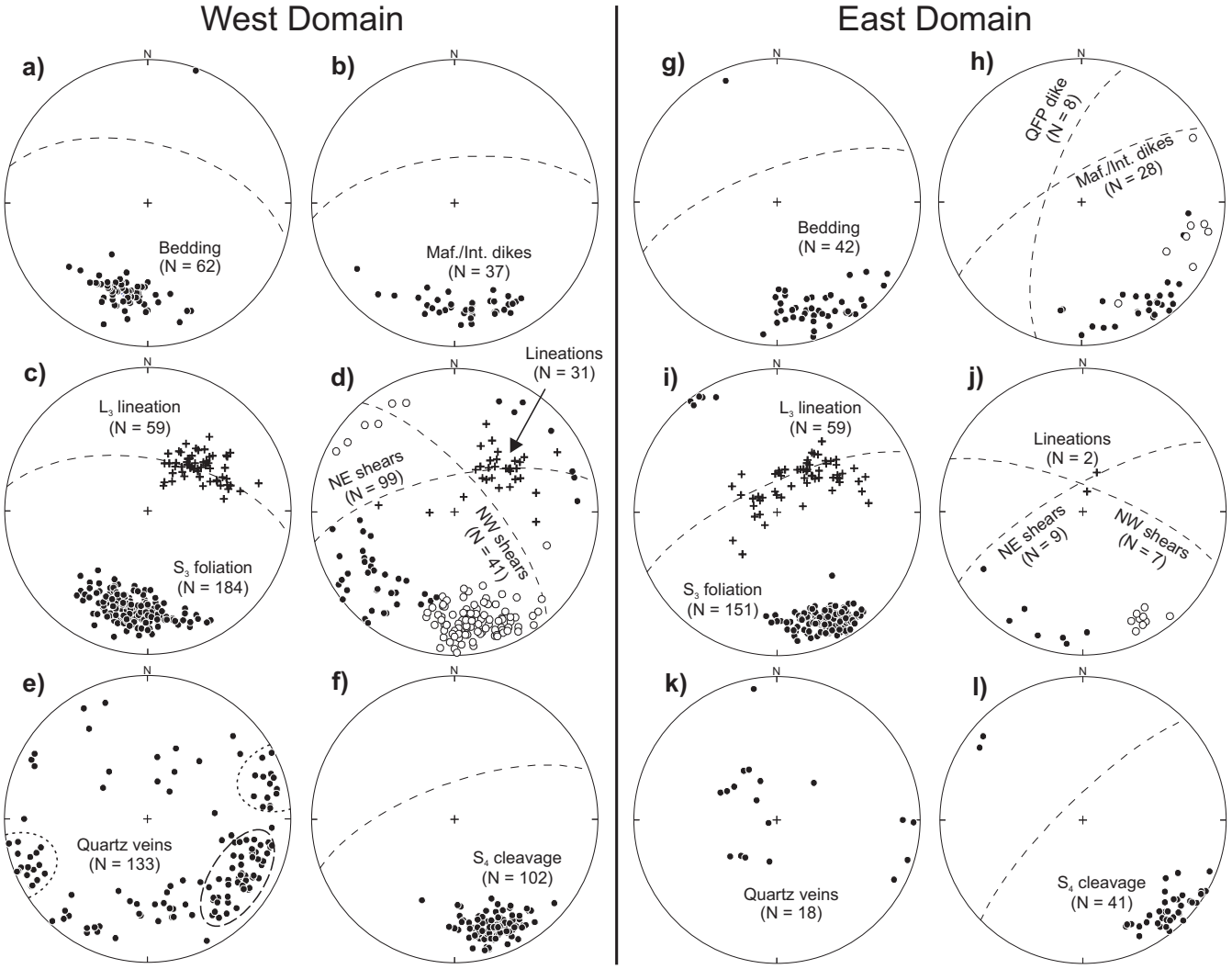

Figure 14: *Lower-hemisphere, equal-area projections of structural data in the western (a–f) and eastern (g–l) domains of the mine trend:* ***a)*** *and* ***g)*** *poles to bedding;* ***b)*** *and* ***h)*** *poles to contacts of mafic and intermediate dikes; quartz-feldspar porphyry dikes in eastern domain indicated by open circles;* ***c)*** *and* ***i)*** *L_3 linear fabric (crosses) and poles to S_3 planar fabric (circles);* ***d)*** *and* ***j)*** *poles to northwest-trending shears (NW shears; filled circles) and northeast-trending shears (NE shears; open circles), with associated slickenline or chlorite lineations (crosses);* ***e)*** *and* ***k)*** *poles to quartz veins; ellipses indicate the two main clusters in the data from the western domain; long-dashed ellipse indicates extension veins associated with NE shears, whereas short-dashed ellipse indicates extension veins associated with NW shears;* ***f)*** *and* ***l)*** *poles to the S_4 crenulation cleavage. Great circles (dashed lines) indicate the mean orientation of the corresponding planar structures. Abbreviations: Int., intermediate; Maf., mafic.*

southwest and dips steeply to the northwest (Figure 14c, i). In both domains, the S_3 fabric crosscuts primary structures at a very shallow (~5°) counter-clockwise angle (beds thus face east on S_3) and dips slightly more steeply than bedding. Mesoscopic F_3 folds are lacking. The associated L_3 stretching lineation is most prominently defined by plagioclase crystals in the Townsite dacite; in some locations, these rocks are L>S tectonites. The G_3 shape fabric locally intensifies into narrow (<2 m) widely spaced zones of chloritic or sericitic mylonite that contain intense S-L fabrics and record distinctly higher G_3 strain than the surrounding rocks.

Local asymmetric fabrics and folds in these zones indicate sinistral-reverse non-coaxial shear; these zones are interpreted to represent ductile precursors to the brittle-ductile shears described below. Outside these zones, the G_3 shape fabric is less intense and generally symmetric (Lau and Brisbin, 1996); hence, G_3 strain appears to have been strongly partitioned on a macroscopic scale (Anderson, 2008). The L_3 lineation has a very consistent orientation in the western domain and plunges moderately to the northeast in the plane of the S_3 fabric (Figure 14c). The orientation of the L_3 fabric in the eastern domain shows significant scatter (Figure 14i), which is interpreted to result from reorientation during late (G_5) shear along the NCSZ.

Brittle-ductile G_3 structures

The G_3 shape fabric is overprinted throughout the Rice Lake mine trend by discrete brittle-ductile shear zones and shear fractures (hereafter referred to as 'shears'), which are the principal controlling structures for the auriferous quartz-carbonate veins systems. These shears are separated into two sets on the basis of orientation and kinematics. Mutual overprinting

and crosscutting relationships indicate that they evolved synchronously (Anderson, 2011b).

Northeast-trending shears (NE shears)

The NE shears are well developed throughout the mine trend and generally coincide in outcrop with pronounced topographic lineaments, particularly where they follow early mafic or intermediate dikes. These lineaments are well-defined by high-resolution light detection and ranging (LiDAR) data (Figure 15) and are traced along strike for up to 3 km. The most prominent of these lineaments/shears are shown on Figure 12. In the western domain, the NE shears strike to the west-southwest and dip steeply or moderately to the northwest, whereas they strike to the southwest and dip steeply to the northwest in the eastern domain (Figure 14d, j). Within both domains, NE shears have fairly consistent orientations: they cut at a shallow counter-clockwise angle across primary structures and the S_3–L_3 shape fabric, and are oriented roughly parallel to mafic and intermediate dikes. The latter relationship indicates that NE shears may have been controlled by the anisotropy of the dikes in some cases.

Highly variable characteristics within and between individual NE shears relate to differing stages of development in a progressive deformation. Incipient NE shears are marked by en échelon arrays of synthetic shear or extension fractures. At an early stage of development, these fractures were joined by discrete, through-going shear fractures, which are typically marked by planar slip-surfaces and discontinuous seams of cataclasite. This progression is clearly evident at the lateral tips of NE shears, which dissipate along strike into en échelon or horsetail arrays of shear or extension fractures, and abruptly terminate at wing cracks. In later stages of development, the shears are characterized by continuous zones of chloritic or sericitic mylonite that range up to several metres in thickness and contain lenticular to tabular fault-fill quartz veins. The fault-fill veins vary from laminated to brecciated to massive, and contain stylolitic pressure-solution seams marked by fine-grained pyrite, tourmaline and chlorite. Slickenline and chlorite lineations on slip-surfaces and foliation planes plunge moderately to the northeast, roughly parallel to the L_3 fabric in the wallrocks. Pressure fringes on pyrite cubes in narrow sulphidization haloes surrounding the fault-fill veins are also aligned parallel to the L_3 lineation. The external S_3 shape fabric is either sharply truncated at the margins of the shears or is continuously transposed into parallelism with the internal fabric.

The best-documented examples of NE shears occur in the Rice Lake deposit, where they host major fault-fill veins referred to as '16-type' in local mine terminology (e.g., Poulsen et al., 1986; Lau, 1988; Lau and Brisbin, 1996). A typical example is illustrated in Figure 16. Fault-fill veins hosted by NE shears also constitute orebodies in the Cohiba, Hinge, L10, L13, 007 and SG1 deposits. In the Rice Lake deposit, these veins are preferentially hosted by leucogabbro in the upper portion of the SAM unit, presumably on account of its higher competency, and form a right-stepping, en échelon array along the strike of the sill (Figure 17, 18). Sill contacts are offset in a left-lateral sense and are locally back-rotated between adjacent NE shears (Figure 18). The fault-fill veins form tabular or lenticular orebodies that range up to 200 m in length, up to 2.5 m in thickness and, in the case of the namesake No. 16 vein in the Rice Lake mine, have been traced down-dip in excess of 700 m. The thickest segments tend to coincide with left-stepping dilational jogs

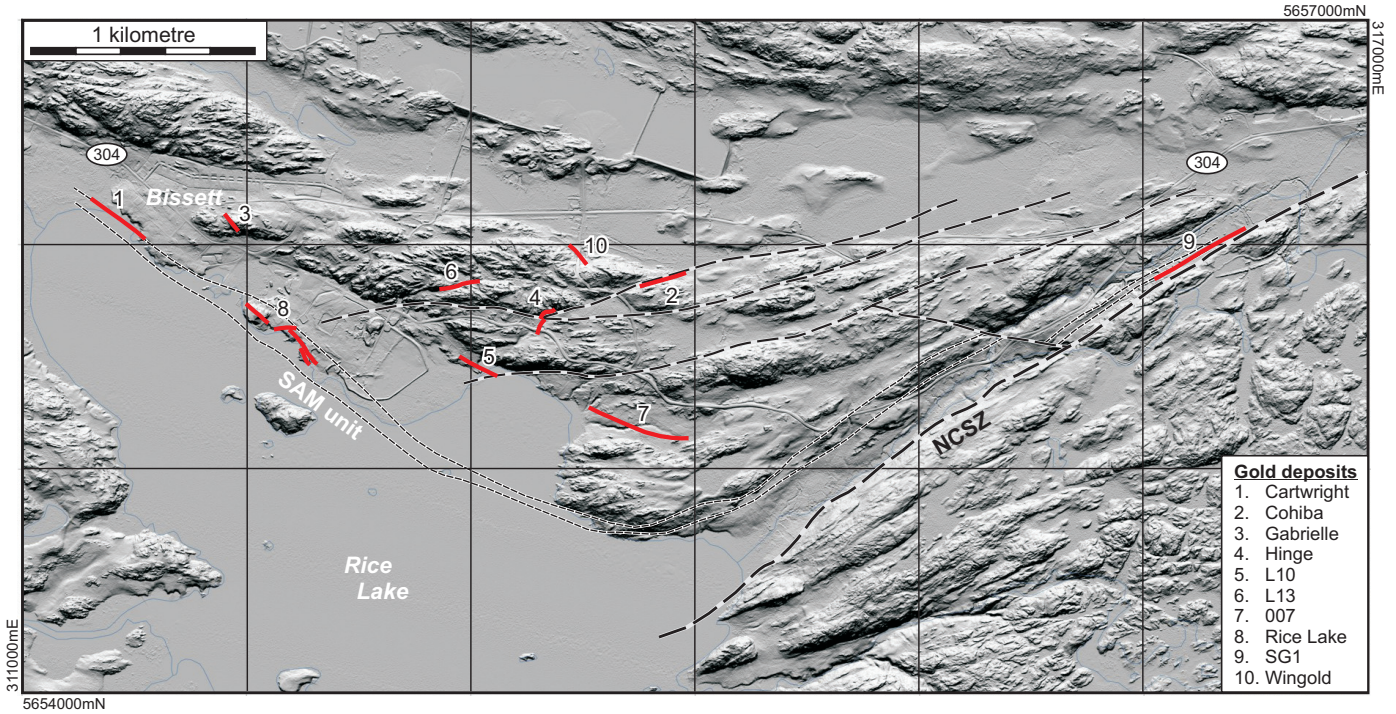

Figure 15: *Digital elevation model of the 'bare-earth' surface derived from light detection and ranging (LiDAR) data, illuminated from the north at an angle of -40° (3x vertical exaggeration). Approximate surface trace of the major gold deposits are shown in red (projected up-dip). Long-dashed lines indicate the major NE shears. Short-dashed lines indicate the contacts of the SAM unit. NCSZ, Normandy Creek shear zone.*

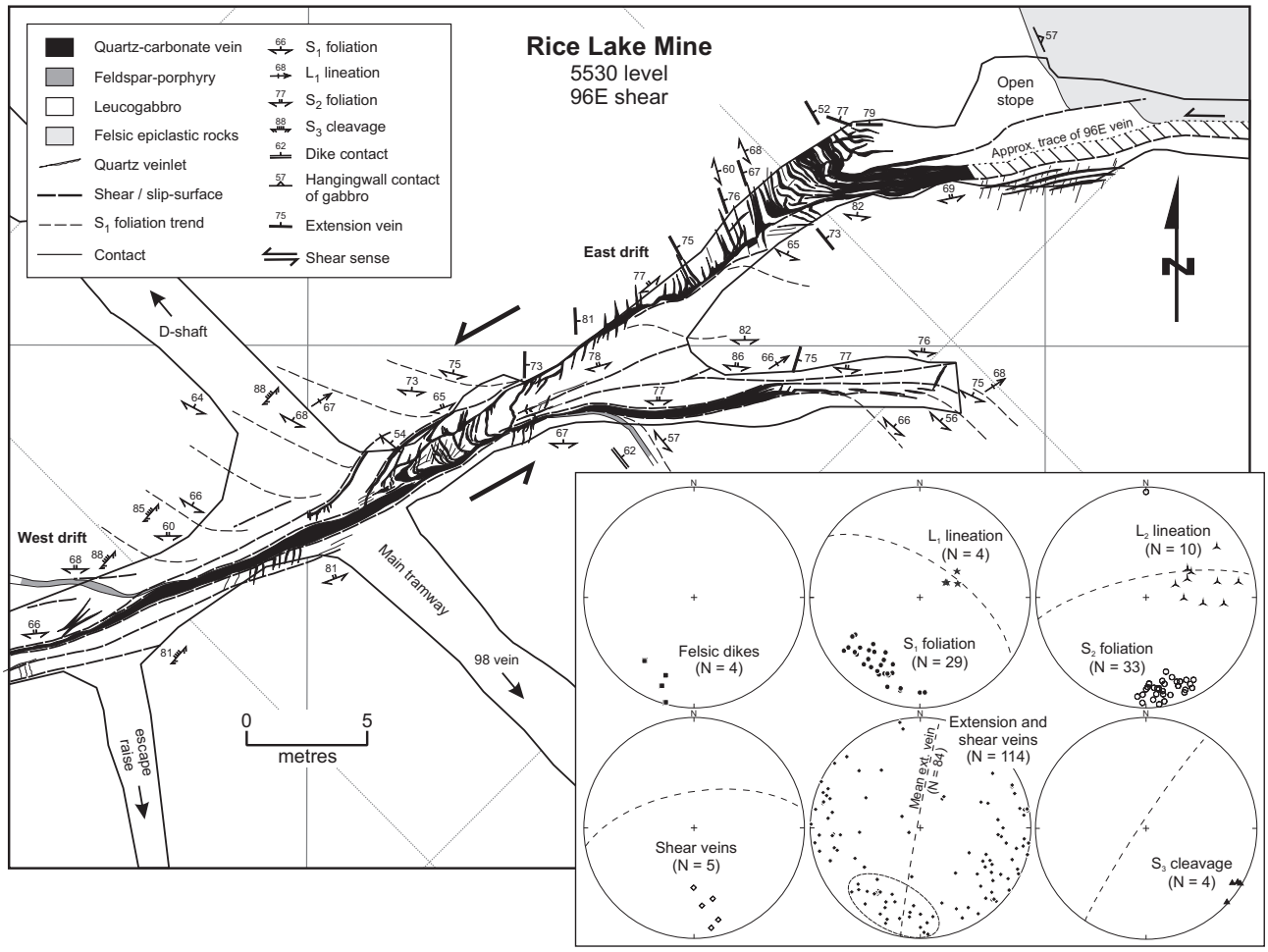

Figure 16: *Detailed map of a typical NE shear and 16-type vein at 5530 level in the Rice Lake mine (96E vein). Structural data are plotted on lower-hemisphere, equal-area stereonets (ellipse indicates veins that parallel the wallrock S_1 foliation). Local generations of structure correspond to the regional generations as follows: S_1-L_1 = ductile G_3; S_2-L_2 = brittle-ductile G_3; S_3 = G_4. Note the left-lateral offset of the hangingwall contact of the SAM unit and refraction of the shear across the contact.*

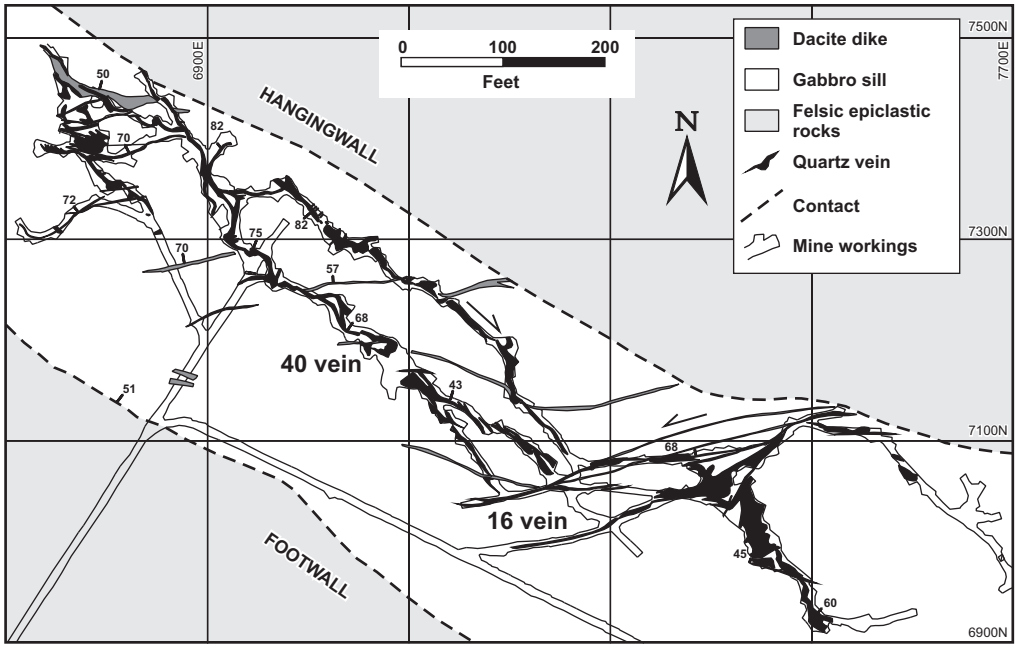

Figure 17: *Simplified geology at 7750 level of the Rice Lake mine, showing the distribution and geometry of NE shears (host to the 16 vein) and NW shears (host to the 40 vein) in the upper portion of the SAM unit (from mine geology plans; after Rhys, 2001). Note the left-lateral offset of the hangingwall sill contact along NE shears and right-lateral offset of dacite dikes long NW shears.*

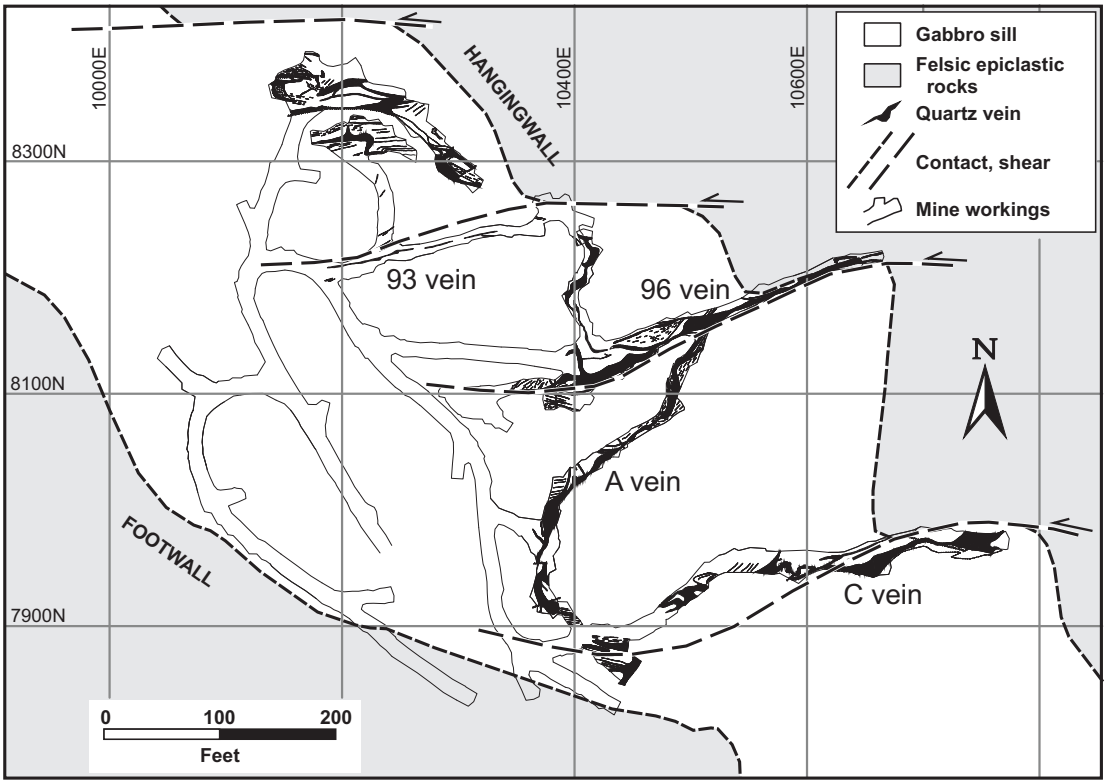

Figure 18: *Simplified geology at 4980 level of the Rice Lake mine, showing the distribution and geometry of NE shears (host to the C, 96 and 93 veins) and NW shears (host to the A vein) in the upper portion of the SAM unit (from mine plans; after Rhys, 2001). Note the left-lateral offset of the hangingwall sill contact along the NE shears, and apparent back-rotation of this contact and the A vein in structural blocks bounded by NE shears. Note also that the footwall contact is not offset, indicating that the displacements were accommodated internally, perhaps due to the lesser competence of the melagabbro.*

that formed where the host shears refracted into the sill across the hangingwall contact (Figure 16). Left-stepping dilational jogs also host major orebodies in the Hinge deposit, where they appear to result from refraction of NE shears through the stratified lithofacies of the Townsite dacite (Figure 19). The fault-fill veins are characterized by laminated, massive and brecciated textures, with multiple slip surfaces and stylolitic pressure-solution seams, indicating repeated cycles of fault-slip, dilation, hydraulic fracturing, hydrothermal sealing and stress accumulation consistent with fault-valve behaviour (e.g., Sibson et al., 1988; Cox, 1995).

Most shears are associated with peripheral arrays of en échelon extension fractures (quartz-filled) that vary from planar to prominently sigmoidal (S-asymmetric; Figure 16). In the western domain, the lateral tips of these fractures typically strike to the south-southwest and dip steeply northwest (Figure 14e, 16). The geometry of the peripheral extension veins, coupled with asymmetric fabrics in the shears, offset markers and the geometry of the dilational jogs indicate sinistral-reverse oblique-slip shear. Apparent displacements are generally less than 10 m, but range up to approximately 50 m for the thickest, most-continuous shears. The bulk-slip vector calculated from the mean orientations of NE shears in the western domain plunges shallowly to the east-northeast (Figure 20), at a shallower angle than the lineations in the shear planes (Figure 14d). This discrepancy may be due to reactivation or may indicate a non-ideal stress configuration during shearing (e.g., the intermediate principal stress, σ_2, may not have coincided with the shear plane; Blenkinsop, 2008).

Northwest-trending shears (NW shears)

The NW shears are also developed throughout the mine trend, but tend to be thinner, less continuous and more widely spaced than NE shears. They coincide in outcrop with topographic lineaments that also tend to be more subtle and less continuous than those associated with NE shears. The one exception occurs in the eastern domain, where a major NW shear is traced along strike for 900 m (Figure 15). In the western domain, NW shears typically strike to the northwest and dip steeply or moderately to the northeast (Figure 14d) but also include a minor subset of shears that dip steeply to the southwest. In the eastern domain, they strike to the west-northwest and dip steeply to the northeast (Figure 14j). Within both domains, NW shears crosscut primary structures at a clockwise angle but tend to be more variable in orientation than NE shears. The apparent absence of a pre-existing anisotropy in the northwest direction likely explains the comparatively poor development and variable orientations of NW shears.

In most locations, these shears are characterized by discrete planar slip-surfaces or narrow (<50 cm) zones of cataclasite that truncate the external S_3 shape fabric. Unlike NE shears, NW shears do not contain continuous zones of mylonite and most appear to have been arrested in the early stages of development. Incipient NW shears are typically marked by

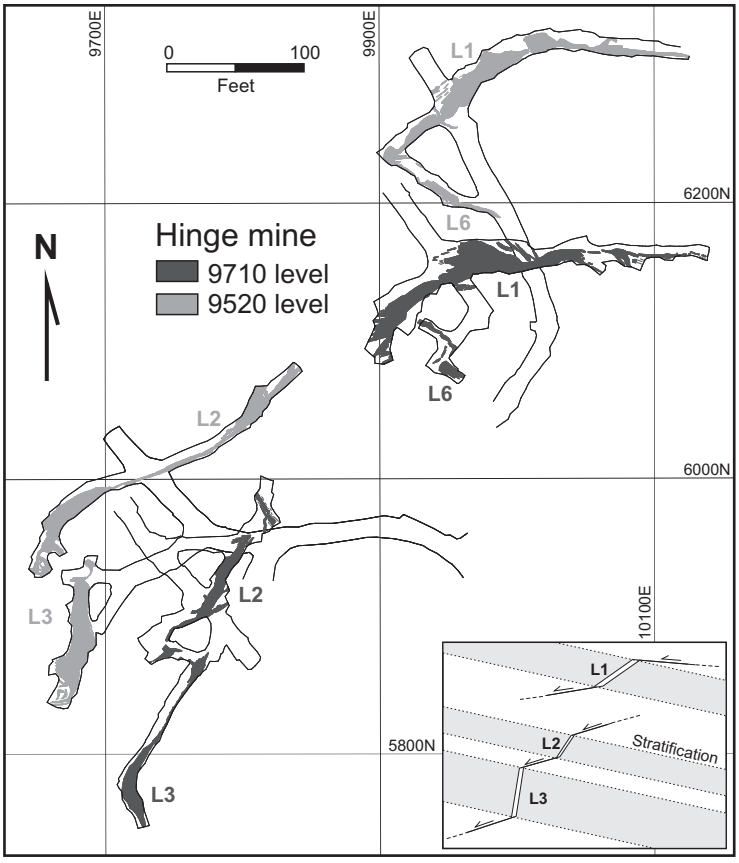

Figure 19: *Composite plan of vein systems at 9710 and 9520 levels of the Hinge mine (simplified from mine plans), showing the geometry of the main ore lenses (L1–L3) and a schematic model (inset) involving refraction of NE shears through a multi-layer system (stratified lithofacies of the Townsite dacite) and vein emplacement in left-stepping dilational jogs.*

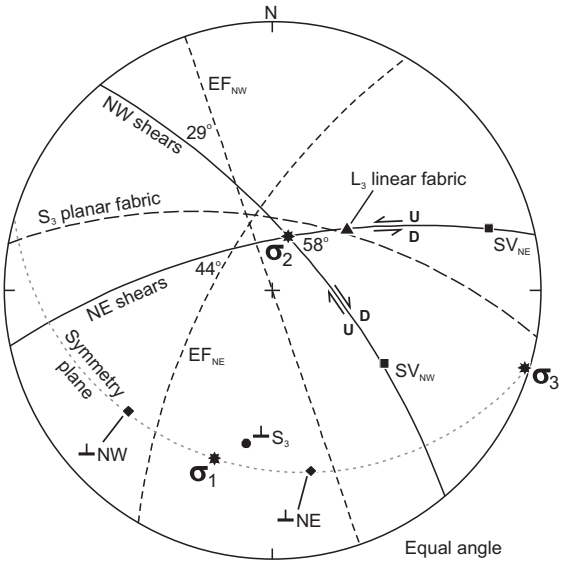

Figure 20: *Lower hemisphere, equal-angle stereographic projection showing the mean orientations of the principal G_3 deformation structures in the western domain of the mine trend, and the calculated orientations of the near-field principal stress axes during development of the shears and associated quartz vein systems. EF_{NE}, mean extension fracture associated with NE shears; EF_{NW}, mean extension fracture associated with NW shears; SV_{NE}, calculated slip vector for NE shears (90° from the line of intersection between the mean shear and extension fracture); SV_{NW}, calculated slip vector for NW shears. The symmetry plane contains the poles to the mean NE and NW shears.*

en échelon arrays of subvertical extension fractures that trend north-northwest (in the western domain) and are quartz filled. In some locations, it is apparent that these extension veins nucleated on, and locally linked, small-scale heterogeneities in the rock mass, such as out-sized boulders in conglomerate. At a later stage of development, these veins were linked by through-going slip surfaces and fault-fill veins, which tend to be thin and discontinuous in comparison to those along NE shears. These veins have weakly laminated internal structures and local stylolitic pressure-solution seams composed of fine-grained pyrite, tourmaline and/or chlorite.

The lateral tips of NW shears appear to be mostly defined by NE shears; the resulting lines of intersection plunges steeply to the north. Offsets of markers are right-lateral and apparent displacements are generally less than 2 m. Peripheral arrays of en échelon quartz-filled extension fractures vary from planar to sigmoidal (Z-asymmetric). In the western domain, the lateral tips of these fractures typically strike to the north-northwest and dip subvertically (Figure 14e). Coupled with offsets and dilational jogs, the geometry of the extension veins indicates dextral-normal oblique-slip shear along the NW shears. Slickenlines and chlorite lineations on slip-surfaces plunge steeply or moderately to the northeast, roughly parallel to the L_3 lineation in the NE shears and wallrocks. In contrast, the bulk-slip vector calculated for NW shears in the western domain plunges moderately to the southeast, at a significant angle to lineations in the shear planes (Figure 14d). As with the NE shears, this discrepancy may indicate a non-ideal stress configuration

during shearing, but is thought to be more likely a result of reactivation.

In the Rice Lake deposit, NW shears consist of relatively discrete brittle faults that are preferentially hosted by leucogabbro in the upper portion of the SAM unit. Intermediate dikes are offset in a right-lateral sense across the faults (Figure 17); apparent displacements are generally less than a few metres (Lau, 1988; Lau and Brisbin, 1996). The faults host irregular stockwork-breccia veins, referred to as '38-type' in local mine terminology, that constitute major orebodies in the Rice Lake deposit, where they range up to 500 m in length and up to 10 m in thickness. Stockwork-breccia veins are locally developed elsewhere, most notably in the Gabrielle, 007 and Wingold deposits. Fully developed stockwork-breccia veins consist of sinuous zones of silica-cemented hydrothermal breccia, laminated fault-fill quartz and complex vein stockworks that transition outward into peripheral arrays of extension fractures that vary from subhorizontal to subvertical, with the latter being of highly variable strike (Figure 21, 22). Jigsaw-fit textures of wallrock fragments indicate in situ fragmentation during intense hydraulic fracturing. Fault-fill veins are a relatively minor component and are typically less complex and continuous as compared to those hosted by NE shears. In the upper levels of the Rice Lake mine, subvertical stockwork-breccia veins strike roughly parallel or very slightly clockwise to the SAM unit and are arranged en échelon down the dip. They are limited in dip extent by the leucogabbro contacts. With increasing depth in the deposit, the veins develop a more pronounced left-stepping geometry in plan view that appears to reflect the oblique slip direction of the NE shears, coupled with back-rotation of shear-bounded blocks (Figure 18; see below).

Discussion

The NE shears transect stratigraphy at shallow counterclockwise angles and appear to have been controlled, at least in part, by primary anisotropy (dikes) in relatively competent rock types. They contain tabular or lenticular fault-fill veins that record incremental emplacement during progressive shear. In contrast, NW shears transect stratigraphy at oblique clockwise angles and do not appear to be controlled by primary anisotropy. They contain irregular stockwork-breccia veins that were evidently emplaced by a less incremental process, perhaps associated with catastrophic releases of overpressured fluids during discrete rupture events. Nevertheless, the close spatial association and mutual crosscutting relationships indicate that NW and NE shears were coeval (e.g., Poulsen et al., 1986). Similarities in the mineralogy of veins and associated wallrock alteration indicates that they probably also channelled the same or similar fluids.

The geometry and kinematics of the shears are compatible with a conjugate set (e.g., Stockwell, 1938; Rhys, 2001), with NW shears being antithetic and subsidiary to NE shears. Their broadly symmetrical arrangement to the ductile S_3-L_3 shape fabric is interpreted to indicate that they formed during a later increment of the same deformation, which accommodated north-northeast – south-southwest–directed shortening at a near-orthogonal angle to the hostrock primary anisotropy. The brittle-ductile nature of the shears may relate to transiently higher strain rates or fluid pressures, or strain-hardening effects during late increments of this deformation.

Antithetic faults are a common feature of 'linking damage zones' in natural fault systems, and typically develop between the lateral tips of overstepping or understepping segments of subparallel and adjacent faults (Kim et al., 2003). Antithetic faults develop in subparallel arrays at high angles to principal faults and typically delimit en échelon rectilinear structural blocks, which are commonly rotated. This structural geometry is observed at scales varying from centimetres (Kim et al., 2004) to tens of kilometres (Nicholson et al., 1986), and has been reproduced in analogue model experiments of strike-slip faulting in zones of distributed shear deformation (Schreurs, 1994). As shown schematically in Figure 23, the sense of slip on subsidiary faults may vary in response to local boundary conditions, or due to differential slip on principal faults, leading to rigid-block rotation and, depending on the sense of rotation, contraction or extension across the damage zone. The later scenario is evident in the deeper levels of the Rice Lake mine, where NW shears define the western edges of tabular or wedge-shaped blocks that were apparently back-rotated in the overstep areas between adjacent NE shears (Figure 18). Down-dip slickenline lineations indicate that some NW shears were also reactivated, perhaps as compressional oversteps during a later increment of G_3 deformation (Figure 23). Reactivation may explain why NW shears in the Rice Lake mine are flanked by peripheral arrays of subhorizontal extension fractures, the geometry of which is difficult to reconcile with the right-lateral offsets of markers across the shears (e.g., Lau, 1988; Lau and Brisbin, 1996).

Field trip road log and stop descriptions

This field trip is designed to take place over a period of three full days. Stops on Day 1 (Figure 4) are intended to provide an overview of the geology, stratigraphy, structural evolution and tectonic setting of the Rice Lake district, and will include opportunities to examine most of the principal map units and deformation structures. Stops on Day 2 (Figure 12) will focus specifically on the Rice Lake mine trend, and will provide participants with an opportunity to examine: 1) the character and stratigraphy of the volcanic, volcaniclastic and subvolcanic intrusive hostrocks to gold mineralization; 2) the geometry and overprinting relationships of mesoscopic deformation structures and associated arrays of auriferous quartz-carbonate veins; 3) the effects of hydrothermal alteration. Day 3 of the field trip will provide an underground tour of quartz-carbonate vein systems in the one of the active mines in the Rice Lake mine trend, with the location determined by the production schedule on that day.

From Winnipeg, take Highway 59 north from the north perimeter (Highway 101) to the junction with Provincial Road 304 (approximately 70 km driving distance). Turn right (east) onto PR304 and travel approximately 35 km to the town of Powerview-Pine Falls. Continue north across Highway 11 (crossing the Winnipeg River at the Pine Falls hydroelectric generating station) and follow PR304 north then east for 119 km to the town of Bissett (total driving distance approximately 224 km; plan for 3 hours driving time). Note that PR304 is unpaved from

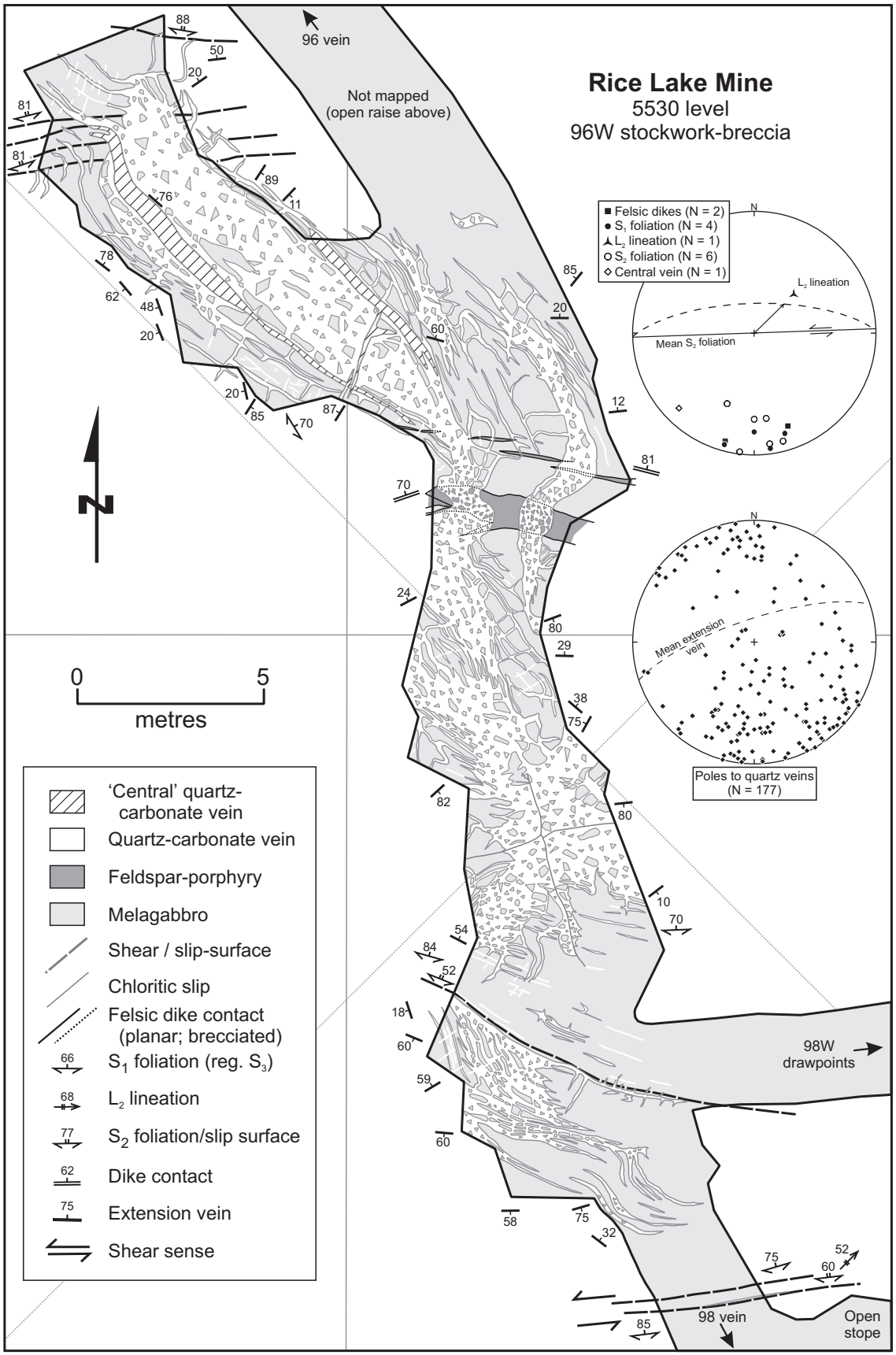

Figure 21: *Detailed map of a typical NW shear and stockwork-breccia (38-type) vein at 5530 level in the Rice Lake mine (96W vein), showing the characteristic internal complexity. This structure splays off the hangingwall of a major NE shear to the south, which hosts the fault-fill–type 98 vein. Note that the vein overprints feldspar-porphyry dikes and several subsidiary NE shears without significant offset. Structural data are plotted on lower-hemisphere, equal-area stereonets. Local generations of structure correspond to the regional generations as follows: S_1 = ductile G_3; S_2-L_2 = brittle-ductile G_3.*

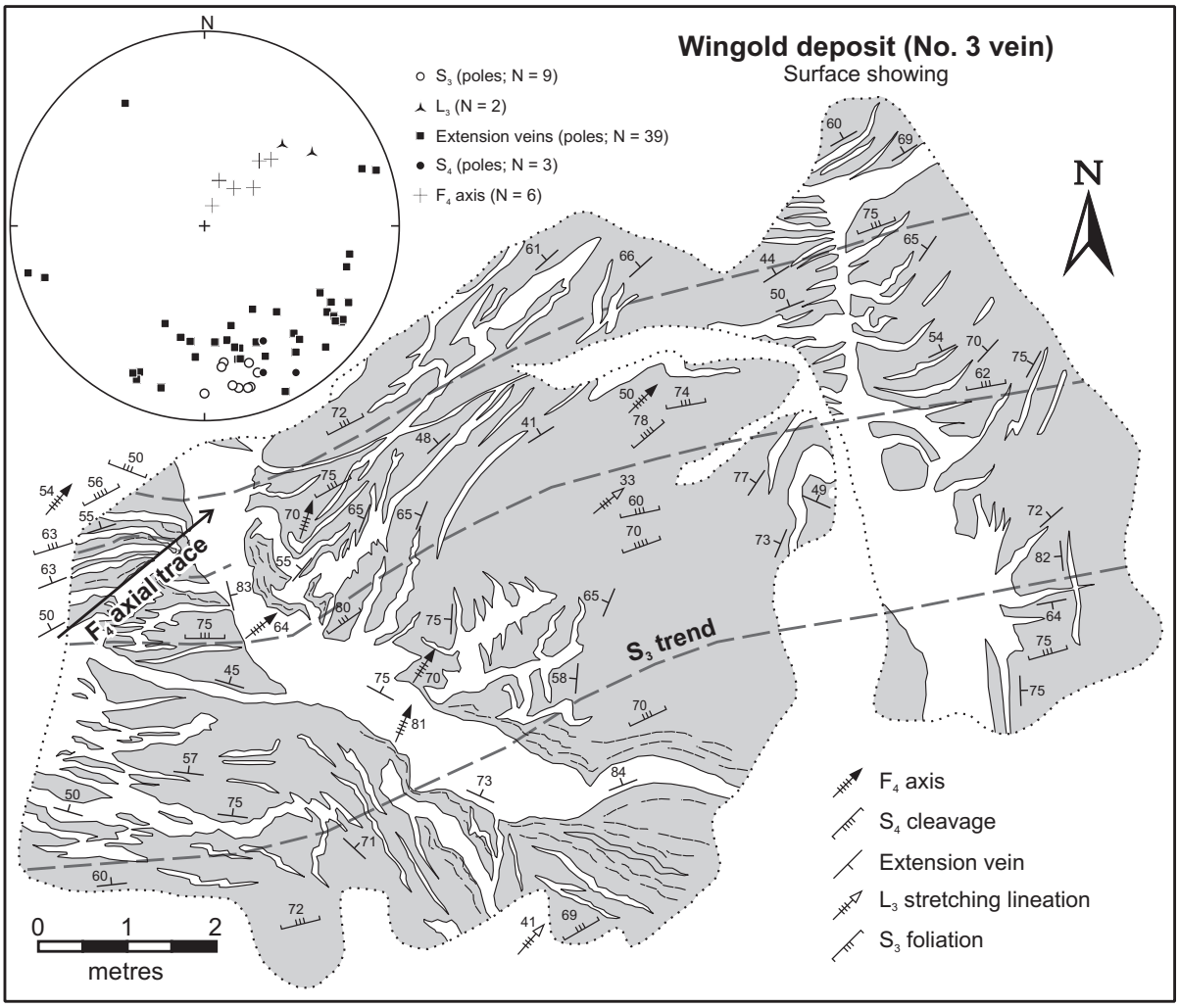

Figure 22: *Detailed map of the surface showing of the Wingold deposit (see Figure 15 for location), showing a NW shear vein, with peripheral arrays of extension veins. The fault-fill vein cuts the regional S_3-L_3 shape fabrics in the hostrock and is overprinted by the northeast-trending S_4 cleavage and open F_4 folds. Structural data are plotted on a lower-hemisphere, equal-area stereonet.*

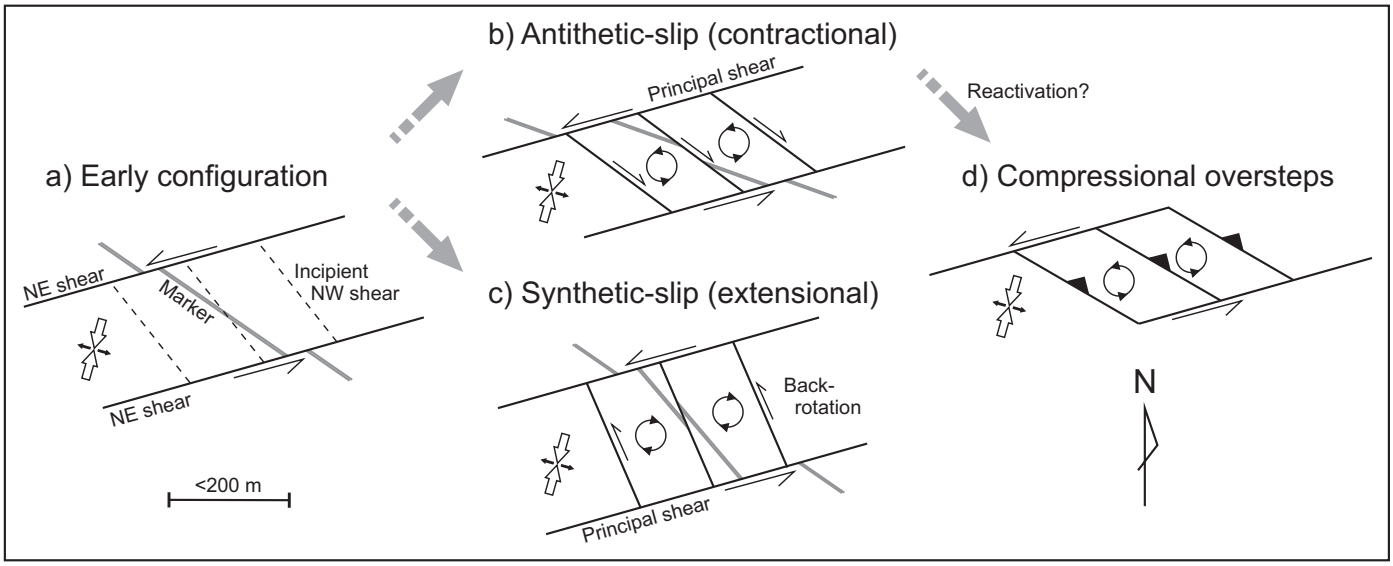

Figure 23: *Schematic plan view illustrating the structural geometry of NE and NW shears, and two kinematic models that incorporate differential slip, subsidiary faulting and block-rotation to explain the observed geometry:* ***a)*** *initial configuration;* ***b)*** *counter-clockwise rotation of blocks and antithetic slip on NW shears, with resulting contraction across the block-faulted domain;* ***c)*** *clockwise rotation of blocks and synthetic slip on NW shears, with resulting extension across the block-faulted domain;* ***d)*** *reactivation (northeast-side-up) of antithetic NW shears in a compressional overstep joining two NE shears.*

the bridge over the Manigotagan River to the town of Bissett (45 km) and includes many sharp corners. The shoulders along this section of road are steep and locally clay-based, and are extremely soft and slippery when wet. Use caution when making way for oncoming traffic.

Locations for all field trip stops are provided in Universal Transverse Mercator (UTM) grid co-ordinates (Zone 15; NAD83 datum).

Day 1: Geological setting of the Rice Lake district

Set the odometer to zero at the post office in Bissett (look for the dilapidated log cabin on the north side of PR 304, approximately 400 m east of Wynne's Place restaurant and store). From the post office drive 7.7 km east on PR304 to the junction with the Rainy Lake logging road on the right (look for the orange gate and millstones approximately 200 m south of PR304). Park at the intersection and walk south on the logging road for 2.5 km (approx. 30 minutes travel time) to a large clean outcrop in an open area 50 m to the left (east) of the road, on the north margin of the bog.

Stop 1-1 (319721mE, 5654228mN): Ross River pluton

This outcrop is located 300 m south of the north contact of the Ross River pluton and provides an opportunity to examine auriferous quartz-carbonate veins hosted by a granitoid intrusion, which is a somewhat atypical setting for mineralization in the Rice Lake belt. In this area, the Ross River pluton consists of medium to coarse-grained tonalite or granodiorite that contains sparse phenocrysts of plagioclase, hornblende and biotite. It also contains rare mafic xenoliths and aplitic dikes, but is otherwise homogeneous and massive. Along the north margin of the pluton large rafts and angular xenoliths of gabbro indicate its intrusive relationship with the Rainy Lake Road unit of the Gem assemblage to the north. Homogeneous biotite granodiorite from the central portion of this pluton yielded a U-Pb zircon age of 2724 ±1 Ma, indicating that it was emplaced broadly coeval with the Gem assemblage (Anderson, 2008).

At Stop 1-1, the granodiorite contains a series of brittle-ductile shear zones associated with moderate to strong ankerite-chlorite-sericite-silica alteration and minor quartz-carbonate veins. Outside the shear zones, alteration is manifest by replacement of primary hornblende and biotite by chlorite and epidote. The shear zones trend toward the west or northwest and range up to 1.5 m thick. They are defined by discrete zones of intense foliation development and closely-spaced shear fractures that dip steeply north or northeast and contain chlorite or slickenline lineations that plunge shallowly to the east. Asymmetric fabrics (e.g., S-C fabric, shear bands, asymmetric boudins and drag-folds) typically indicate dextral shear (one shear trends toward the west-southwest and contains sinistral kinematic indicators, compatible with a conjugate relationship). Late slip-surfaces, perhaps resulting from reactivation, are associated with thin seams of black pseudotachylite. Granodiorite along the margins of these structures is strongly fractured and contains quartz-carbonate veins up to 20 cm thick that locally contain coarse visible gold. The veins consist of microcrystalline smoky-grey quartz, which is more typical of veins along the southeast margin of the Ross River pluton in the vicinity of the past-producing Ogama-Rockland mine.

Return to the logging road and walk north for approximately 1.1 km to a low, south-facing outcrop ledge just off the right (east) shoulder of the road.

Stop 1-2 (319840mE, 5655241mN): Gem assemblage, Rainy Lake Road unit

This outcrop exposes thin-bedded feldspathic greywacke, mudstone and chert in the medial section of the Rainy Lake Road unit of the Gem assemblage (Figure 4, 8), which is interpreted to record deposition in a relatively quiescent marine setting, in the hangingwall of the postulated synvolcanic subsidence structure (G_1) immediately to the west. Planar beds dip at moderate angles to the northwest and include normally-graded beds with well-developed load structures, indicating deposition via downslope turbidity flows. The outcrop contains two generations of asymmetric folds. The older generation, consisting of contorted and locally disrupted beds, are locally truncated by overlying beds and are thus interpreted to represent soft-sediment slump structures. The younger generation, consisting of open to tight S-folds of bedding with an associated fine-scale axial planar cleavage, are interpreted to be parasitic to the macroscopic Beresford Lake anticline (G_3) that dominates the structure in the eastern Rice Lake belt (Figure 2). Further up section, these rocks are intruded by thick sills of MORB-like tholeiitic gabbro. The lower contact of one of these sills is exposed in the northern portion of this outcrop and shows a particularly thick chilled margin, consistent with high-level emplacement.

Proceed north (back toward PR304) on the logging road for 300 m to a south-facing outcrop just off the left (west) shoulder of the road, near the base of a low outcrop ridge.

Stop 1-3 (319689mE, 5655519mN): Gem assemblage, Rainy Lake Road unit

This outcrop shows a 25 m thick section of well-stratified felsic epiclastic rocks at the top of the medial section of the Rainy Lake Road unit (Figure 4, 8). Thick to thin-bedded, pebbly volcanic sandstone in this section contains subordinate interbeds of laminated sulphidic mudstone and heterolithic pebble conglomerate. Planar sandstone beds vary from massive to normally-graded; local scours indicate these rocks are upright. A sharp depositional contact separates these epiclastic rocks from overlying pillowed to massive flows of MORB-like tholeiitic basalt, which dominate the upper section of the basin-fill and are interpreted to record incipient rifting of the underlying Bidou assemblage.

A crudely-graded layer of volcanic conglomerate in this section was sampled for U-Pb geochronological analysis to constrain the age of basin infilling. The layer is 3.0 m thick and is marked at the base by a sharp undulatory contact that locally cuts down through an underlying bed of black mudstone. It is reversely size-graded at the base and normally-graded in the upper portion, consistent with a subaqueous debris flow. The conglomerate is matrix supported and poorly sorted, and contains angular to subrounded clasts of feldspar-phyric dacite, with subordinate clasts of porphyritic andesite, aphyric and

quartz-phyric rhyolite, felsic tuff, amygdaloidal basalt, mudstone and solid sulphide. The sulphide clasts are angular and consist mainly of pyrrhotite with minor chalcopyrite, consistent with derivation from a proximal fault-controlled exhalative site.

U-Pb (TIMS) analyses of single detrital zircons yielded one concordant analysis with a $^{207}Pb/^{206}Pb$ age of 2747 ±6 Ma, and one near-concordant (–0.5%) analysis with an age of 2727 ±1 Ma. Two other single zircon crystals gave slightly discordant analyses with ages of 2731 ±0.5 Ma (1.1% discordant) and 2727 ±3 Ma (3.2% discordant), whereas a multigrain fraction (5 grains) gave a slightly discordant analysis (2.6%) with an age of 2737 ±1 Ma. The essentially identical ca. 2727 Ma $^{207}Pb/^{206}Pb$ ages of two of the single-zircon analyses give a weighted-average age of 2727 ±2 Ma, which is interpreted to represent the maximum depositional age. In keeping with the heterolithic nature of the conglomerate, the slightly older ages are interpreted to reflect slightly older detrital components, likely derived from the Bidou assemblage in the footwall of the subsidence structure.

Return to PR304. Drive 2.5 km west (back toward Bissett) on PR304 to an unmarked turnoff leading to a large rock quarry on the right (north) side of the road. Turn right off PR304 and park in front of the large boulders blocking the entrance to the quarry. Caution: due to the possibility of falling rock, participants are asked to remain well back from the quarry walls.

Stop 1-4 (317247mE, 5656681mN): Gem assemblage, Round Lake unit

The quarry in this location is situated along the south margin of the Wanipigow fault (WF) and exposes strongly deformed felsic epiclastic rocks of the Round Lake unit of the Gem assemblage (Figure 4). In the walls of the quarry, thin intervals of planar-bedded volcanic sandstone separate 1–3 m thick layers of heterolithic, poorly sorted, pebble to cobble volcanic conglomerate. Bedding dips steeply north and normally-graded sandstone beds and rare scours indicate these rocks are upright. To the north, these rocks are cut by a slightly discordant quartz-feldspar porphyry intrusion that yielded a U-Pb age of 2715 ±2 Ma (Anderson, 2008), which represents the minimum depositional age for the Gem assemblage at Rice Lake.

Aspect ratios of deformed clasts in horizontal vs. vertical exposures define a shallowly east-plunging stretching lineation, which is interpreted as a composite fabric formed via reorientation and attenuation of the regional L_3 shape fabric during progressive non-coaxial shear (G_4 and G_5) along the south margin of the WF (Figure 5). Vertical outcrop surfaces show a somewhat less pronounced planar shape fabric. Seams of mylonite and ultramylonite are conspicuous in the clean outcrop surface on the eastern flank of the quarry and are interpreted as G_5 structures resulting from transcurrent shear deformation. Shear bands, porphyroclast systems and asymmetric boudins in these outcrops indicate dextral shear; antithetic shear bands may indicate a component of synkinematic zone-normal shortening.

Return to PR304. Drive 300 m west (back toward Bissett) on PR304 to an unmarked turnoff leading to a gravel pit on the right (north) side of the road. Turn right and park in the bottom of the pit.

Stop 1-5 (316965mE, 5656619mN): Gem assemblage, Round Lake unit

Outcrops along the north side of the sand quarry in this location consist of heterolithic volcanic conglomerate of the Round Lake unit, at approximately the same stratigraphic position as the previous outcrop (Figure 4). Significantly higher finite strain has all but obliterated the primary clastic textures in this location. Aspect ratios of deformed clasts in the horizontal outcrop surface locally exceed 100:1 (X:Z), which is anomalous in comparison to other rocks in the area. Locally asymmetric fabrics indicate dextral shear. The unusually high finite strain recorded by these rocks may be a consequence of their location near the confluence of the Wanipigow fault and Normandy Creek shear zones (Figure 4).

Return to PR304. Drive back through Bissett on PR304 to the intersection with Quesnel Lake road (5.7 km from the post office in Bissett). Turn left (south) and proceed along the Quesnel Lake road for 6.6 km to the short causeway at the outlet of Red Rice Lake (marked by small wooden sign on right side of road). Caution: the Quesnel Lake Road is narrow, with soft shoulders and abundant sharp curves. Drive 100 m further south along Quesnel Lake road to an unmarked turnoff to a partially overgrown bush-road on the left (east) side of the road.

Park at the turnoff and walk east along the bush road for 550 m to a fork in the road. Follow the orange flagging tape in a general northwesterly direction along an overgrown skidder trail to a large stripped outcrop (approximately 750 m walking distance).

Stop 1-6 (311477mE, 5653788mN): San Antonio assemblage

As originally described by Stockwell (1938), this outcrop shows the intact unconformable contact between the San Antonio assemblage and underlying intermediate volcaniclastic rocks of the Independence Lake unit of the Bidou assemblage (Figure 4). In this location, it is also possible to demonstrate the angular nature of the unconformity (Figure 24). Crudely stratified tuff breccia at the east end of the outcrop is crosscut by an andesite dike and contains three generations of planar fabric, corresponding to the regional S_3, S_4 and S_5 fabrics. The S_3 fabric trends northwest, slightly clockwise from S_0, and is defined by flattened clasts and a continuous chlorite foliation in the matrix. This fabric is overprinted by a finely-spaced crenulation cleavage (S_4) that trends west-northwest and is well-preserved in the flattened clasts, where it transects the long axes at shallow counter-clockwise angles. Both of these fabrics are overprinted by a spaced shear-band cleavage (S_5) that trends north-northwest and has a dextral sense of asymmetry. A north-trending crenulation cleavage in the andesite dike may correspond to the regional S_6 fabric or, alternatively, the S_5 fabric that was refracted through the dike.

The base of the San Antonio assemblage is marked by a 1–1.5 m thick layer of pebble-cobble conglomerate composed mostly of intermediate volcanic detritus, with scattered pebbles of vein quartz. Near the top, the conglomerate contains interbeds of quartz arenite up to 1 m thick. These rocks are overlain

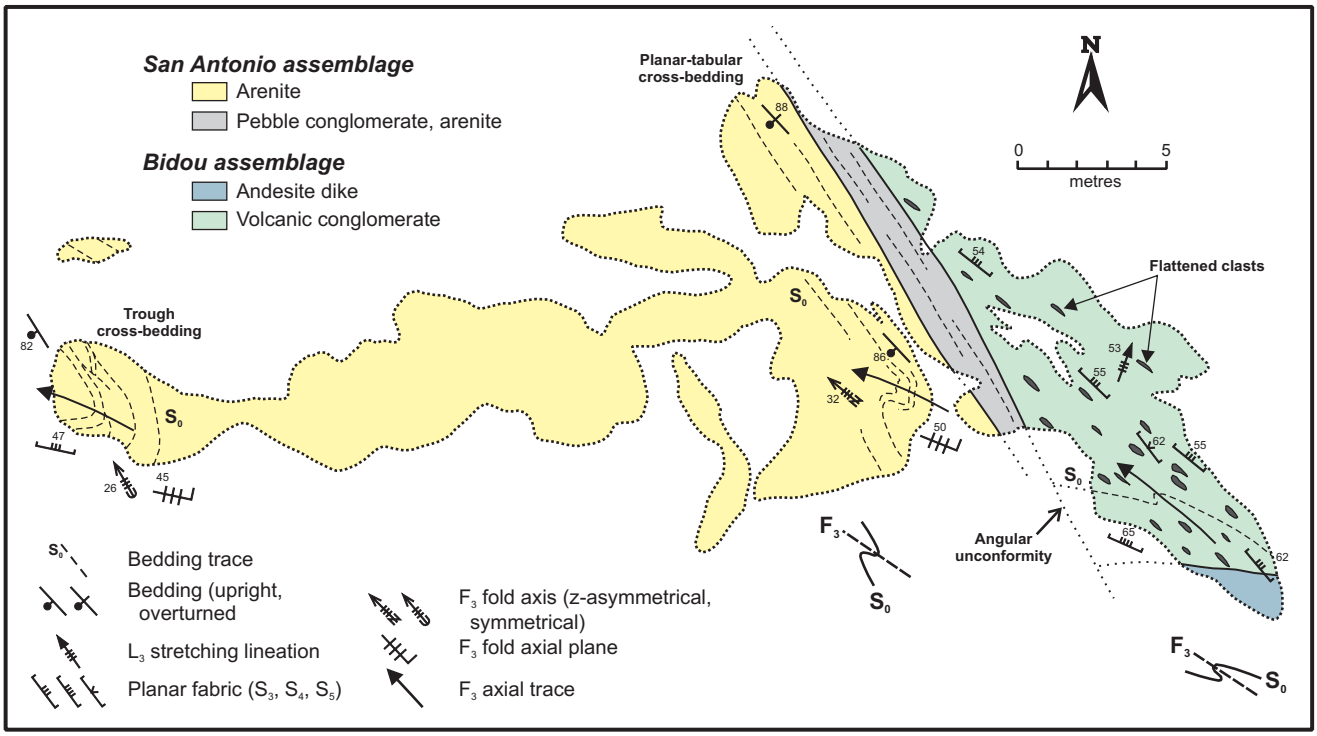

Figure 24: *Detailed outcrop map showing the angular unconformity at the base of the San Antonio assemblage. This locality, 600 m northeast of Red Rice Lake, was originally mapped and described by Stockwell (1938). The change in fold vergence across the contact in this location indicates the angular nature of the unconformity.*

to the west by medium-grained quartz arenite that contains crossbeds and local ripple cross laminations; bedding here dips steeply southwest or northeast (overturned), oblique to stratification in the underlying rocks. The S_3 fabric trends northwest, slightly counter-clockwise from S_0, and is defined by a weak chlorite-sericite foliation; the change in S_0-S_3 vergence indicates the angular nature of the unconformity. Further up section, coarser-grained pebbly arenite is trough crossbedded.

Detrital zircons from arkosic greywacke near the base of the San Antonio assemblage along strike to the west (north of Red Rice Lake) range in age from 2.98 to 2.7 Ga and define two population modes at 2.98–2.84 and 2.76–2.71 Ga (Percival et al., 2006a). The older population distinguishes these rocks from superficially similar sandstones in the Bidou and Gem assemblages, and is interpreted to signal the arrival of detritus from the uplifted margin of the North Caribou terrane. The youngest analyzed zircon from this sample has an age of 2705 ±5 Ma (Percival et al., 2006a), representing the maximum depositional age of the assemblage.

Return to Quesnel Lake road. Drive south for 500 m to a sharp left turn at the southeast corner of Red Rice Lake. Park in the cleared area on the right side of the road at the turn.

Stop 1-7 (311100mE, 5652607mN): San Antonio assemblage

This outcrop shows tonalitic conglomerate and sandstone at the base of the San Antonio assemblage, on the southern limb of the G_3 Gold Creek syncline. The outcrop on the south side of the trail to the lake consists of unstratified monomictic conglomerate composed of closely-packed subangular to rounded cobbles and boulders of medium-grained, equigranular tonalite in a matrix of pebbly feldspathic wacke and rare mudstone. Erosion and transport of tonalite, as opposed to in-situ brecciation, is indicated by aplite dikes in some clasts that cannot be traced through the matrix or into adjacent clasts. These rocks have been interpreted to represent a landslide facies that was deposited in close proximity to a basin-bounding fault scarp (Weber, 1971b). The easternmost tip of this outcrop may expose the unconformable contact with underlying volcaniclastic rocks of the Bidou assemblage, which appear to be cut by a pale pink felsic dike that does not extend into the adjacent conglomerate.

The conglomerate coarsens toward the west, where it is exposed in a series of outcrops that extend up to the contact of the large tonalite pluton of the Ross River plutonic suite. Boulders in these outcrops range up to several metres across and are surrounded by a distinctly muddy matrix. As described by Stockwell (1938) and Davies (1963), a nonconformable contact between the conglomerate and underlying pluton is exposed further along strike to the west.

The outcrop on the north side of the trail leading down to Red Rice Lake consists of a heterogeneously transposed section of interbedded medium- to very coarse grained pebbly feldspathic wacke (tonalite grit), pebble conglomerate and sericitic mudstone. Lenticular packets of intact, moderately northwest-dipping bedding are separated by northwest-trending zones of intense transposition and foliation development. Within these packets, a spaced crenulation cleavage is oriented nearly orthogonal to bedding and overprints an early bedding-parallel (S_2?) foliation. The transposition fabric and crenulation cleavage (S_3) are axial planar to the G_3 Gold Creek syncline, which plunges shallowly to the northwest, and are transected at

a shallow counter-clockwise angle by the S_4 crenulation cleavage. The surface of the outcrop is oriented nearly parallel to the F_3 enveloping surface, obscuring its bedded aspect.

Return to PR304. Turn left and proceed 100 m west on PR304 to an unmarked turnoff on the right (north) side of the road. Turn right and drive north for 100 m to the low washed outcrop on the right (east), approximately 50 m south of the entrance to the rock quarry.

Stop 1-8 (307249mE, 5657456mN): San Antonio assemblage

This outcrop shows pebbly quartz arenite in the upper portion of the San Antonio assemblage, near the hinge of the G_3 Horseshoe Lake anticline (Figure 4). Here, the quartz arenite contains large-scale trough crossbeds, with bottomsets locally defined by diffuse pebble-lag deposits. The lag deposit in the central portion of the outcrop consists of sericitized clasts of intermediate volcanic and plutonic material. Flattened pebbles and a penetrative sericite foliation define the S_3 planar fabric in this outcrop, which deviates from the regional northwest trend on account of refraction through the overturned limb of the anticline (Figure 4, 5). This fabric is overprinted at a shallow counter-clockwise angle by a finely-spaced S_4 crenulation cleavage. The long axes of the flattened pebbles accentuate the near-orthogonal angular relationship between bedding and S_3, in keeping with the structural location near the hinge of the macroscopic G_3 anticline.

Immediately west of this location, the San Antonio assemblage lies in contact with intermediate volcaniclastic rocks of the Gem assemblage (Gold Creek unit of Anderson, 2008), which likewise face west on the regional S_3 fabric. This older-over-younger map pattern is interpreted to result from imbrication by a G_2 thrust fault.

Return to PR304. Drive west for 4.5 km to the turnoff to Currie's Landing on the right (north) side of the road (marked by small wooden sign and bright yellow "Designated Route R" sign). Proceed 1.1 km northwest along the Currie's Landing road to the turnoff of the Pointer Lake forestry access road on the right. Caution: this road is not maintained and may not be passable by vehicles with low ground-clearance. Turn right (east) and drive for 2.4 km to the bridge over the Wanipigow River. Park 100 m north of the bridge on the right (east) side of the road (location marked by orange flagging). Walk east approximately 50 m to a low bush outcrop.

Stop 1-9 (305114mE, 5661278mN): San Antonio assemblage

This outcrop is situated along the main trace of the Wanipigow fault and shows a spectacular example of strongly-deformed polymictic conglomerate of the San Antonio assemblage (Figure 4). The conglomerate is clast-supported, unsorted and contains minor interbeds of feldspathic wacke. Well-rounded and roughly equant clasts of more competent tonalite contrast with strongly flattened clasts of less competent intermediate to felsic volcanic material. The tonalite clasts typically have well-developed asymmetric tails (σ-type), with local synthetic and/or antithetic shear factures or extension fractures filled with quartz-fibre veins. Gentle to tight Z-folds, which are a characteristic feature of the core of the Wanipigow fault, plunge shallowly east in this location.

U-Pb analyses of detrital zircons from a sample of feldspathic greywacke collected just west of the bridge over the Wanipigow River (Silver Falls) define two distinct age populations at 3010–2940 and 2750–2710 Ma (Anderson, 2008), which is typical of the coarse fluvial-alluvial clastic rocks that define late fault-bounded basins along the NCT-Uchi interface in Manitoba.

Return to PR304. End of Day 1.

Day 2: Stratigraphy and structure of the Rice Lake mine trend

From the post office in Bissett proceed 1.4 km east on PR 304 to the intersection with the access road for the tailings impoundment on the left (north) and the Cohiba portal on the right (south). Turn right (south) and proceed past the portal and over the large outcrop ridge to the intersection with the SG1 road (0.9 km). You are now on the Rice Lake mine property of San Gold Corporation – permissions are required. Turn left and proceed east along the SG1 road for a distance of 2.6 km to the SG1 portal. Caution: use care when passing heavy equipment.

Stop 2-1 (315988mE, 5656048mN): Townsite dacite (SG1 deposit)

Two outcrops will be examined in this location. The first, located at the portal to the SG1 mine, exposes porphyritic volcaniclastic rocks of the 'breccia' lithofacies of the Townsite dacite. This outcrop is situated just above the upper contact of the Shoreline basalt, which was previously well-exposed but was excavated for the portal. The breccia is very strongly deformed and contains a penetrative chlorite foliation and prominent S-L shape fabric defined by flattened and stretched clasts. The stretching lineation plunges at moderate angles to the northeast, and is particularly apparent in the west wall of the portal. The foliation intensifies into narrows zones of chloritic mylonite that locally contain tightly folded and transposed quartz veins; a particularly good example is exposed in the clean outcrop above the portal.

A similarly intense structural overprint characterizes quartz-carbonate veins in the SG1 deposit, which is located beneath the drift-covered area southeast of the portal. The abrupt topographic break on the far side of the cleared area is the fault-scarp corresponding to the main strand of the Normandy Creek shear zone. The SG1 deposit is situated in the immediate hangingwall of this structure, at the contact between felsic volcanic sandstone and conglomerate of the Hares Island formation on the southeast and mafic volcanic rocks that are probably equivalent to the Shoreline basalt on the northwest. The SG1 orebodies consist of quartz-carbonate-pyrite veins and narrow zones of intense, proximal, chlorite-sericite-ankerite-pyrite alteration (large boulders of this material can be examined in the rock dump south of the portal). Both are enveloped by chloritic or sericitic phyllonite and mylonite that contain intense down-dip stretching lineations, with the result that orebodies are strongly

attenuated along strike and down-dip. The mylonitic foliation overprints the regional S_4 cleavage and is thus assigned to the G_5 generation of structure.

The second outcrop to be examined at this stop provides an exposure of the upper contact of the Shoreline basalt, which in this location is separated from the overlying Townsite dacite by a 20–30 m thick unit of volcanic sandstone and conglomerate (Hares Island formation). The basalt is aphyric, non-amygdaloidal and contains irregular epidote nodules, which are a characteristic feature of the Shoreline basalt. The volcanic conglomerate is poorly-sorted, crudely stratified and contains angular to subrounded cobbles and boulders of mafic to intermediate volcanic material. Minor interlayers of bedded volcanic sandstone range up to 20 cm thick and dip steeply to the northwest. Normally-graded beds and low-angle scours indicate these rocks are upright.

Proceed back toward the west on the SG1 road for approximately 1.3 km and park on the right (north) side of the road at the base of the large outcrop ridge to the north. Proceed on foot up onto the outcrop ridge and toward the northeast for approximately 200m.

Stop 2-2 (315058mE, 5655506mN): SAM unit and Shoreline basalt

This large outcrop provides a continuous exposure through the eastern portions of the SAM unit and Shoreline basalt, which are separated in this location by a thin unit of volcanic sandstone and conglomerate. The section here is approximately 100 m thick and, although strongly tectonized, is considered to be primary. Significant gold mineralization is hosted along or within the upper and lower margins of the gabbro and basalt in several locations along strike, most notably in the 007, L10, SG1 and Cartwright deposits.

The SAM unit at the base of the section is composed of fine-grained melagabbro that is very strongly foliated and altered. The deeply pitted outcrop surface is due to preferential weathering of carbonate. Contacts are exposed along strike to the southwest in several locations and are planar, sharp and chilled, and cut at shallow angles across bedding in the country rocks. In this location the gabbro contains large rafts (up to 10 m thick) of felsic volcanic sandstone and conglomerate, the contacts of which are strongly sheared.

The gabbro lies in sharp intrusive contact to the northwest with a 10 m thick unit of heterolithic volcanic conglomerate that is dominated by clasts of plagioclase-phyric dacite and contains up to 5% quartz in the matrix. The conglomerate contains minor interlayers of volcanic sandstone and mudstone; beds dip steeply to the north-northwest. The upper contact with the Shoreline basalt is well-exposed and clearly depositional. Flattened clasts in the conglomerate define the regional S_3 shape fabric. It is overprinted at a shallow counter-clockwise angle by the S_4 crenulation cleavage and at a shallow clockwise angle by the locally developed, spaced, S_5 fracture cleavage.

The Shoreline basalt defines the top of the section and is approximately 30 m thick in this location. Immediately above the basal contact, the basalt is very fine-grained and aphyric, with sparse quartz amygdules up to 5 mm across. The lower portion of this basalt is mostly massive, whereas the top is mostly pillowed, with the latter consisting of bun-shaped pillows up to 50 cm across that have strongly epidotized cores and only minor interpillow hyaloclastite. The medial portion is less well-exposed, but appears to consist of thin alternating flow units of massive, pillowed or brecciated basalt.

Return to the vehicles and proceed west along the SG1 road for approximately 1.4 km to the intersection with the Rice Lake access road. Turn left (south) and, staying left, proceed along the road for approximately 300 m to the 007 vent raise. Park in the cleared area near the raise and proceed on foot in a general southeasterly direction along a drill road for approximately 750 m to a large outcrop near the shore of Rice Lake.

Stop 2-3 (313952mE, 5654806mN): SAM unit (hangingwall contact)

This stop provides an opportunity to examine the SAM unit immediately along strike to the southeast of the Rice Lake deposit, and includes two exposures of the hangingwall contact. The SAM unit in this location is 40–60 m thick and, in contrast to the previous outcrop, is coarser-grained and mesocratic, and contains a variably developed but generally weak foliation. These differences highlight important role of composition and competency in determining the style and intensity of deformation in the SAM unit. Here, the gabbro is typically medium-grained, equigranular and homogeneous, and contains 40–60% intact plagioclase laths. It contains a weak to moderate S_3 foliation that dips steeply toward the north-northwest and is defined by fine-grained chlorite and actinolite. The hangingwall contact dips steeply to the north-northwest, subparallel to the S_3 foliation.

The overlying rocks consist of felsic volcanic sandstone, with minor interbeds of pebble conglomerate and mudstone. Medium to coarse-grained pebbly sandstone defines planar beds up to 1 m thick that are normally-graded and are locally capped by thin beds of mudstone. Bedding dips steeply toward the north-northwest, and is cut at a shallow counter-clockwise angle by the gabbro contact. These rocks contain only patchy weak alteration, in contrast to felsic volcanic sandstone in the equivalent stratigraphic position at the Rice Lake deposit, which is intensely altered (sericite-ankerite-pyrite). The same contact is exposed 150 m further along strike to the west (313802mE, 5654746mN), and is cut by minor shear fractures and quartz veins.

Return to the drill road and walk back toward the vehicles for approximately 550 m, to a point where the road passes between two outcrops. Proceed toward the left (west) along the outcrop ridge for approximately 200 m to a large stripped outcrop near its northwestern extent. Caution: outcrop is extremely slippery when wet.

Stop 2-4 (313555mE, 5655104mN): Shoreline basalt (footwall contact)

This outcrop provides an opportunity to examine the footwall contact of the Shoreline basalt unit in the immediate footwall of the 007 deposit. The contact in this location is unusually well-preserved, with only a minor structural overprint. It trends northwest, dips moderately to the northeast and separates felsic epiclastic rocks of the Hares Island formation from overlying

volcaniclastic rocks of the Shoreline basalt. The stratigraphic section in the stripped portion of the outcrop is approximately 25 m thick. Buff to pale grey felsic volcanic sandstone at the base of the section defines a 10–15 m thick fining-upward cycle. The lower portion of this cycle consists of medium to coarse-grained, massive to faintly stratified sandstone that contains 5–10% quartz grains and 10–15% lithic pebbles. Grain size and bed thickness both decrease upsection and the cycle is capped by a 3 m thick interval in which fine to medium-grained felsic volcanic sandstone is thinly-interbedded with feldspathic greywacke and mudstone. Normally-graded beds, scours and possible ripples indicate these rocks are upright.

The top of the section, above the basal contact of the Shoreline basalt, defines a coarsening-upward cycle approximately 10 m thick, which is capped by massive basalt. Laminated to thin-bedded mafic tuff at the base of this cycle is overlain by stratified lapilli-tuff and lapillistone composed of closely packed, angular to subangular clasts of basalt with delicate shard-like or cuspate shapes. These rocks are in turn overlain by monolithic, clast-supported lapillistone and breccia composed of very angular to subangular basalt clasts ranging up to 30 cm across. The overlying flow is fine-grained and sparsely plagioclase-phyric, with rare quartz amygdules and patchy epidote alteration. This cycle is interpreted to represent a distal to proximal facies transition within an apron of resedimented hyaloclastite (laminated tuff), in-situ hyaloclastite (lapilli-tuff and lapillistone) and hyaloclastic or autoclastic breccia, which were deposited in front of the massive flow and were subsequently overridden.

Walk back along the outcrop ridge to the drill road and from there return to the vehicles. Drive north from the 007 vent raise to the intersection with the SG1 road. Park in the large cleared area southeast of the intersection and continue north on foot along the access road toward PR 304 for approximately 200 m to an outcrop on the left (west) side of the road.

Stop 2-5 (313721mE, 5655612mN): Townsite dacite (stratified lithofacies)

This outcrop exposes faintly stratified breccia and crystal-lithic lapilli-tuff near the footwall contact of the stratified lithofacies of the Townsite dacite, immediately along strike to the east from the Hinge deposit. This outcrop provides a particularly good example of the crosscutting and geometrical relationships of bedding, felsic dikes, ductile S_3-L_3 shape fabrics, and late-G_3 brittle-ductile NW and NE shears.

Diffuse beds of clast-supported breccia in this outcrop strike toward the west-northwest and dip steeply or moderately north. Along the south side of the outcrop, bedding is crosscut by a 20–50 cm thick dike of pale grey aphanitic dacite and both are overprinted by the S_3 fabric, defined here by a continuous foliation and flattened clasts. Both the dike and S_3 fabric dip steeply to the north and are oriented at shallow counter-clockwise angles to bedding. The L_3 stretching lineation is defined by elongate clasts and plagioclase phenocrysts that plunge moderately to the northeast. All of these features are crosscut by northwest or northeast-dipping brittle-ductile shears, corresponding to NE and NW shears of the late-G_3 generation, respectively. Both sets are defined by one or more discrete, planar, slip surfaces and narrow zones of cohesive cataclasite, with minor quartz veins and sericite alteration. Offsets of the dacite dike are right-lateral on the NW shears and left-lateral on the NE shears; mutual overprinting indicates the shears were contemporaneous.

Return along the access road to the vehicles. Drive west along the SG1 road toward the Rice Lake mine to the access road to the Hinge vent raise (approximately 600 m). Park the vehicles in the large cleared area north of the SG1 road and proceed on foot for approximately 150 m to the surface showing of the historical Gold Standard deposit, located 50 m east of the Hinge vent raise. Caution: there is a steep drop-off at the east end of this outcrop.

Stop 2-6 (313354mE, 5655710mN): Townsite dacite (Gold Standard showing)

This outcrop includes the surface showing of the historical Gold Standard deposit, which corresponds to the upper extension of the Hinge deposit. It provides one of the few surface exposures of a mineralized fault-fill quartz vein ('16-type') and its host NE shear.

The outcrop consists of clast-supported breccia in the immediate hangingwall of the stratified lithofacies of the Townsite dacite. A moderate to strong G_3 shape fabric in these rocks is highlighted by rare cream-coloured dacite clasts exposed in the blasted vertical face at the east end of the outcrop. The S_3 fabric dips moderately to the north-northeast and the L_3 lineation plunges moderately to the northeast. The quartz vein is exposed over 10–15 m of strike length in a trench along the south face of the outcrop. It ranges up to 45 cm thick and consists of massive to faintly laminated quartz, with minor stylolitic pressure solution seams (chlorite±tourmaline), and accessory carbonate, chlorite and pyrite.

The vein is hosted by a 1–2 m thick zone of chloritic mylonite that dips moderately towards the northwest. Along its hangingwall margin, the wallrock S_3 fabric curves into parallelism with the mylonitic foliation, and altered plagioclase phenocrysts define a prominent stretching lineation that plunges toward the north-northeast at a shallower angle than the wallrock L_3 lineation. The vein pinches and swells slightly, perhaps due to incipient boudinage (the boudin axis appears to plunge shallowly to the west). Shallowly-dipping extension veins in the hangingwall contain quartz fibres oriented subparallel to the wallrock L_3 lineation. The overall structural geometry is consistent with sinistral-reverse oblique-slip along the NE shear.

The NE shear and fault-fill vein represent the up-dip extension of the L1 lens of the Hinge deposit (Figure 19), which has been mined to within 80 m of surface beneath this outcrop. The prominent left-stepping dilational-jog geometry of major orebodies in the Hinge deposit is interpreted to result from refraction of this shear through layers of varying competency in the stratified lithofacies of the Townsite dacite, which passes just south of this outcrop and will be examined at the next stop.

Continue on foot toward the west for approximately 200 m, past the Hinge vent raise, to a large and flat cleared outcrop. Caution: this outcrop may be littered with broken glass.

Stop 2-7 (313169mE, 5655739mN): Townsite dacite (stratified lithofacies)

This outcrop corresponds to the type locality of the 'stratified' lithofacies of the Townsite dacite (Figure 12), approximately 150 m along strike to the west from the Hinge deposit. The unusually large flat outcrop in this location provides a continuous exposure over a stratigraphic thickness of at least 50 m and facilitates detailed examination of the internal stratigraphy of this unit (Figure 25).

The lithofacies in this location consists of interlayered heterolithic volcanic conglomerate and bedded volcanic sandstone. The conglomerate layers range up to 15 m thick and are poorly sorted, matrix supported and unstratified. They consist of angular to subrounded clasts of plagioclase-phyric dacite that range up to 80 cm in maximum dimension. Subordinate clast types include aphyric andesite, epidotized basalt and rare melagabbro. Most layers are massive, with thin (<50 cm) reversely graded bases and normally graded tops, whereas others show diffuse normal or reverse size-grading throughout; basal contacts are sharp and scoured. These features are consistent with high-density debris flow deposits. Some layers also contain diffuse beds of volcanic sandstone, indicating that they represent more than one debris-flow unit.

Volcanic sandstone defines six discrete layers in this location, which vary from 0.3 to 1 m in thickness and dip steeply to the north. Most layers consist of a relatively thick (15–30 cm), normally graded bed of pebbly volcanic sandstone at the base. The tops consist of thin (<10 cm) normally-graded beds of medium- to coarse-grained volcanic sandstone. Some beds are reversely graded at the base, or contain low-angle crossbeds; sharp scoured bases are indicative of high-density turbidity flows. Collectively, the volcanic conglomerate and sandstone are interpreted to record influxes of reworked detritus during a transition from grain-flow–dominated (massive lithofacies) to mass-flow–dominated (breccia lithofacies) sedimentation in the Townsite unit, likely in a shallow submarine fan setting.

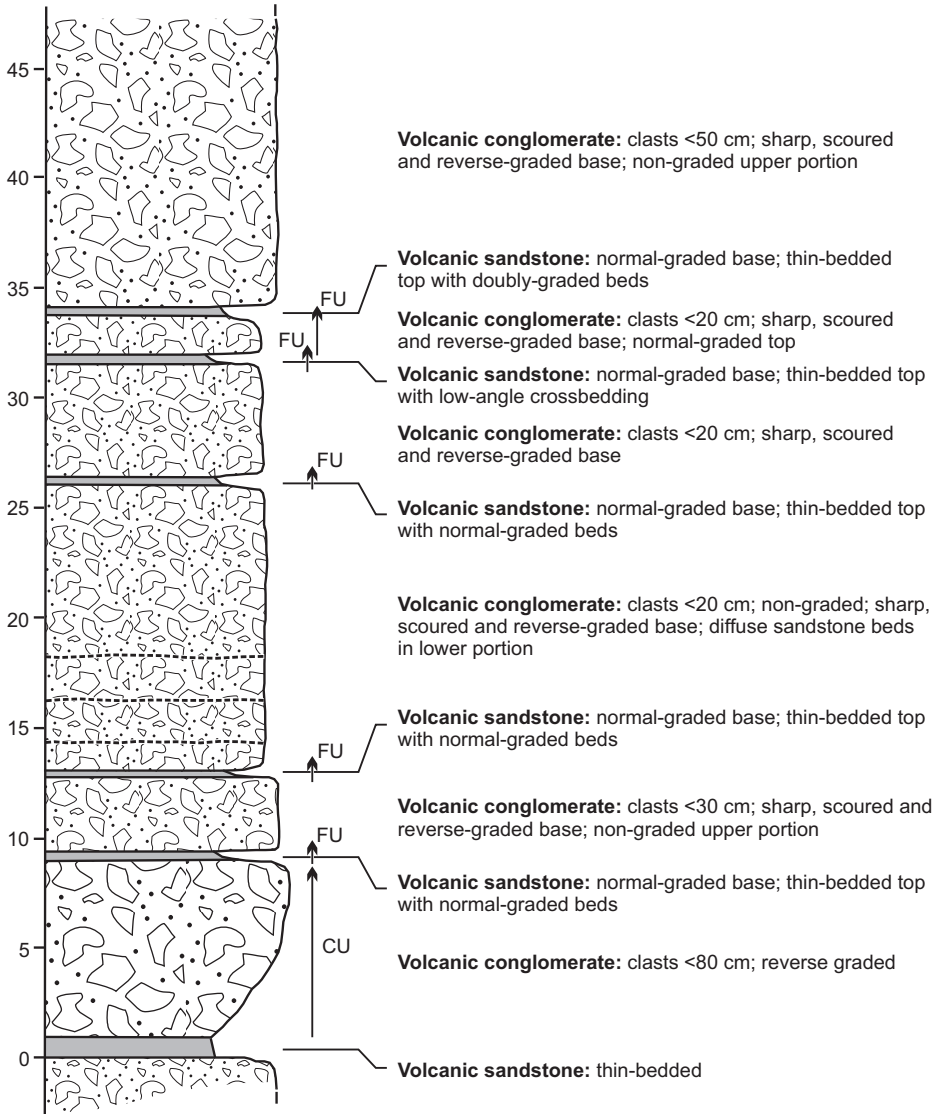

Figure 25: *Measured section of the stratified lithofacies of the Townsite dacite at the type locality 100 m west of the Gold Standard/ Hinge deposit. The volcanic conglomerate layers are heterolithic, matrix supported and poorly sorted, and are internally unstratified except where indicated. The volcanic sandstone layers are planar bedded, medium to coarse grained and pebbly. Arrows indicate coarsening upward (CU) and fining-upward (FU) trends within individual layers. Vertical scale is metres.*

As noted previously, the trace of this lithofacies in outcrop coincides with the surface projections of the Hinge and L13 deposits. Counter-clockwise refraction of NE shears across layers of varying competency in this lithofacies are interpreted to account for the prominent left-stepping geometry of dilational jogs in the Hinge deposit (Figure 19).

From the west end of the outcrop at Stop 2-7, proceed west on foot for approximately 100m to the site of the historical 'Big Four' shaft, and from there follow a drill road north then east for approximately 150 m to a large clean outcrop in the roadbed.

Stop 2-8 (313099mE, 5655838mN): Townsite dacite (breccia lithofacies)

This outcrop consists of the breccia lithofacies of the Townsite dacite, and includes particularly good examples of overprinting relationships between the regional S_3 and S_4 fabrics. The matrix-supported breccia and tuff-breccia consist of angular to rounded clasts of plagioclase-phyric dacite up to 50 cm across. Variably flattened clasts define the regional S_3 shape fabric that dips steeply north and is overprinted at a shallow counter-clockwise angle by the S_4 crenulation cleavage, which is finely-spaced and dips steeply to the northwest. At the east end of the outcrop, the S_3 fabric is overprinted by a planar, northwest-trending shear fracture, corresponding to a NW shear, and a subparallel array of sigmoidal extension veins, representing an incipient NW shear. The sense of vein asymmetry indicates dextral shear.

From Stop 2-8 proceed across the outcrop ridge in a northwesterly direction to a large flat outcrop that has been stripped and washed (approximately 150 m walking distance).

Stop 2-9 (312997mE, 5655941mN): Townsite dacite (breccia lithofacies)

This outcrop provides an exposure of the breccia lithofacies of the Townsite dacite and an opportunity to examine the geometry and kinematics of NE and NW shears.

The breccia is crudely stratified, matrix or clast-supported and consists of angular to subrounded clasts of plagioclase-phyric dacite up to 50 cm across in a matrix of crystal-lithic lapilli-tuff. In this location the breccia contains a thin (1–2 m) interlayer of bedded, fine to medium-grained, volcanic sandstone that dips moderately to the north-northeast (Figure 26). Flattened clasts in the breccia define a weak to moderate S_3 shape fabric that dips steeply to the north and transects bedding at a shallow counter-clockwise angle, and is likewise transected by the S_4 crenulation cleavage, which dips steeply to the north-northwest. At the north end of the outcrop, the S_3 fabric intensifies into a narrow (~0.5 m), subparallel zone of chloritic mylonite. The mylonitic foliation contains a local quartz-fibre lineation that plunges moderately to the northeast and is overprinted by the S_4 crenulation cleavage. Minor en échelon extension veins in the footwall are compatible with sinistral-reverse oblique-slip shear along this zone, which thus corresponds to a NE shear of the late-G_3 generation.

Discrete brittle-ductile shears in the footwall of the NE shear correspond to NW shears of the late-G_3 generation. The shears are defined by planar slip surfaces that dip steeply to the northeast and are associated with arrays of planar to sigmoidal quartz-filled extension fractures (Figure 26). The geometry of the extension veins and offsets of the bedded volcanic sandstone indicate right-lateral movement along the shears. Adjacent and subparallel NW shears bound rectilinear structural blocks of various sizes in which bedding has apparently been rotated up to 20° from its orientation in adjacent blocks (Figure 26). Apparent displacements of the sandstone layer vary up to 2 m; however, the NW shears do not displace the NE shear, nor have they been observed in the immediate hangingwall. Although it is possible that the NW shears entirely pre-date the NE shear in this location, their geometry and kinematics, coupled with mutual overprinting relationships observed elsewhere, indicate a conjugate set. The NW shears and associated block-rotations are thought to represent 'linking damage' that occurred in the area between the NE shear exposed in this outcrop and a subparallel shear to the immediate south, which is not exposed at surface but hosts the L13 deposit at depth (Figure 12, 15).

Return to the vehicles by the reciprocal route (approximately 400 m in a southeasterly direction). Drive west along the SG1 road for approximately 1.2 km, past the Hinge portal, to the stop sign. Turn right (north) and proceed north to a road cut on the left (west) side of the road, just before the San Antonio Hotel.

Stop 2-10 (312178mE, 5656030mN): Townsite dacite (massive lithofacies)

This outcrop consists of the massive lithofacies of the Townsite dacite, which in this location contains moderate to strong ankerite-albite-sericite-pyrite alteration and minor quartz-carbonate veins along strike from the Gabrielle deposit approximately 200 m to the west (Figure 12). The outcrop contains a penetrative S-L fabric (G_3) defined by flattened and stretched plagioclase crystals. The S_3 foliation dips moderately to the north-northeast and contains a northeast-plunging L_3 stretching lineation. These fabrics locally intensify into narrow zones of G_3 mylonite and are cut at very shallow angles by discrete brittle-ductile NE shears that contain chlorite, quartz-fibre or slickenline lineations that plunge at steep to moderate angles toward the northeast, subparallel to the L_3 lineation in the wallrock. The G_3 fabric is also overprinted by the weak S_4 crenulation cleavage, which dips steeply towards the north-northwest. Narrow zones of intense sericitization along the margins of quartz-carbonate veins in this outcrop locally contain a prominent crenulation lineation associated with the S_4 cleavage and/or open crenulations of the G_6 generation (the latter being axial planar to the macroscopic open flexure of the mine stratigraphy). Quartz-filled pressure fringes on pyrite porphyroblasts in these zones define a lineation that parallels the L_3 stretching lineation, suggesting that mineralization and alteration occurred prior to the latest increments of G_3 fabric development. Minor shallow-dipping extension veins in this outcrop contain well-developed quartz fibres; these veins are common along the margins of most major orebodies in the Rice Lake mine trend.

Proceed back along the road to the south, verging right at the base of the hill and then left toward the marina and beach, and continuing on towards the west along the residential road

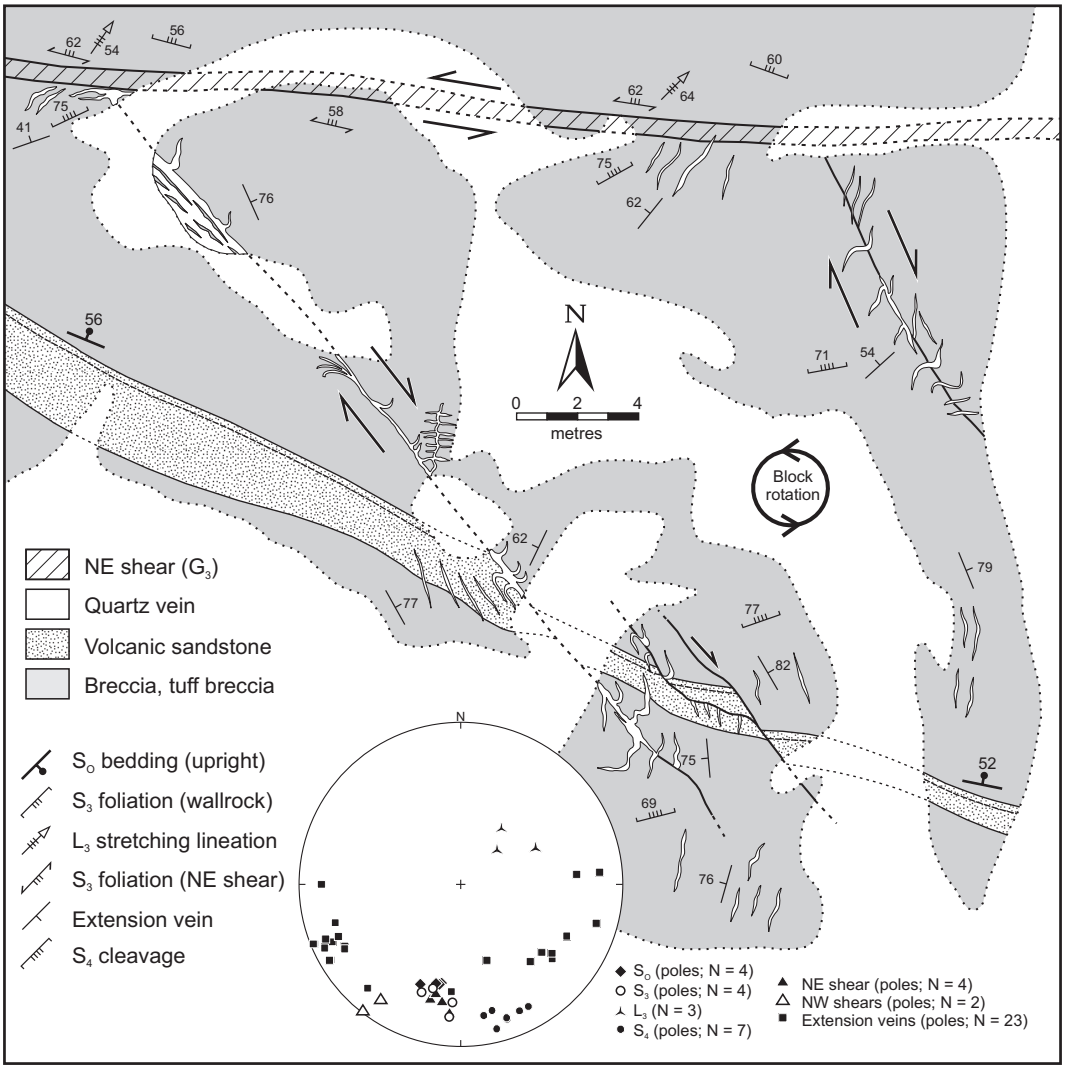

Figure 26: *Outcrop map of NW and NE shears in the Townsite dacite, approximately 100 m north of the L13 deposit. Rotation of the shear-bounded block in the eastern portion of the outcrop is indicated by the counter-clockwise deflection (<20°) of bedding. Structural data are plotted on a lower-hemisphere, equal-area sterographic projection.*

to the Bissett curling club (approximately 600 m driving distance). Park in the parking lot and proceed on foot to the historical monument and stamp mill at the shoreline of Rice Lake. Note: access to this site requires crossing private property; please seek permission from owners.

Stop 2-11 (311592mE, 5655918mN): SAM unit (Gabrielle showing)

This outcrop provides an exposure of the SAM unit approximately 500 m along strike to the northwest from the Rice Lake deposit. As indicated by the monument and bronze plaque, this locality has considerable historical significance: it was the site of the original Gabrielle discovery in 1911 and the first gold mill in the Province of Manitoba.

Here, the gabbro is homogeneous, fine-grained and melanocratic. It contains a weak to moderate fabric, which in places can be seen to consist of the penetrative S_3 foliation overprinted at a shallow angle by the spaced S_4 cleavage (as in the small outcrop 40 m to the east of the monument). The southern portion of the outcrop, near the waterline, contains an example of stockwork-breccia–style veins and associated ankerite alteration. If water levels are sufficiently low, additional examples of stockwork-breccia veins, locally associated with NE shears, can be observed in several small outcrops of gabbro to the northwest along the shoreline.

Return to the vehicles. Drive northeast for 100m to the intersection with Antonio Street. Turn left (west) and proceed 250 m to the northwest, past the intersection with PR 304, to the intersection with Currie Drive (just past Northern Wings B&B). Turn right (north) and proceed along Currie Drive for approximately 750 m to the large field on the left (north) side of the road. Proceed on foot to the north across the field to a series of clean outcrops at the eastern end of the large outcrop ridge.

Stop 2-12 (312227mE, 5656314mN): Townsite – Round Lake contact

The erosional contact between the Townsite dacite and overlying Round Lake unit is well exposed along the southern edge of the outcrop ridge in this location (Figure 12). Along

strike to the east, the Wingold deposit is hosted by a NW shear in the immediate footwall of this contact.

Crudely stratified monolithic tuff breccia and breccia at the base of the section define the top of the Townsite dacite and consist of angular to subrounded clasts of coarsely plagioclase-phyric dacite in a matrix of crystal-lithic lapilli tuff. These rocks are crosscut along strike by sanukitoid basalt dikes up to 3 m thick that have planar or irregular contacts and thick chilled margins.

The Townsite dacite is overlain by the basal heterolithic volcanic conglomerate of the Round Lake unit. This conglomerate is crudely stratified, matrix supported, poorly sorted and contains well-rounded to subangular clasts that range up to 2.5 m across. Despite significant subaerial transport, as indicated by an abundance of rounded and subspherical clasts, the detritus appears to be mostly representative of underlying units. The conglomerate includes minor interlayers of pebbly volcanic sandstone that range up to 50 cm thick and dip moderately to the north-northeast. The proportion of porphyritic dacite clasts systematically decreases upsection over 35–40 m of stratigraphic thickness. Mafic dikes are absent. However, the conglomerate contains a high proportion (locally up to 80%) of mafic clasts, some of which have very angular cuspate shapes suggestive of proximal autoclastic or hyaloclastic detritus. Near the top of the section, the conglomerate includes a thick (10–15 m) layer of sanukitoid-affinity basaltic lapilli-tuff, indicating that sedimentation was coeval with sanukitoid volcanism in this location.

Deformed clasts in the conglomerate define a moderate to strong G_3 shape fabric that dips moderately to the north-northeast and includes a moderate to strong L_3 stretching lineation that plunges northeast. The S_4 crenulation cleavage is weakly developed. Diffuse northwest-trending arrays of planar to slightly sigmoidal quartz-filled extension fractures are developed locally and, in one location, appear to have nucleated at the lateral tips of outsized boulders, emphasizing the important role of heterogeneity in localizing deformation and veining. The extension veins are locally linked by through-going shear fractures and narrow fault-fill veins. The geometrical relationships indicate dextral movement on the shear fractures, which would thus correspond to NW shears of the late-G_3 generation.

In an outcrop approximately 100 m to the west (312132mE, 5656313mN), plagioclase-phyric breccia of the Townsite dacite is cut by a particularly thick basaltic dike. The outcrop includes a good example of quartz-filled 'wing-cracks' at the lateral termination of a northeast-trending shear fracture.

Return to vehicles. End of Day 2.

Day 3: Underground tour

This portion of the field trip is intended to include a tour of an active mine in the Rice Lake mine trend, during which participants will have the opportunity to examine auriferous quartz-carbonate vein systems, as well as their hostrocks, controlling structures and associated hydrothermal alteration, in newly-developed underground workings. Unfortunately, due to the vagaries of production and staff schedules, it is not possible to specify in advance which mine will be visited, nor the specific features that might be available for detailed examination.

Background – history of the Rice Lake mine trend

The original gold discovery at Rice Lake was made in 1911 by Captain E.A. Pelletier, based on samples of vein quartz provided by Duncan Twohearts, an aboriginal trapper from Fort Alexander, Manitoba. The original claim, named Gabrielle, was staked in March, 1911. An adjacent claim, staked in May, 1911, was the namesake for the San Antonio deposit. In the summer of 1912, the occurrence was documented by E.S. Moore of the Geological Survey of Canada (Moore, 1914) and a stamp mill was erected on the Gabrielle claim, representing the first gold mill in Manitoba.

Underground development of the San Antonio deposit commenced in 1927, but its economic viability did not become apparent until 1929, with the discovery of the No. 16 vein. Mill construction took place in 1931 and commercial production was achieved in 1932 at a rate of 136 tonnes per day, increasing to 500 tonnes per day by 1948. During this time period, the bulk of production came from the No. 16 and No. 38 veins, the latter discovered in 1937. Several prospect shafts were excavated on adjacent claims during this early phase of exploration and development (e.g., Big Four, Emperor, Gabrielle, Gold Cup, Gold Standard, San Norm and Wingold), but none were proved viable.

Access to the San Antonio mine was initially by the No.1 and No. 2 shafts, which were replaced in 1934 by the larger No. 3 shaft (now known as 'A' shaft). Underground exploration and development were carried out by driving footwall drifts parallel to the strike of the host gabbro sill at 150 foot vertical intervals and then drilling horizontal holes on standard (50 foot) centres to establish the locations of veins. Ore was mined by shrinkage stoping, trammed to the shafts and hoisted to surface. As development progressed down the dip of the inclined sill, three internal winzes were added (B, C and D shafts), such that ore from the deepest levels of the mine, below D shaft, had to be trammed and hoisted four times over a cumulative distance of nearly 3 km to surface. Ore was processed by standard crushing and milling, followed by gravity concentration and finishing in a Merrill Crowe cyanide plant.

The surface hoist was destroyed by fire in 1968, resulting in the end of production and a declaration of bankruptcy by San Antonio Gold Mines Ltd. In 1980, the mill was also destroyed by fire. The property saw limited work during the period 1980–87, until being acquired in 1989 by Rea Gold Corporation ('Rea Gold'). At that time, the mineral reserve was estimated to be 1.1 million tonnes grading 7.5 g/t gold (Ginn and Michaud, 2013). Between 1994 and 1997, Rea Gold completed a major program of underground rehabilitation and exploration, including the deepening of A shaft to 1219 m, and construction of a modern 900 tonne per day processing facility. Prior to commencing production however, Rea Gold was placed into receivership. Harmony Gold (Canada) Inc. ('Harmony') took over the project in 1998 and established a new ramp system and longhole stoping operation in the deepest levels of the mine. Harmony operated the mine for three years and placed it on a care and maintenance in 2001 due to low gold prices. In 2001, the measured and indicated mineral resources were estimated to be 1.2 million tonnes grading 8.9 g/t gold, with an inferred

mineral resource of 670,000 tonnes grading 10.6 g/t gold (Ginn and Michaud, 2013).

In 2004, the predecessors to San Gold Corporation ('San Gold') entered into a joint venture agreement to acquire the property from Harmony. From 2005 to the present, intensive exploration drilling by San Gold resulted in the discovery or delineation of several significant gold deposits, which collectively define the Rice Lake mine trend. Underground exploration and development of the SG1 deposit commenced in 2005, followed closely by the Hinge deposit in 2008, and the 007, Cohiba and L10 deposits in 2010, all of which are accessed via ramps from surface. Mining of the Rice Lake (San Antonio) deposit was resumed in 2006. Ore is currently being extracted from three underground mines (007, Hinge and Rice Lake); workings in the latter extend 1,675 m below surface. Mining methods vary according to deposit geometry, but are mostly mechanized cut-and-fill with localized longhole stoping in locations where vein widths and continuity are suitable. Currently, all material from the Hinge and 007 mines is transported to surface via underground trucks.

In 2011, an expansion of the crushing plant allowed mill throughput to be increased to 2300 tonnes per day. Ore is ground by ball mill, passed through gravity concentrators and upgraded on a shaking table to recover gold for direct smelting. Tails from the concentrators and shaking table are returned to the grinding circuit and recovered using a six stage carbon-in-pulp process. Current mill recovery is 93.5% based on a feed grade of 5.5 grams per tonne. As of December 31, 2012, the Rice Lake mine complex had produced close to 1.72 million ounces of gold, and had estimated total resources of 3.51 million ounces (Ginn and Michaud, 2013).

Acknowledgements

San Gold Corporation is gratefully acknowledged for allowing access to the Rice Lake property and mine complex, and for providing proprietary company data, without which this field trip and guidebook would not be possible. The author also acknowledges past and present staff from Mine Geology (J. Wong, J. Harvey, L. Norquay, A. Kathler, D. Pickell, S. Horte and D. Berthelsen), Exploration (B. Ferreira and K. Murphy) and management (D. Ginn, R. Boulay, M. Michaud), for discussions, tours and free access to company data.

References

Ames, D.E. 1988: Stratigraphy and alteration of gabbroic rocks near the San Antonio gold mine in the Rice Lake area, southeastern Manitoba; M.Sc. thesis, Carleton University, Ottawa, Ontario, 202 p.

Ames, D.E., Franklin, J.M. and Froese, E. 1991: Zonation of hydrothermal alteration at the San Antonio gold mine, Bissett, Manitoba, Canada; Economic Geology, v. 86, p. 600–619.

Anderson, S.D. 2008: Geology of the Rice Lake area, Rice Lake greenstone belt, southeastern Manitoba (parts of NTS 52L13, 52M4); Manitoba Science, Technology, Energy and Mines, Manitoba Geological Survey, Geoscientific Report GR2008-1, 97 p.

Anderson, S.D. 2011a: Detailed geological mapping of the Rice Lake mine trend, southeastern Manitoba (part of NTS 52M4): stratigraphic setting of gold mineralization; *in* Report of Activities 2011, Manitoba Innovation, Energy and Mines, Manitoba Geological Survey, p. 94–110.

Anderson, S.D. 2011b: Detailed geological mapping of the Rice Lake mine trend, southeastern Manitoba (part of NTS 52M4): structural geology of hostrocks and auriferous quartz-vein systems; *in* Report of Activities 2011, Manitoba Innovation, Energy and Mines, Manitoba Geological Survey, p. 111–126.

Anderson, S.D. 2011c: Geology and structure of the Rice Lake mine trend, Rice Lake greenstone belt, southeastern Manitoba (part of NTS 52M4); Manitoba Innovation, Energy and Mines, Manitoba Geological Survey, Preliminary Map PMAP2011-3, scale 1:5000.

Anderson, S.D. 2013: Geology of the Garner–Gem lakes area, Rice Lake greenstone belt, southeastern Manitoba (parts of NTS 52L11, 14); Manitoba Innovation, Energy and Mines, Manitoba Geological Survey, Geoscientific Report GR2013-1 (in press, May 2013).

Bailes, A.H. and Percival, J.A. 2005: Geology of the Black Island area, Lake Winnipeg, Manitoba (parts of NTS 62P1, 7 and 8); Manitoba Industry, Economic Development and Mines, Manitoba Geological Survey, Geoscientific Report GR2005-2, 33 p.

Bailes, A.H., Percival, J.A., Corkery, M.T., McNicoll, V.J., Tomlinson, K.Y., Sasseville, C., Rogers, N., Whalen, J.B. and Stone, D. 2003: Geology and tectonostratigraphic assemblages, West Uchi map area, Manitoba and Ontario; Manitoba Geological Survey, Open File OF2003-1, 1:250 000 scale with marginal notes.

Bethune, K.M., Helmstaedt, H.H. and McNicoll, V.J. 2006: Structural analysis of the Miniss River and related faults, western Superior Province: post-collisional displacement initiated at terrane boundaries; Canadian Journal of Earth Sciences, v. 43, p. 1031–1054.

Bleeker, W. 2012: Targeted Geoscience Initiative 4. Lode gold deposits in ancient deformed and metamorphosed terranes: the role of extension in the formation of Timiskaming basins and large gold deposits, Abitibi greenstone belt—a discussion; *in* Ontario Geological Survey, Summary of Field Work and Other Activities 2012, Open File Report 6280, p. 47-1–47-12.

Bleeker, W., Ketchum, J.W.F., Jackson, V.A. and Villeneuve, M.E. 1999: The Central Slave Basement Complex, Part I: its structural topology and autochthonous cover; Canadian Journal of Earth Sciences; v. 36, p. 1083–1109.

Blenkinsop, T.G. 2008: Relationship between faults, extension fractures and veins, and stress; Journal of Structural Geology, v. 30, p. 622–632.

Bragg, J.G. 1943: Rock alteration at the San Antonio mine; Canadian Mining Journal, v. 64, p. 553–556.

Breaks, F.W. 1991: English River Subprovince; *in* Geology of Ontario, P.C. Thurston, H.R. Williams, R.H. Sutcliffe and G.M. Stott (ed.), Ontario Geological Survey, Special Volume 4, Part 1, p. 239–277.

Brommecker, R. 1991: The structural setting of gold occurrences in the southeast Rice Lake greenstone belt, southeast Manitoba; M.Sc. thesis, Queen's University, Kingston, Ontario, 267 p.

Brommecker, R. 1996: Geology of the Beresford Lake area, southeast Manitoba; Geological Survey of Canada, Open File 3318, 127 p.

Brommecker, R., Scoates, R.F.J. and Poulsen, K.H. 1993: Komatiites in the Garner Lake–Beresford Lake area: implications for tectonics and gold metallogeny of the Rice Lake greenstone belt, southeast Manitoba; *in* Current Research, Part C, Geological Survey of Canada, Paper 93-1C, p. 259–264.

Campbell, F.H.A. 1971: Stratigraphy and sedimentation of part of the Rice Lake Group, Manitoba; *in* Geology and Geophysics of the Rice Lake Region, Southeastern Manitoba (Project Pioneer), W.D. McRitchie and W. Weber (ed.), Manitoba Department of Mines and Natural Resources, Mines Branch, Publication 71-1, p. 135–188.

Card, K.D. 1990: A review of the Superior Province of the Canadian Shield, a product of Archean accretion; Precambrian Research, v. 48, p. 99–156.

Card, K.D. and Ciesielski, A. 1986: Subdivisions of the Superior Province of the Canadian Shield; Geoscience Canada, v. 13, p. 5–13.

Cooke, H.C. 1922: Geology and mineral resources of Rice Lake and Oiseau River areas, Manitoba; Canada Department of Mines, Geological Survey, Summary Report, 1921, Part C, 36 p.

Corcoran, P.L. and Mueller, W.U. 2007: Time-transgressive Archean unconformities underlying molasse basin-fill successions of dissected oceanic arcs, Superior Province, Canada; The Journal of Geology, v. 115, p. 655–674.

Corfu, F. and Stone, D. 1998: Age structure and orogenic significance of the Berens River composite batholiths, western Superior Province; Canadian Journal of Earth Sciences, v. 35, p. 1089–1109.

Corfu, F. and Stott, G.M. 1993: U-Pb geochronology of the central Uchi Subprovince, Superior Province; Canadian Journal of Earth Sciences, v. 30, p. 1179–1196.

Corfu, F., Davis, D.W., Stone, D. and Moore, M.L. 1998: Chronostratigraphic constraints on the genesis of Archean greenstone belts, northwestern Superior Province, Ontario, Canada; Precambrian Research, v. 92, p. 277–295.

Corfu, F., Stott, G.M. and Breaks, F.W. 1995: U-Pb geochronology and evolution of the English River Subprovince, an Archean low P-high T metasedimentary belt in the Superior Province; Tectonics, v. 14, p. 1220–1233.

Cox, S.F. 1995: Faulting processes at high fluid pressures: an example of fault valve behaviour from the Wattle Gully Fault, Victoria, Australia; Journal of Geophysical Research, v. 100, p. 12 841–12 859.

Davies, J.F. 1953: Geology and gold deposits of southern Rice Lake area; Manitoba Department of Mines and Natural Resources, Mines Branch, Publication 52-1, 41 p.

Davies, J.F. 1963: Geology and gold deposits of the Rice Lake–Wanipigow River area, Manitoba; Ph.D. thesis, University of Toronto, Ontario, 142 p.

Davis, D.W. 1994: Report on the geochronology of rocks from the Rice Lake belt, Manitoba; Royal Ontario Museum, Geology Department, Toronto, Ontario, unpublished report.

Davis, D.W. 1996: Provenance and depositional age constraints on sedimentation in the Western Superior Transect area from U-Pb ages of zircons; *in* LITHOPROBE Western Superior Transect, Second Annual Workshop, R.M. Harrap and H. Helmstaedt (ed.), LITHOPROBE Secretariat, University of British Columbia, LITHOPROBE Report 53, p. 18–23.

Davis, D.W. 1998: Speculations on the formation and crustal structure of the Superior Province from U-Pb geochronology; *in* Western Superior LITHOPROBE Transect, Fourth Annual Workshop, R.M. Harrap and H.H. Helmstaedt (ed.), LITHOPROBE Secretariat, University of British Columbia, LITHOPROBE Report 65, p. 21–28.

De Lury, J.S. 1927: The mineral resources of southeastern Manitoba, Rice Lake District, Oiseau River District, Boundary District; Industrial Development Board of Manitoba, Winnipeg, Manitoba, 55 p.

Diamond, L.W., Marshall, D.D., Jackman, J.A. and Skippen, G.B. 1990: Elemental analysis of individual fluid inclusions in minerals by secondary ion mass spectrometry (SIMS): application to cation ratios of fluid inclusions in an Archaean mesothermal gold-quartz vein; Geochimica et Cosmochimica Acta, v. 54, p. 545–552.

Dresser, J.A. 1917: Gold-bearing district of southeastern Manitoba; *in* Summary Report of the Geological Survey, Department of Mines, for the calendar year 1916, Sessional Paper No. 26, p. 169–175.

Dubé, B., Williamson, K., McNicoll, V., Malo, M., Skulski, T., Twomey, T. and Sanborn-Barrie, M. 2004: Timing of gold mineralization at Red lake, northwestern Ontario, Canada: new constraints from U-Pb geochronology at the Goldcorp high-grade zone, Red Lake mine, and the Madsen mine; Economic Geology, v. 99, p. 1611–1641.

Ermanovics, I.F. and Wanless, R.K. 1983: Isotopic age studies and tectonic interpretation of Superior Province in Manitoba; Geological Survey of Canada, Paper 82-12, 22 p.

Fretzdorff, S., Livermore, R.A., Devey, C.W., Leat, P.T. and Stoffers, P. 2002: Petrogenesis of the back-arc East Scotia Ridge, South Atlantic Ocean; Journal of Petrology, v. 43, p. 1435–1467.

Geological Survey of Canada 1986: Manitoba (Flin Flon) – Area 300 Bisset, aeromagnetic survey; Geological Survey of Canada, Geoscience Data Repository (available on-line at http://gdrdap.agg.nrcan.gc.ca/geodap/index_e.html).

Gibson, J.C. and Stockwell, C.H. 1948: San Antonio mine; *in* Structural Geology of Canadian Ore Deposits, Canadian Institute of Mining and Metallurgy, Geology Division, Symposium Volume, p. 315–321.

Ginn, D. and Michaud, M. 2013: Technical report on the Rice Lake mining complex, Bissett, Manitoba; San Gold Corporation, 77 p.

Gribble, R.F., Stern, R.J., Newman, S., Bloomer, S.H. and O'Hearn, T. 1998: Chemical and isotopic composition of lavas from the northern Mariana Trough: implications for magma genesis in back-arc basins; Journal of Petrology, v. 39, p. 125–154.

Groves, D.I., Goldfarb, R.J., Gebre-Mariam, M., Hagemann, S.G. and Robert, F. 1998: Orogenic gold deposits: a proposed classification in the context of their crustal distribution and relationship to other gold deposit types; Ore Geology Reviews, v. 13, p. 7–27.

Hodgson, C.J. 1993: Mesothermal lode-gold deposits; *in* Mineral Deposit Modelling, R.V. Kirkham, W.D. Sinclair, R.I. Thorpe and J.M. Duke (ed.), Geological Association of Canada, Special Paper 40, p. 635–678.

Hoffman, P.F. 1989: Precambrian geology and tectonic history of North America; *in* The Geology of North America—an overview, A.W. Bally and A.R. Palmer (ed.), Geological Society of America, The Geology of North America, v. A, p. 447–512.

Hollings, P. and Kerrich, R. 2000: An Archean arc basalt–Nb-enriched basalt–adakite association: the 2.7 Ga Confederation assemblage of the Birch-Uchi greenstone belt, Superior Province; Contributions to Mineralogy and Petrology, v. 139, p. 208–226.

Hollings, P., Wyman, D. and Kerrich, R. 1999: Komatiite-basalt-rhyolite volcanic associations in northern Superior Province greenstone belts: significance of plume-arc interaction in the generation of the proto continental Superior Province; Lithos, v. 46, p. 137–161.

Hrabi, R.B. and Cruden, A.R. 2006: Structure of the Archean English River Subprovince: implications for the tectonic evolution of the western Superior Province, Canada; Canadian Journal of Earth Sciences, v. 43, p. 947–966.

Kelemen, P.B., Johnson, K.T.M., Kinzler, R.J. and Irving, A.J. 1990: High-field-strength element depletions in arc basalts due to mantle-magma interaction: Nature, v. 345, p. 521–524.

Kerrich, R. and Cassidy, K.F. 1994: Temporal relationships of lode gold mineralization to accretion, magmatism, metamorphism and deformation — Archean to present: a review; Ore Geology Reviews, v. 9, p. 263–310.

Kerrich, R. and Wyman, D. 1990: Geodynamic setting of mesothermal gold deposits: an association with accretionary tectonic regimes; Geology, v. 18, p. 882–885.

Kim, Y-S., Peacock, D.C.P. and Sanderson, D.J. 2004: Fault damage zones; Journal of Structural Geology, v. 26, p. 503–517.

Krogh, T.E., Ermanovics, I.F. and Davis, G.L. 1974: Two episodes of metamorphism and deformation in the Archean rocks of the Canadian Shield; Carnegie Institution of Washington, Geophysical Laboratory Yearbook, 1974, v. 73, p. 573–575.

Larbi, Y., Stevenson, R., Breaks, F., Machado, N. and Gariépy, C. 1999: Age and isotopic composition of late Archean leucogranites: implications for continental collision in the western Superior Province; Canadian Journal of Earth Sciences, v. 36, p. 495–510.

Lau, M.H.S. 1988: Structural geology of the vein system in the San Antonio gold mine, Bissett, Manitoba, Canada; M.Sc. thesis, University of Manitoba, Winnipeg, Manitoba, 154 p.

Lau, M.H.S. and Brisbin, W.C. 1996: Structural geology of the San Antonio mine, Bissett, Manitoba; Geological Survey of Canada, Open File 1699, 65 p.

Lemkow, D.R., Sanborn-Barrie, M., Bailes, A.H., Percival, J.A., Rogers, N., Skulski, T., Anderson, S.D., Tomlinson, K.Y., McNicoll, V., Parker, J.R., Whalen, J.B., Hollings, P. and Young, M. 2006: GIS compilation of geology and tectonostratigraphic assemblages, western Uchi Subprovince, western Superior Province, Ontario and Manitoba; Manitoba Geological Survey, Open File OF2006-30, CD-ROM.

Lesher, C.M., Goodwin, A.M., Campbell, I.H. and Gorton, M.P. 1986: Trace-element geochemistry of ore-associated and barren, felsic metavolcanic rocks in the Superior Province, Canada; Canadian Journal of Earth Sciences, v. 23, p. 222–237.

Martin, H. 1999: Adakitic magmas: modern analogues of Archaean granitoids; Lithos, v. 46, p. 411–429.

Martin, H., Smithies, R.H., Rapp, R., Moyen, J-F. and Champion, D. 2005: An overview of adakite, tonalite-trondhjemite-granodiorite (TTG), and sanukitoid: relationships and some implications for crustal evolution; Lithos, v. 79, p. 1–24.

McCuaig, T.C. and Kerrich, R. 1998: P–T–t–deformation–fluid characteristics of lode gold deposits: evidence from alteration systematics; Ore Geology Reviews, v. 12, p. 381–453.

McRitchie, W.D. and Weber, W. 1971: Metamorphism and deformation in the Manigotagan Gneissic Belt, south-eastern Manitoba; *in* Geology and Geophysics of the Rice Lake Region, Southeastern Manitoba (Project Pioneer), W.D. McRitchie and W. Weber (ed.), Manitoba Department of Mines and Natural Resources, Mines Branch, Publication 71-1, p. 235–284 (and accompanying Maps 69-1 to -4).

Moore, E.S. 1914: Region east of the south end of Lake Winnipeg; *in* Summary Report of the Geological Survey, Department of Mines, for the calendar year 1912, Sessional Paper 26, p. 262–270.

Nicholson, C., Seeber, L., Williams, P. and Sykes, L.R. 1986: Seismic evidence for conjugate slip and block rotation within the San Andreas fault system, southern California; Tectonics, v. 5, p. 629–648.

Pan, Y., Therens, C. and Ansdell, K. 1998: Geochemistry of mafic-ultramafic rocks from the Werner–Gordon Lake area: back-arc origin for the English River Subprovince?; *in* Western Superior LITHOPROBE Transect, Annual Meeting, R.M. Harrap and H.H. Helmstaedt (ed.), LITHOPROBE Secretariat, University of British Columbia, LITHOPROBE Report 65, p. 29–34.

Percival, J.A., McNicoll, V. and Bailes, A.H. 2006a: Strike-slip juxtaposition of ca. 2.72 Ga juvenile arc and >2.98 Ga continent margin sequences and its implications for Archean terrane accretion, western Superior Province, Canada; Canadian Journal of Earth Sciences, v. 43, p. 895–927.

Percival, J.A., Sanborn-Barrie, M., Skulski, T., Stott, G.M., Helmstaedt, H. and White, D.J. 2006b: Tectonic evolution of the western Superior Province from NATMAP and LITHOPROBE studies; Canadian Journal of Earth Sciences, v. 43, p. 1085–1117.

Perfit, M.R., Gust, D.A., Bence, A.E., Arculus, R.J. and Taylor, S.R. 1980: Chemical characteristics of island-arc basalts: implications for mantle sources; Chemical Geology, v. 30, p. 227–256.

Poulsen, K.H. 1987: Structural and alteration studies, Bissett area; *in* Report of Field Activities 1987, Manitoba Energy and Mines, Minerals Division, p. 169–170.

Poulsen, K.H. 1989: Structure and hydrothermal alteration, Rice Lake gold district, southeastern Manitoba; *in* Investigations by the Geological Survey of Canada in Manitoba and Saskatchewan during the 1984-1989 Mineral Development Agreements, A.G. Galley (comp.), Geological Survey of Canada, Open File 2133, p. 42–49.

Poulsen, K.H., Ames, D.E., Lau, S. and Brisbin, W.C. 1986: Preliminary report on the structural setting of gold in the Rice Lake area, Uchi Subprovince, southeastern Manitoba; *in* Current Research, Part B, Geological Survey of Canada, Paper 86-1B, p. 213–221.

Poulsen, K.H., Davis, D.W., Weber, W. and Scoates, R.F.J. 1993: Geological and geochronological studies in the Rice Lake Belt; *in* Report of Activities 1993, Manitoba Energy and Mines, Geological Services, p. 152.

Poulsen, K.H., Robert, F. and Dubé, B. 2000: Geological classification of Canadian gold deposits; Geological Survey of Canada, Bulletin 540, 106 p.

Poulsen, K.H., Weber, W., Brommecker, R. and Seneshen, D.N. 1996: Lithostratigraphic assembly and structural setting of gold mineralization in the eastern Rice Lake greenstone belt, Manitoba; Geological Association of Canada–Mineralogical Association of Canada, Joint Annual Meeting, May 27–29, 1996, Winnipeg, Manitoba, Field Trip A4 Guidebook, 106 p.

Poulsen, K.H., Weber, W., Garson, D.F. and Scoates, R.F.J. 1994: New geological observations in the Rice Lake belt, southeastern Manitoba; *in* Report of Activities 1994, Manitoba Energy and Mines, Geological Services, p. 163–166.

Reid, J.A. 1931: The geology of the San Antonio gold mine, Rice Lake, Manitoba; Economic Geology, v. 26, p. 644–661.

Rhys, D.A. 2001: Report on a structural geology study of the, San Antonio Mine, Bissett, Manitoba; prepared for Harmony Gold (Canada) Inc.; unpublished technical report prepared by Panterra Geoservices Inc., 74 p.

Richards, J.P. and Kerrich, R. 2007: Adakite-like rocks: their diverse origins and questionable role in metallogenesis; Economic Geology, v. 102, p. 537–576.

Sanborn-Barrie, M., Skulski, T. and Parker, J. 2001: Three hundred million years of tectonic history recorded by the Red Lake greenstone belt, Ontario; Geological Survey of Canada, Current Research 2001-C19, 14 p.

Sasseville, C., Tomlinson, K.Y., Hynes, A. and McNicoll, V. 2006: Stratigraphy, structure, and geochronology of the 3.0–2.7 Ga Wallace Lake greenstone belt, western Superior Province, southeast Manitoba, Canada; Canadian Journal of Earth Sciences, v. 43, p. 929–945.

Schreurs, G. 1994: Experiments on strike-slip faulting and block rotation; Geology, v. 22, p. 567–570.

Shirey, S.B. and Hanson, G.N. 1984: Mantle derived Archaean monzodiorites and trachyandesites; Nature, v. 310, p. 222–224.

Sibson, R.H., Robert, F. and Poulsen, K.H. 1988: High-angle reverse faults, fluid-pressure cycling, and mesothermal gold-quartz deposits; Geology, v. 16, p. 551–555.

Sinton, J.M., Ford, L.L., Chappell, B. and McCulloch, M.T. 2003: Magma genesis and mantle heterogeneity in the Manus back-arc basin, Papua New Guinea; Journal of Petrology, v. 44, p. 159–195.

Stephenson, J.F. 1972: Gold deposits of the Rice Lake–Beresford Lake area, southeastern Manitoba; Ph.D. thesis, University of Manitoba, Winnipeg, 294 p.

Stern, R. 1989: Petrogenesis of the Archaean Sanukitoid Suite; State University at Stony Brook, New York, 275 p.

Stern, R.A., Hanson, G.N. and Shirey, S.B. 1989: Petrogenesis of mantle-derived, LILE-enriched Archean monzodiorites and trachyandesites (sanukitoids) in southwestern Superior Province; Canadian Journal of Earth Sciences, v. 26, p. 1688–1712.

Stockwell, C.H. 1938: Rice Lake–Gold Lake area, southern Manitoba; Geological Survey of Canada, Memoir 210, 79 p.

Stockwell, C.H. 1940: Gold mines and prospects in Rice Lake–Beresford Lake area, Manitoba; Transactions of the Canadian Institute of Mining and Metallurgy, v. 43, p. 613–626.

Stockwell, C.H. 1945: Rice Lake; Geological Survey of Canada, Map 810A, scale 1:63 360.

Stockwell, C.H. and Lord, C.S. 1939: Halfway Lake–Beresford Lake area, Manitoba; Geological Survey of Canada, Memoir 219, 67 p., and accompanying Maps 535A, 536A and 537A, scale 1:12 000.

Stott, G.M. and Corfu, F. 1991: Uchi Subprovince; *in* Geology of Ontario, P.C. Thurston, H.R. Williams, R.H. Sutcliffe and G.M. Stott, (ed.), Ontario Geological Survey, Special Volume 4, Part 1, p. 145–236.

Stott, G.M., Corkery, M.T., Percival, J.A., Simard, M. and Goutier, J. 2010: Project units 98-006 and 98-007: a revised terrane subdivision of the Superior Province; *in* Summary of Field Work and Other Activities 2010, Ontario Geological Survey, Open File Report 6260, p. 20-1–20-10.

Sun, S.-S. and McDonough, W.F. 1989: Chemical and isotopic systematics of oceanic basalts: implications for mantle composition and processes; *in* Magmatism in the Ocean Basins, A.D. Saunders and M.J. Norry, (ed.), Geological Society of London, Special Publication 42, p. 313–345.

Theyer, P. 1994a: Mineral deposits and occurrences in the Bissett area, NTS 52M/4; Manitoba Energy and Mines, Geological Services, Mineral Deposit Series, Report 18, 101 p.

Theyer, P. 1994b: Mineral deposits and occurrences in the Flintstone Lake area, NTS 52L/11; Manitoba Energy and Mines, Geological Services, Mineral Deposit Series Report 22, 60 p.

Theyer, P. and Ferreira, K.J. 1990: Mineral deposits and occurrences in the Garner Lake area, NTS 52L/14; Manitoba Energy and Mines, Geological Services, Mineral Deposit Series Report 10, 173 p.

Theyer, P. and Yamada, P.H. 1989: Mineral deposits and occurrences in the Manigotagan Lake area, NTS 52L/13; Manitoba Energy and Mines, Geological Services, Mineral Deposit Series, Report 4, 108 p.

Thurston, P.C. and Chivers, K.M. 1990: Secular variation in greenstone sequence development emphasizing Superior Province, Canada; Precambrian Research, v. 46, p. 21–58.

Thurston, P.C., Osmani, I.A. and Stone, D. 1991: Northwestern Superior Province: review and terrane analysis; *in* Geology of Ontario, P.C. Thurston, H.R. Williams, R.H. Sutcliffe and G.M. Stott (ed.), Ontario Geological Survey, Special Volume 4, Part 1, p. 81–142.

Tirschmann, P.A. 1986: Physical volcanology and sedimentology of part of the Archean Rice Lake Group, Rice Lake greenstone belt, southeastern Manitoba; B.Sc. thesis, University of Manitoba, Winnipeg, Manitoba, 99 p.

Tomlinson, K.Y., Stevenson, R.K., Hughes, D.J., Hall, R.P., Thurston, P.C. and Henry, P. 1998: The Red Lake greenstone belt, Superior Province: evidence of plume-related magmatism at 3 Ga and evidence of an older enriched source; Precambrian Research, v. 89, p. 59–76.

Turek, A. and Weber, W. 1991: New U-Pb zircon ages from the Rice Lake area: evidence for 3 Ga crust; *in* Report of Activities 1991, Manitoba Energy and Mines, Minerals Division, p. 53–55.

Turek, A. and Weber, W. 1994: The 3 Ga granitoid basement to the Rice Lake supracrustal rocks, southeast Manitoba; *in* Report of Activities 1994, Manitoba Energy and Mines, Minerals Division, p. 167–169.

Turek, A., Keller, R., Van Schmus, W.R. and Weber, W. 1989: U-Pb zircon ages for the Rice Lake area, southeastern Manitoba; Canadian Journal of Earth Sciences, v. 26, p. 23–30.

Weber, W. 1971a: Geology of the Wanipigow River–Manigotagan River region; *in* Geology and Geophysics of the Rice Lake Region, Southeastern Manitoba (Project Pioneer), W.D. McRitchie and W. Weber (ed.), Manitoba Department of Mines and Natural Resources, Mines Branch, Publication 71-1, Map 71-1/4.

Weber, W. 1971b: The evolution of the Rice Lake–Gem Lake greenstone belt, southeastern Manitoba; *in* Geoscience Studies in Manitoba, A.C. Turnock (ed.), Geological Association of Canada, Special Paper 9, p. 97–103.

Whalen, J.B., Percival, J.A., McNicoll, V.J. and Longstaffe, F.J. 2003: Intra-oceanic production of continental crust in a Th-depleted ca. 3.0 Ga arc complex, western Superior Province, Canada; Contributions to Mineralogy and Petrology, v. 146, p. 78–99.

Whiting, B.H. 1989: The lithology and lithogeochemistry of the San Antonio gold mine, Bissett, Manitoba; M.Sc. thesis, University of British Columbia, Vancouver, British Columbia, 250 p.

Williams, H.R., Stott, G.M., Thurston, P.C., Sutcliffe, R.H., Bennett, G., Easton, R.M. and Armstrong, D.K. 1992: Tectonic evolution of Ontario: summary and synthesis; *in* Geology of Ontario, P.C. Thurston, H.R. Williams, R.H. Sutcliffe and G.M. Stott (ed.), Ontario Geological Survey, Special Volume 4, Part 2, p. 1255–1332.

Wright, J.F. 1923: Rice Lake map-area, southeastern Manitoba; Canada Department of Mines, Geological Survey, Summary Report, 1922, Part C, p. 45–88.

Wright, J.F. 1932: Geology and mineral deposits of a part of southeastern Manitoba; Geological Survey of Canada, Memoir 169, 150 p.